

# **Generating CAR $\gamma\delta$ T cells for effective targeting of B lymphomas**

Marilee Larrivée

Thesis submitted to the University of Ottawa  
in partial fulfillment of the requirements for the degree of  
Master of Science in Microbiology and Immunology

Department of Biochemistry, Microbiology and Immunology  
Faculty of Medicine  
University of Ottawa

## Abstract

Chimeric antigen receptor (CAR) T-cell therapy has attracted growing interest in the treatment of various malignancies and represents the most advanced technology to date. This approach involves the use of genetically engineered immune cells expressing a surface receptor, called CAR, that specifically detects tumor-associated antigens (TAAs). Here, we generate polyclonal CAR  $\gamma\delta$  T cells, as these cells do not require patient-donor compatibility and are ideal candidates due to their natural cytotoxicity. The cells are modified to express a B lymphoma-specific CAR, featuring one of the two designs: either 1) an anti-CD19 murine single-chain variable fragment (scFv), a CD28-hinge domain, a 4-1BB costimulatory domain, and a CD3 $\zeta$  activation domain; or 2) an anti-CD22 camelid single-domain antibody (sdAb), a CD8 hinge-domain, a 4-1BB costimulatory domain, and a CD3 $\zeta$  activation domain. Using a recently developed packaging and producer line of 293SF-PacLV, we have produced and stocked the lentiviral vector (LV) for these CAR constructs. Lentiviral titration was performed on HEK 293A cells and validated by flow cytometry.  $\gamma\delta$  T cells were then transduced with the CAR lentivirus at different multiplicities of infection (MOIs). Analyses using flow cytometry showed a CAR transduction efficacy of over 30%, surpassing the clinical threshold required for therapeutic applications. Importantly, all  $\gamma\delta$  T cell subsets were efficiently transduced. This transduction rate represents a significant milestone in our research, and polyclonal CAR  $\gamma\delta$  T cells could be a promising off-the-shelf immunotherapy platform for treating B-cell malignancies.

## Acknowledgments

I would like to express my profound gratitude to my thesis supervisor, Dr. Zakia Djaoud, for believing in me and providing me the opportunity to undertake this project. I am extremely grateful for your constant support, availability and valuable advice. Thank you for checking in with me and always answering my questions, cheering me up when things went wrong, and for always lending a helping hand. You have marked my journey, not only professionally, but also personally. I have become more confident over the past three years, and it is partly thanks to you. I could not have had a better mentor than you.

To Dr. Marceline Côté, thank you for being a part of my thesis advisory committee and examiner for my thesis defence. Your expertise, advice and feedback have been greatly appreciated.

To Dr. Tommy Alain, thank you for accepting to be part of my thesis advisory committee, and for your advice during our common lab meetings.

To Dr. Scott McComb, thank you for your implication in my project and for taking the time to answer to all my questions.

To Dr. Carolina Ilkow, thank you for being an examiner for my thesis defence.

To Dr. Jonathan Angel, thank you for your interest in my work and your collaboration for the blood sampling.

To Dr. Vera Tang and Dr. Roland Pilgram, thank you for your trainings at the Cytometry & Virometry Core Facility and the Pre-Clinical Imaging Core Facility.

To my lab mates, Yeganeh and Mahya, a big thank you for providing advice, support and encouragement through all my experiments, troubles and woes.

A huge shout out to the members of the Alain lab, Pena lab and Beug lab; Eknoor, Salar, Negar, Huy-Dung, Pallavi, Simran, Mariam, Mikaela and Allan. I am so grateful for your friendship, help and support my entire time at the CHEO RI II. I would like to extend my gratitude to all the people working at the CHEO RI II.

I would like to thank Linda Doucet for proofreading my thesis. Your advice has been invaluable.

And above all, to my parents, thank you for your unconditional love, encouragement and support. Thank you for taking the time to listen to all my presentations, wiping my tears, making me laugh, hug me and always believing in my potential.

This is for you Juliane.

# Table of Contents

Abstract.....	ii
Acknowledgments.....	iii
List of Figures and Tables.....	vi
List of Abbreviations.....	vii
<b>Chapter 1: Introduction .....</b>	<b>1</b>
1.1 Cancer.....	1
1.1.1 Cancer metabolism .....	2
1.1.2 Cancer treatments .....	3
1.2 B-cell non-Hodgkin lymphomas .....	4
1.3 Adoptive cell therapy .....	6
1.4 Discovery of $\gamma\delta$ T cells.....	9
1.4.1 $\gamma\delta$ T cells.....	11
1.5 Current perspective of $\gamma\delta$ T cell-based therapies .....	14
1.6 Generating CAR $\gamma\delta$ T cells.....	16
1.7 Hypothesis and aims.....	19
<b>Chapter 2: Materials and Methods .....</b>	<b>22</b>
2.1 Cell culture .....	22
2.2 Flow cytometry .....	23
2.3 PBMC isolation.....	23
2.4 Maxipreparation of CD19 CAR and CD22 CAR plasmids .....	24
2.5 Lentivirus production in HEK 293SF-PacLV .....	25
2.6 Titration of CD19 and CD22 CAR lentiviruses .....	26
2.7 Isolation of $\gamma\delta$ T cells .....	27
2.8 Production of CAR $\gamma\delta$ T cells .....	27

<b>Chapter 3: Results</b> .....	<b>33</b>
3.1 <i>Aim 1: Production of CD19 scFv-CAR and CD22 sdAb-CAR lentiviruses in HEK 293SF-PacLV</i> .....	33
3.1.1 Both plasmids maintained their integrity upon maxipreparation .....	33
3.1.2 Transfection of HEK 293SF-PacLV with the CD19 CAR plasmid showed higher levels of GFP-expressing cells than with the CD22 CAR plasmid.....	36
3.1.3 Titration of CD19 CAR and CD22 CAR lentiviruses with HEK 293A cells .....	38
3.2 <i>Aim 2: Transduction of <math>\gamma\delta</math> T cells with CD19 or CD22 CAR lentivirus</i> .....	42
3.2.1 Generating CD19 CAR $\gamma\delta$ T cells .....	42
3.2.2 Comparing different protocols of transduction to numerically transduce and expand CAR $\gamma\delta$ T-cell products .....	45
3.2.3 Identification of the optimal MOI .....	46
3.2.4 Generating CD22 CAR $\gamma\delta$ T cells .....	51
 <b>Chapter 4: Discussion</b> .....	 <b>54</b>
4.1 Conclusion and future directions.....	60
4.2 References .....	61
4.3 Contributions of collaborators.....	74
4.4 Supplementary Materials.....	75

## List of Figures and Tables

Figure 1: A second-generation CAR design .....	8
Figure 2: Antitumor activity of $\gamma\delta$ T cells .....	13
Figure 3: Current $\gamma\delta$ T cell-based therapies.....	16
Figure 4: The second-generation CAR constructs .....	21
Figure 5: Production of CD19 scFv-CAR or CD22 sdAb-CAR lentivirus in HEK 293SF-PacLV and titration with HEK 293A cells.....	30
Figure 6: First protocol for generating CD19 CAR and CD22 CAR $\gamma\delta$ T cells .....	31
Figure 7: Second protocol for generating CD19 CAR and CD22 CAR $\gamma\delta$ T cells.....	32
Figure 8: CD19 CAR plasmids isolated from minipreparations .....	34
Figure 9: DNA sequence of the CD19 CAR plasmid .....	35
Figure 10: GFP expression of HEK 293SF-PacLV .....	37
Figure 11: CD19 and CD22 CAR lentiviruses titration on HEK 293A cells.....	40
Figure 12: Transduction of $\gamma\delta$ T cells using the original CD19 CAR lentivirus stock and the first protocol of transduction .....	44
Figure 13: Transduction of $\gamma\delta$ T cells using the original CD19 CAR lentivirus stock and the second protocol of transduction .....	46
Figure 14: Effects of different MOIs by using CD19 CAR lentivirus on the viability and transduction rate of $\gamma\delta$ T cells .....	49
Figure 15: Transduction rate assessed by GFP expression over time .....	50
Figure 16: Effects of different MOIs by using CD22 CAR lentivirus on the viability and transduction rate of $\gamma\delta$ T cells .....	53
Supplemental Figure 1: Feeder cells viability at day 7 post-irradiation.....	75
Table 1: Titrations of CD19 lentivirus stocks .....	41
Table 2: Titrations of CD22 lentivirus stocks .....	41

## List of abbreviations

aAPC	Artificial antigen-presenting cell
$\alpha\beta$	Alpha-beta
ABC-DLBCL	Activated B-cell-like diffuse large B-cell lymphoma
ADC	Antibody-drug conjugate
ADCC	Antibody-dependent cellular cytotoxicity
APC	Antigen-presenting cell
ATC	Adoptive cell therapy
ASIR	Age-standardized incidence rate
ASMR	Age-standardized mortality rate
4-1BBL	4-1BB ligand
B-ALL	B-cell acute lymphoblastic leukemia
BCMA	B-cell maturation antigen
BCR	B-cell receptor
BiTE	Bi-specific T-cell engager
BL	Burkitt lymphoma
B-NHL	Non-Hodgkin B-cell lymphoma
CAR	Chimeric antigen receptor
ccRCC	Clear cell renal cell carcinoma
CHOP	Cyclophosphamide, hydroxydaunorubicin (doxorubicin), oncovin (vincristine), prednisone
CLL/SLL	Chronic lymphocytic leukemia/ Small lymphocytic lymphoma
CMV	Cytomegalovirus
CR	Complete remission
CRC	Colorectal cancer
CRS	Cytokine release syndrome
CSR	Class switch recombination
CTLA-4	Cytotoxic T lymphocyte antigen-4
DLBCL	Diffuse large B-cell lymphoma
DMSO	Dimethyl sulfoxide
EGFR	Epidermal growth factor receptor
ERK	Extracellular signal-regulated kinase
ETP	Early thymic precursor
FasL	Fas ligand
FBS	Fetal bovine serum
FDA	Food and drug administration
FL	Follicular lymphoma
GBM	Glioblastoma multiforme
GCB-DLBCL	Germinal center B-cell-like diffuse large B-cell lymphoma

GFP	Green fluorescent protein
GRB2	Growth factor receptor bound 2
GvHD	Graft versus host disease
HEK	Human embryonic kidney
HIV-1	Human immunodeficiency virus-1
HLA	Human leukocyte antigen
HSCT	Hematopoietic stem cell transplantation
ICANS	Immune effector cell-associated neurotoxicity syndrome
ICI	Immune checkpoint inhibitor
IFN- $\gamma$	Interferon- $\gamma$
IL-2	Interleukin-2
IL-15	Interleukin-15
IPI	International prognostic index
IPP	Isopentenyl pyrophosphate
KIR	Killer immunoglobulin-like receptor
LPL	Lymphoplasmacytic lymphoma
LV	Lentiviral vector
mAb	Monoclonal antibody
MAPK	Mitogen-activated protein kinase
MCL	Mantle cell lymphoma
MHC	Major histocompatibility complex
MM	Multiple myeloma
MOI	Multiplicity of infection
MTD	Maximum tolerated dose
mTOR	Mammalian target of rapamycin
MZL	Marginal zone lymphoma
NCR	Natural cytotoxic receptor
NHL	Non-Hodgkin lymphoma
NK	Natural killer cell
NRC	National Research Council
NSCLC	Non-small cell lung cancer
OHRI	Ottawa Hospital Research Institute
OKT3	Anti-human CD3 antibody
ORR	Overall response rate
pAg	Phosphoantigen
PBMC	Peripheral blood mononuclear cell
PCIC	Pre-Clinical Imaging Core Facility
PD-1	Programmed cell death protein 1
PD-L1	Programmed death ligand 1
PEI	Polyethylenimine
PFA	Paraformaldehyde
PDGFR	Platelet-derived growth factor receptor
PI3K	Phosphoinositide 3-kinase

PMBCL	Primary mediastinal large B-cell lymphoma
RAG	Recombination activator gene
R-ICE	Rituximab, ifosfamide, carboplatin, etoposide
ROS	Reactive oxygen species
r/r	Relapsed and/or refractory
RTK	Receptor tyrosine kinase
sCAR-T cell	Standard CAR-T cell
scFv	Single-chain variable fragment
sdAb	Single-domain antibody
SLE	Systemic lupus erythematosus
SOP	Standard operating procedure
TAA	Tumor-associated antigen
TCR	T-cell receptor
TLR	Toll-like receptor
TM	Transmembrane domain
TNBC	Triple negative breast cancer
TNF	Tumor necrosis factor
TOI	Transgene of interest
TRAIL	TNF-related apoptosis-inducing ligand
Treg	Regulatory T cell
TRM	Tissue-resident memory
VSV-G	Vesicular stomatitis virus G protein
WHO	World Health Organisation
ZOL	Zoledronic acid

## **1. Introduction**

### **1.1 Cancer**

Cancer is a leading cause of death worldwide, accounting for nearly 10 million deaths and 20 million new cases in 2022, according to the World Health Organisation (WHO). In 2050, it is estimated that there will be almost 19 million cancer related deaths, and more than 35 million people worldwide will be diagnosed with cancer. In Canada, nearly half of the population, 45%, will develop a cancer, and about one quarter of Canadians are expected to die from the disease<sup>1</sup>. Although the age-standardized incidence rate (ASIR) and age-standardized mortality rate (ASMR) are expected to decline for several common cancers, such as lung cancer, colorectal cancer, and prostate cancer, these rates are expected to increase for other cancers, including liver and intrahepatic bile duct cancer, kidney cancer, melanoma, and non-Hodgkin lymphoma<sup>2</sup>.

Cancer is defined as a complex disease driven by genetic and epigenetic dysregulations, resulting in uncontrollable cell growth and proliferation<sup>3</sup>. In 2000, Douglas Hanahan and Robert Weinberg have identified six physiological phenomena happening during the development of human tumors. They defined these as hallmarks of cancer, which include sustaining proliferative signaling, evading growth suppressors, resisting cell death (apoptosis), enabling replicative potential, inducing angiogenesis, and activating invasion and metastasis<sup>4</sup>. In 2011, two new hallmarks have been added to this list: reprogramming of energy metabolism and evading immune destruction<sup>5</sup>. In addition, recruited normal cells contribute to the multistep of cancer progression since they acquire the hallmark traits and thus create the ‘‘tumor microenvironment’’ (TME)<sup>4</sup>.

### 1.1.1 Cancer metabolism

Cancer cells are self-sufficient in growth signals. Indeed, they have an increased amount of growth factors that induce two key signaling pathways: the mitogen-activated protein kinase (MAPK)/extracellular signal-regulated kinase (ERK) pathway and the phosphoinositide 3-kinase (PI3K) pathway<sup>6</sup>.

For instance, the MAPK/ERK and PI3K signaling pathways are amplified in human cancers with mutated RAS GTPase. In fact, RAS gene is the most mutated gene in human cancers. One out of four cancers have activating mutations in RAS oncogenes. The RAS family encodes small GTPases, including KRAS, NRAS and HRAS, that play a central role in cell survival, differentiation and proliferation. Approximately 30% of all human cancers are driven by RAS oncoproteins, including 40%-50% of colorectal cancers and over 90% of pancreatic cancers<sup>7,8</sup>. In normal RAS pathway, a growth factor binding to receptor tyrosine kinase (RTK), such as the stem cell factor receptor KIT, epidermal growth factor receptor (EGFR) or platelet-derived growth factor receptor (PDGFR), leads to the autophosphorylation of the receptor and recruitment of the adaptor protein growth factor receptor bound 2 (GRB2). In turn, GRB2 recruits the guanine exchange factor SOS1/2, activating RAS. RAS can then self-inactivate by cleaving the phosphate group on the GTP, which converts it to its inactive state RAS-GDP<sup>9</sup>. However, mutations in RAS genes, like KRAS, favour GTP binding and lead to constitutive activation of RAS.

On one hand, a main effector of the RAS pathway is the RAF/MEK/ERK cascade that leads to the transcription of different target genes, such as FOS, MYC, MDM2, MITF, implicated in cell proliferation, survival and cell cycle progression<sup>10</sup>. On the other hand, PI3K pathway is known to activate the mammalian target of rapamycin (mTOR), a serine/threonine kinase, which stimulates cap-dependant mRNA translation and cell growth, while inhibiting catabolic reaction mediated by

autophagy<sup>11</sup>. The PI3K-mTOR signaling pathway represents a major regulator of cell proliferation, survival and angiogenesis. As well as uncontrolled proliferation, the mutagenic RAS oncogene has been implicated in tumor immune resistance by causing upregulation of programmed death ligand 1 (PD-L1)<sup>12</sup>. RAS oncogenes are present in high proportions in many cancers: myeloid leukemia (~30%), lung carcinoma (~40%), sporadic colorectal (~50%) and pancreatic cancer (~90%)<sup>8</sup>.

### **1.1.2 Cancer treatments**

Three traditional treatments are widely used for treating cancers, which include surgery, radiotherapy and chemotherapy. Surgery implies the physical removal of cancerous tissues whereas radiotherapy and chemotherapy use high doses of radiation or cytotoxic agents, respectively. Radiotherapy aims to damage DNA, while chemotherapy aims to stop cancer cells from growing and dividing, which eventually leads to their death<sup>13,14,15</sup>. Although these methods are effective in most cases for early-stage cancer, they suffer from many limitations, such as a lack of tumor specificity, toxicity toward healthy tissues, and the development of drug resistance, leading to disease recurrence and poor outcomes. As a result, there is an urgent need to develop more targeted and less toxic strategies. Immunotherapy, which harnesses the body's own immune system to recognize and eliminate cancer cells, has emerged as a promising fourth pillar of cancer treatment. They comprise approaches known to reactivate the host's immunity, such as myeloid depletion, cytokine therapies and checkpoint inhibitors, while others stimulate a direct antitumor response and include cancer vaccines, oncolytic viruses, targeted antibodies, gene therapy and adoptive cell therapy<sup>16</sup>.

## 1.2 B-cell non-Hodgkin lymphomas

Non-Hodgkin lymphomas (NHLs) are the most common hematological malignancies worldwide, accounting for nearly 3% of cancer related deaths. In 2022, there were an estimated 553,389 new cases of cancer and 250,679 cancer related deaths, according to WHO. NHLs can either be derived from T-cell or B-cell. Non-Hodgkin B-cell lymphomas (B-NHLs) constitute a heterogeneous group of neoplasms characterized by the uncontrolled proliferation of B lymphocytes, which affects the lymphatic system, especially the lymph nodes. They can affect any organ and manifest themselves through distinct clinical symptoms, ranging from asymptomatic to indolent, or very aggressive cases<sup>17</sup>. The most common symptom in patients with B-NHL is adenopathy, which is the inflammation of the lymph nodes. Swollen lymph nodes usually appear in the neck, armpits or groin folds, but can also appear in the mediastinal, area between the lungs, and the abdomen. The adenopathy can be either localized or generalized. Localized adenopathy refers to a condition affecting continuous groups of lymph nodes, while lymphadenopathy refers to a condition affecting two or more non-contiguous areas. The uncontrolled proliferation of B lymphocytes in B-NHLs increases the lymph nodes size, which affects their functions. Indeed, lymph nodes function as an antigen filter for the body's reticuloendothelial system. They sequentially expose B lymphocytes, T lymphocytes and macrophages to an afferent extracellular fluid, allowing the immune system to recognize and react to potential foreign antigens<sup>18</sup>.

Among B-NHLs, aggressive subtypes include diffuse large B-cell lymphoma (DLBCL) (31%), mantle cell lymphoma (MCL) (6%), Burkitt lymphoma (BL) (2%) and primary mediastinal large B-cell lymphoma (PMBCL) (2%). On the other hand, indolent cases comprise follicular lymphoma (FL) (22%), marginal zone lymphoma (MZL) (8%), chronic lymphocytic leukemia/small lymphocytic lymphoma (CLL/SLL) (6%) and lymphoplasmacytic lymphoma (LPL) (1%)<sup>19</sup>. The

causes of B-NHLs are complex, involving genetic and metabolomic factors<sup>19</sup>. For instance, the two subtypes of DLBCL, termed activated B-cell-like (ABC) and germinal center B-cell-like (GCB) DLBCL, are characterized by distinct gene expression profile, genetic aberrations and outcomes. Most DLBCL cases involve genetic alterations in B-cell receptor's key components (BCR) or its downstream signaling effectors. Consequently, signaling pathways such as PI3K, MAPK, NF- $\kappa$ B and/or NFAT pathways are dysregulated<sup>20</sup>.

To date, although several treatment options are available for B-NHLs, these lymphomas often become refractory or relapse after chemotherapy. The International Prognostic Index (IPI) has been created to evaluate and predict outcome for patients with aggressive subtypes of B-NHL, like DLBCL. Poor prognosis factors include age 60 or older, advanced stage disease (stage 3 or 4), an aggressive type of B-NHL, and widespread or generalized lymphoma. Nevertheless, numerous options exist for treating DLBCL; chemotherapy in combination with targeted therapy using rituximab, hematopoietic stem cell transplantation (HSCT), radiotherapy and immunotherapy<sup>21,22</sup>.

For instance, Rituximab, a humanized glycoengineered anti-CD20 monoclonal antibody (mAb), was approved by the Food and Drug Administration (FDA) for relapse/refractory (r/r) indolent B-NHLs in 1997. Rituximab became the standard of care, in combination with chemotherapy and CHOP (cyclophosphamide, doxorubicin, vincristine, prednisone) treatment, for FL, DLBCL and CCL<sup>23,24,25</sup>. Unfortunately, more than 30% of DLBCL will ultimately relapse<sup>24</sup>. New therapies need to be developed to treat DLBCL. Ibrutinib, a B-cell receptor inhibitor, has shown efficacy against activated B-cell-like (ABC)-DLBCL as a single agent and in combination with the R-ICE (rituximab, ifosfamide, carboplatin and etoposide) chemotherapy treatment<sup>26,27</sup>. Pembrolizumab, an immune checkpoint inhibitor (ICI) binding the programmed cell death protein 1 (PD-1) receptor expressed on cancer cells and thus removing the protection from T-cell recognition, has shown

efficacy in PMBCL with overall response rates (ORR) of 48% and 45%, in phase I and phase II clinical trials, respectively<sup>28,29,30</sup>. Obinotuzumab, a glycoengineered anti-CD20 mAb enhancing Fc-receptor affinity, has shown efficacy in rituximab-sensitive/rituximab-resistant cell lines<sup>31</sup>. A new class of biologic drugs is antibody-drug conjugate (ADC), which consists of small anticancer molecule that are attached to an antibody. Inotuzumab, a humanized anti-CD22 antibody conjugated with the cytotoxic agent calicheamicin, has shown activity in B-NHLs as a single agent and in combination with rituximab<sup>32</sup>. Moreover, Blinatumomab, a bi-specific T-cell engager (BiTE), which engage patient's own cytotoxic T cells for directed lysis toward cancer cells, has proven highly effective in phase II clinical trial with ORR of 43% in DLBCL<sup>33,34</sup>. Finally, the most recent curative option for treating relapse/refractory B-NHL (r/r B-NHL) is immunotherapy using adoptive cell transfer (ACT), more specifically chimeric antigen receptor (CAR)-T cell therapy. Four CAR-T cell products have been FDA approved for LBCL, FL and MCL: *Axicabtagene ciroleucel* (NCT03153462), *Tisagenlecleucel* (NCT03601442), *Brexucabtagene autoleucel* (NCT05776134) and *Lisocabtagene maraleucel* (NCT06313996).

### **1.3 Adoptive cell therapy**

During past decades, progress has been made in cancer immunotherapies. ACTs have emerged as a safer treatment option for cancer than chemotherapy. Among these, CAR-T cell therapy has attracted growing interest in the treatment of various malignancies and represents the most advanced technology to date. CAR-T cell therapies, in which a patient's own immune cells are genetically engineered *ex vivo* to express a receptor that binds tumor-associated antigen (TAA), have shown efficacy in treating hematologic malignancies<sup>35,36</sup>. CARs are composed of an extracellular antigen-binding domain, a hinge region, a transmembrane domain, and one or more

intracellular signaling domains<sup>37</sup> (**Fig.1A**). Most CAR constructs are designed from human or murine antibodies converted into a single-chain variable fragment (scFv) which is then combined with the constant region of the T-cell receptor (TCR), the CD3- $\zeta$  domain. The scFv domain has the same specificity and affinity as the natural Fab fragment of immunoglobulin G (IgG). This approach therefore produces CAR-T cells with antibody-type specificity<sup>38</sup>. Once the antigen binding domain of the CAR binds to the TAA on the surface of the tumor cell, the intracellular CD3 $\zeta$  domain initiates T-cell activation. This leads to downstream signaling cascades that trigger cytotoxic functions including the release of perforins and granzymes, as well as the production of pro-inflammatory cytokines (**Fig.1B**). CARs also require at least one costimulatory domain, CD28 or 4-1BB, to improve the expansion, persistence and activity of CAR-T cells (i.e cytotoxicity of the targeted cell). Both CAR constructs, equipped with CD28 or 4-1BB costimulatory domain, are effective for treating DLBCL<sup>39,40,41,42</sup>.

An *in vivo* study comparing the antitumor effects of CD28 and 4-1BB-based CD19 CAR-T in lymphoma-bearing mice has shown that adoptive transfer of both CAR-T cell products resulted in complete tumor regression when the administered dose was  $3 \times 10^6$  CAR-T cells. However, when the administered dose was lower,  $8 \times 10^5$  CAR-T cells, the CD28-based CD19 CAR-T cells had lower antitumor activity<sup>43</sup>. Moreover, analysis of CAR stimulation-induced signaling events revealed that stimulation of CD28 CARs activated rapid changes in protein phosphorylation, which correlated with an effector T-cell like phenotype, while 4-1BB CARs preferentially expressed T-cell memory-associated genes and had a more sustained anti-tumor activity against tumors. 4-1BB-based CD19 CAR-T cells were thus more potent than CD28-based CD19 CAR-T cells at eradicating lymphoma *in vivo*<sup>43</sup>.

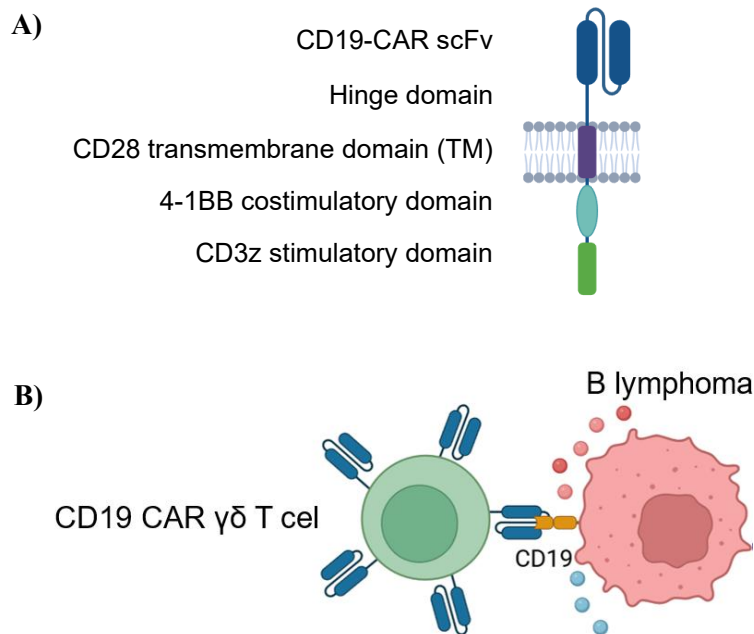


**Figure 1: A second-generation CAR design.** (A) CAR are synthetic receptors that are composed of an antigen-binding domain, a hinge region, a transmembrane domain, and one or more intracellular signaling domains. (B) The antigen binding domain of the CAR recognizes and binds to the tumor-associated antigen (TAA) on the tumor cell surface. This binding activates CAR T cell signaling through the CD3 $\zeta$  domain which initiates cytotoxic functions.

During past decades, alpha-beta ( $\alpha\beta$ ) CAR-T cell therapies targeting CD19 or B-cell maturation antigen (BCMA) have shown remarkable success in treating chemotherapy-refractory patients with leukemia, lymphoma, or myeloma<sup>44</sup>. CD19 is a B-cell-restricted antigen that is highly expressed on B cells of patients with B-NHL. The recent approval of four CD19 CAR-T cell products and two BCMA CAR-T cell products in B-cell malignancies represents a breakthrough in CAR-T cell immunotherapy<sup>45</sup>. Current FDA-approved CAR  $\alpha\beta$  T cells targeting CD19 comprise an anti-CD19 scFv fused to either CD28/CD3 or 4-1BB/CD3 signaling domains<sup>40,46,47,48,49</sup>.

While CAR  $\alpha\beta$  T-cell therapies have marked a major breakthrough in cancer treatment, their clinical application remains limited by key challenges. These include antigen escape, ‘‘on-target, off-tumor’’ effect, cytokine toxicity that often leads to neurotoxicity, as well as graft versus host

disease (GvHD)<sup>50</sup>. Moreover, these therapies have limited tumor trafficking and infiltration due to the immunosuppressive TME. Therefore, they remain inconclusive in the context of solid tumors<sup>51</sup>. Furthermore, most cancers have evolved strategies to escape human leukocyte antigen (HLA)-restricted  $\alpha\beta$  T cells mediated immune recognition by downregulating the expression of HLA at their cell surface<sup>52</sup>.  $\gamma\delta$  T cells, another subset of T lymphocytes, have therefore emerged as a promising candidate for adoptive immunotherapies since they do not require HLA-recognition to be activated and thus, avoid the graft-versus-host effects of HLA-mismatched  $\alpha\beta$  T cells.  $\gamma\delta$  T cells are known to exert natural anti-tumor responses and have been safely used in haploidentical transplants<sup>53</sup>.

#### **1.4 Discovery of $\gamma\delta$ T cells**

In 1984, Tonegawa's group identified two classes of cDNA clones with sequence homology to immunoglobulin variable and constant region genes. These cDNA sequences, which were specifically rearranged and expressed in T cells, encoded the  $\alpha$  and  $\beta$  chains of the TCR, thereby elucidating the complete primary structure of the  $\alpha\beta$  TCR<sup>54</sup>. In 1986, Brenner's and Bank's team identified a novel population of human lymphocytes that expressed a T3 glycoprotein without the  $\alpha$  and  $\beta$  TCR chains<sup>55,56</sup>. Chemical crosslinking experiments revealed that T3-associated polypeptides included a product of the  $\gamma$  TCR gene and further analysis suggested the existence of a fourth TCR chain that they named the  $\delta$  TCR chain. In 1987, Weiss's laboratory successfully cloned and sequenced the  $\delta$  TCR chain<sup>57</sup>. Since then,  $\gamma\delta$  T cells have attracted interest of numerous researchers.

$\gamma\delta$  T cells development is occurring in the thymus of all jawed vertebrates during ontogeny. Hematopoietic stem cells first move from the bone marrow to the thymus. Once in the thymus, the stem cells differentiate into a common progenitor population called “early thymic precursors” (ETPs), which gives rise to both  $\alpha\beta$  and  $\gamma\delta$  T cell lineages<sup>58</sup>. ETPs go through four stages of thymocyte development, DN1, DN2, DN3 and DN4, and each stage is distinguished by specific surface markers. Indeed, thymocytes in DN1 are double negative (CD4<sup>-</sup>, CD8<sup>-</sup>) and characterized by the presence of CD44, whereas thymocytes in DN2 are CD117<sup>+</sup>, CD25<sup>+</sup> and CD44<sup>+</sup>, and thymocytes in DN3 are CD117<sup>low</sup>, CD25<sup>+</sup> and CD44<sup>low</sup><sup>59,60</sup>. During thymocyte transition from DN1 and DN2, TCR formation and differentiation are induced by IL2RA gene expression. Then, gene rearrangement of individual TCR chains starts between the DN2 and DN3 stages, which include the  $\gamma\delta$  TCR chains and the  $\beta$  chain as well as partially the  $\alpha$  chain<sup>61</sup>. Mechanisms by which the lymphocyte differentiation, whether towards  $\alpha\beta$  or  $\gamma\delta$  T cells, is orchestrated are still unclear.

Nevertheless, two theories have been proposed to explain the choice of lymphocyte differentiation: the stochastic model and the instructive model<sup>62</sup>. The stochastic model relies on the idea that each cell belongs to a predetermined group and only the ones that meet their cell fate survive. This process would happen by rearranging *Terg* and *Tcrd* to create  $\gamma\delta$  TCR or rearranging *Tcrb* to create pre-TCR. The second approach, the instructive model, is rather based on a tightly controlled transition of pre-TCR into  $\alpha\beta$  or  $\gamma\delta$  receptor. Finally, a recent model, involving signal strength, has been suggested. Notch receptor family, known to regulate *Il2ra*, *Gata3*, *Bcl11b*, *Notch3* and *Trca*, cooperates with Jagged ligand family. For instance, Jagged2 and Notch1 combination favors  $\alpha\beta$  chains whereas Jagged2 and Notch3 combination promotes  $\gamma\delta$  chains. The process determining ETPs fate toward  $\gamma\delta$  T cells is complex, and despite many studies, further research is needed to elucidate the signaling network<sup>63</sup>.

### 1.4.1 $\gamma\delta$ T cells

$\gamma\delta$  T cells play a central role in the immune response against stressed and abnormal cells, such as virus-infected cells and cancer cells. Only 0.05-5% of T cells circulating in the blood, lymph and secondary tissues are  $\gamma\delta$  T cells. Like  $\alpha\beta$  T cells,  $\gamma\delta$  T cells generate their specific TCRs via V(D)J recombination mediated by the recombination-activating gene (RAG), resulting in theoretical diversity of up to  $10^{17}$  possible TCR combinations<sup>64</sup>.  $\gamma\delta$  T cells express TCRs, which are multimeric transmembrane complexes comprised of a clonotypic heterodimer TCR $\gamma$ /TCR $\delta$ , two CD3 dimers (CD3 $\gamma\epsilon$  and/or CD3 $\delta\epsilon$ ) and a CD3 $\zeta\zeta$  dimer. Based on their TCR  $\delta$  chain,  $\gamma\delta$  T cells are divided into three subsets: V $\delta$ 1, V $\delta$ 2 and V $\delta$ 1/2neg, with the latter predominantly comprising V $\delta$ 3 T cells. Most  $\gamma\delta$  T cells circulating in the blood are V $\delta$ 2 T cells, more specifically V $\gamma$ 9V $\delta$ 2 T cells, while V $\delta$ 1 T cells are mostly found in epithelial and mucosal tissues. V $\delta$ 3 T cell subsets are enriched in the liver and gut. Combinations of  $\gamma$  and  $\delta$  chains are characteristic of specific tissues. For example, V $\delta$ 1 is associated with a greater number of  $\gamma$  chains than V $\delta$ 2 and represents the most abundant subset in the liver (V $\gamma$ 4), skin (V $\gamma$ 4, V $\gamma$ 5, V $\gamma$ 6), spleen (V $\gamma$ 4) and epithelium (V $\gamma$ 7)<sup>61</sup>. In the peripheral blood, at the embryonic stage, V $\delta$ 2 proportions dominate over V $\delta$ 1 T cell subsets. At birth, a drastic decrease in total  $\gamma\delta$  T cells occurs. Later, around the age of 30, V $\delta$ 2 T cells become more prevalent than V $\delta$ 1 T cells, followed by a second decline in the  $\gamma\delta$  T cell population at about age 45. Finally, in later adulthood, V $\delta$ 1 T cells predominate<sup>61</sup>. It is worth noting that the ratio between V $\delta$ 1 and V $\delta$ 2 varies depending on infections and cancer diseases, as well as individual human development.

$\gamma\delta$  T cells have features of both adaptive and innate immunity, positioning them at the intersection of the two systems. It has been shown that they can be activated in both TCR-dependant and independent manners. Indeed, in addition to their TCRs, they express a variety of

innate receptors primarily associated with natural killer cells (NK). The innate-like properties of  $\gamma\delta$  T cells mirror those of NK cells. They share activating and inhibitory killer immunoglobulin-like receptors (KIRs), C-type lectin-like receptors (NKG2s) and natural cytotoxicity receptors (NCRs) with NK cells<sup>65,66</sup>. Moreover, their ability to recognize their target antigens through the TCRs, independently of HLA restriction, allows them to recognize a wide range of structurally different ligands<sup>67</sup>.

$\gamma\delta$  T cells recognize and eliminate cancer cells by engaging their TCRs and/or NK receptors with their respective ligands on the surface of cancer cells, triggering their cytotoxic effector functions and the production of pro-inflammatory cytokines (**Fig.2**). These ligands can either be membrane proteins, phospholipids, soluble proteins, stress molecules, heat shock proteins or small peptides<sup>68</sup>. Phosphorylated compounds known as phosphoantigens (pAgs) are the best characterized ligands for  $\gamma\delta$  T cells. Their recognition, however, is restricted to the subset expressing the V $\gamma$ 9V $\delta$ 2 TCR, referred to as V $\gamma$ 9V $\delta$ 2 T cells. In some cancer cells, the dysregulation of mevalonate pathway leads to the accumulation of isopentenyl pyrophosphate (IPP), a type of PAg. IPP binding to the intracellular B30.2 domain of BTN3A1 induces conformational changes in its extracellular domain, thereby enabling recognition and activation of  $\gamma\delta$  T cells through the V $\gamma$ 9V $\delta$ 2 TCR<sup>69</sup>.

$\gamma\delta$  T cells can induce direct cancer cell killing by the granule exocytosis pathway or by the expression of tumor necrosis factors (TNFs), such as the TNF-related apoptosis-inducing ligand (TRAIL) and the FAS ligand (FASL) that bind TRAIL R1/R2 and FAS, respectively<sup>70-75</sup>. In addition,  $\gamma\delta$  T cells can kill tumor cells by the antibody-dependent cellular cytotoxicity (ADCC) mechanism, upon treatment with tumor-specific antibodies. Once  $\gamma\delta$  T cells are activated, they increase the expression of their CD16 receptor, also called Fc $\gamma$ III, which can then bind antibodies that have been coated on tumor cells beforehand<sup>76-79</sup>. Moreover,  $\gamma\delta$  T cells can bind MICA and

MICB, which are highly polymorphic stress induced molecules for immune cell activation, through NKG2D<sup>80-83</sup>. They can also trigger antitumor responses by antigen-presenting cell (APC) functions, through their HLA-DR, CD80/86 and 4-1BB ligand (4-1BBL), as well as by producing interferon- $\gamma$  (IFN- $\gamma$ )<sup>84</sup>. Alternatively,  $\gamma\delta$  T cells induce a class switch recombination (CSR), a key process where B cells change the type of antibody they produce, which promotes a humoral response<sup>85</sup>.  $\gamma\delta$  T cells are therefore uniquely equipped with multiple independent recognition pathways to sense and kill abnormal cells, which makes them ideal candidates for use in immunotherapy.

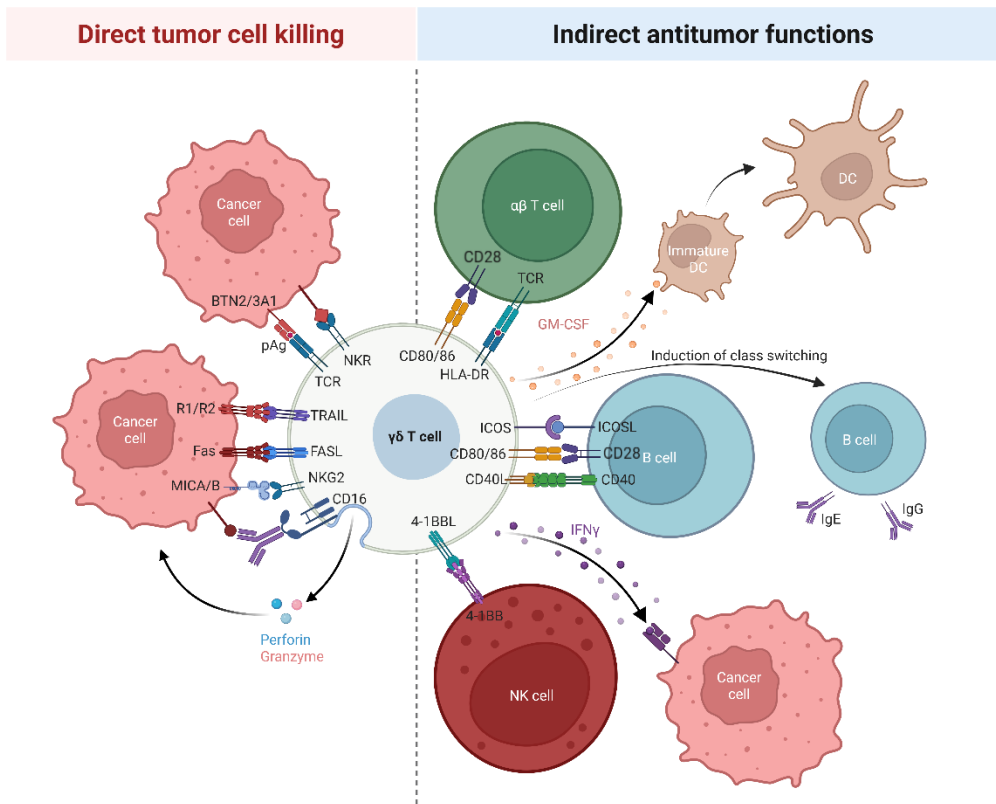


**Figure 2: Antitumor activity of  $\gamma\delta$  T cells.**  $\gamma\delta$  T cells exhibit remarkable functional plasticity. Their ability to recognize their target antigens via TCRs, independently of HLA restriction, enables them to recognize a wide range of structurally different ligands and thus ensure direct tumor cell killing. They also induce indirect tumor cell destruction through their APC functions, by priming  $\alpha\beta$  T cells and regulating NK cells. Adapted from Silva-Santos B, Mensurado S, Coffelt SB's review (2019)<sup>84</sup>.

## 1.5 Current perspective of $\gamma\delta$ T cell-based therapies

$\gamma\delta$  T cells expressing V $\gamma$ 9V $\delta$ 2 TCRs are known to respond to pAgs that are overexpressed in some cancer cells. Therefore, multiple groups have tested the therapeutic potential of V $\gamma$ 9V $\delta$ 2 T cells in human cohorts either by systemic activation, using aminobisphosphonates, or adoptive cell transfer following  $\gamma\delta$  T-cell activation and expansion *in vitro* with aminobisphosphonates or synthetic pAgs. Both methods demonstrated outstanding safety profiles of V $\gamma$ 9V $\delta$ 2 T cells. However,  $\gamma\delta$  T-cell therapies have shown a lower clinical efficacy than expected in many trials<sup>85-90</sup>. Multiple reasons could explain these low response rates, including low variability in the V $\gamma$ 9V $\delta$ 2 TCR repertoire and the exhaustion and dysfunction of chronically activated  $\gamma\delta$  T cells. The first clinical trial involving  $\gamma\delta$  T cells was in 2011 (NCT01404702) and studied the effect of zoledronic acid (ZOL) combined with interleukin-2 (IL-2) against neuroblastoma. This trial showed limited efficacy. Nevertheless, a phase 1 study (NCT05400603) is currently investigating the maximum tolerated dose (MTD) of allogeneic expanded  $\gamma\delta$  T cells, in combination with dinutuximab, temozolomide, irinotecan, and zoledronate, by children with neuroblastoma or refractory/relapsed osteosarcoma<sup>91</sup>.

New strategies have emerged to overcome these limitations, involving both V $\delta$ 1 and V $\delta$ 2  $\gamma\delta$  T cell subsets (**Fig.3**). They can be categorized into three groups:  $\gamma\delta$  T cell-stimulating therapies, combination therapies with other immune components and cell engineering therapies involving genetically modified  $\gamma\delta$  T cells.

$\gamma\delta$  T cell-stimulating therapies comprise ACTs and immunotherapies using bisphosphonate, NKG2D agonists, or cytokines such as IL-2 and IL-15. This approach consists of activating, expanding and enhancing the natural cytotoxic properties of  $\gamma\delta$  T cells with the goal to improve antigen recognition and thus, cancer cell killing. Combination therapies aim to enhance therapeutic

efficacy. For example, combining  $\gamma\delta$  T cells with mAbs such as rituximab to foster ADCC response, with toll-like receptor (TLRs) agonists to trigger dendritic cell activation, or with immune checkpoint inhibitors (ICIs) targeting PD-1 or cytotoxic T lymphocyte antigen-4 (CTLA-4).

Finally, CAR-T cell therapies are the most advanced technology to date among immunotherapies and aim to combine antibody-like high-affinity antigen with TCR signaling, enabling more precise and effective recognition of cancer cells<sup>92,93</sup>. Even though since 2017, some CAR  $\alpha\beta$  T-cell therapies have been approved and have led to durable complete responses for patients with B-cell leukemia or lymphoma, many patients have relapsed.  $\gamma\delta$  T cells are promising candidates for “off-the-shelf” CAR-T cell therapy, not only because they are HLA-independent and therefore do not induce GvHD, but also because they do not induce cytokine storms, a phenomenon that has been observed in  $\alpha\beta$  T cell-based therapies. As of now, there are only 8 active clinical trials on CAR  $\gamma\delta$  T cells, according to ClinicalTrials.gov; (NCT04735471), (NCT06375993), (NCT07100873), (NCT06106893), (NCT05302037), (NCT06375993), (NCT06480565) and (NCT06150885).

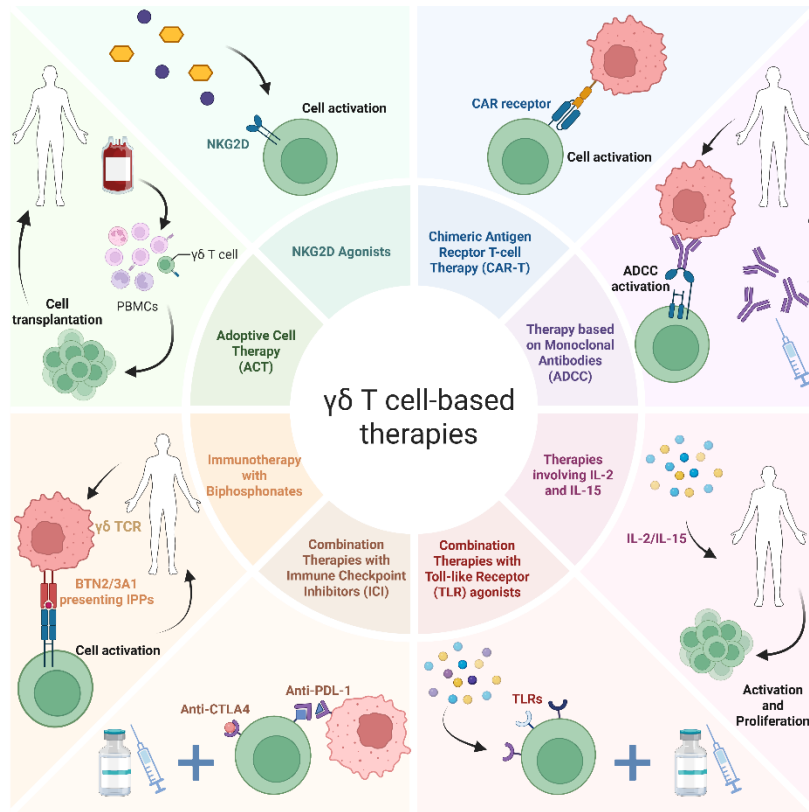


**Figure 3: Current  $\gamma\delta$  T cell-based therapies.** Schematic showing novel therapeutic approaches using  $\gamma\delta$  T cells alone or in combination; ACTs, NKG2D agonists, CAR-Ts, mAbs, cytokines, TLRs, ICIs and bisphosphonates. Adapted from Biały S, Bogunia-Kubik K's review (2025)<sup>61</sup>.

## 1.6 Generating CAR $\gamma\delta$ T cells

Previous studies have shown that  $\gamma\delta$  T cells can robustly kill a wide range of tumor cells and that their infiltration, into the tumor, is the most positive prognostic marker among 22 different immune cell populations in 39 cancer types<sup>94</sup>. Thus, engineering CAR  $\gamma\delta$  T cells against a specific surface-exposed tumor antigen has emerged as a promising therapeutic approach. In 2004, Rossig's laboratory performed the first *in vitro* study to evaluate the potential of  $\gamma\delta$  T cells to exert tumor-specific effector functions by using zoledronate and first generation CAR<sup>95</sup>. Transduced  $\gamma\delta$  T cells with either 14.GD2 CAR or CD19 CAR efficiently recognized and lysed the cell lines expressing

their respective antigen. This study thus confirmed that CAR  $\gamma\delta$  T cells enhance the natural antitumor functions of  $\gamma\delta$  T cells.

Moreover, in 2013, Deniger's laboratory engineered  $\gamma\delta$  T cells with second generation CAR containing CD28 costimulatory domain and successfully expanded CAR  $\gamma\delta$  T cells *in vitro* to clinically relevant numbers using CD19<sup>+</sup> artificial antigen-presenting cells (aAPC)<sup>96</sup>. In 2020, Besser's laboratory generated a CD19 CAR  $\gamma\delta$  T-cell product and compared its efficacy *in vitro* and *in vivo* with standard CAR-T cells (sCAR-T cells). CD19 CAR  $\gamma\delta$  T cells showed similar transduction efficacy and cytotoxicity against Nalm6, a CD19<sup>+</sup> target cell line, *in vitro*, compared to the standard CAR-T cells. *In vivo*, CD19 CAR  $\gamma\delta$  T cells showed inferior anti-tumor effect and persistence, according to the leukemic burden in the bone marrow and the number of CAR  $\gamma\delta$  T cells found in spleen and bone marrow of xenograft NSG mice, in comparison with sCAR-T cells<sup>97</sup>. Nevertheless, Besser's group has demonstrated that CAR  $\gamma\delta$  T cells are effective effector cells for targeting leukemia-specific antigen as well as antigen escape variants in allogeneic settings *in vivo*<sup>97</sup>.

Finally, in 2021, Hayes' laboratory has initiated Phase 1 clinical trial to test Anti-CD20 CAR<sup>+</sup> V $\delta$ 1  $\gamma\delta$  T cells against B-cell malignancies in 34 patients. The CAR construct consists of a novel human anti-CD20 monoclonal antibody (3H7 mAb) linked to CD8 $\alpha$  hinge and transmembrane domains, as well as the 4-1BB and CD3 $\zeta$  signaling domains. The Phase 1 has been successfully completed in June of this year. Despite no results have been published as of now, the results of their preclinical studies were published in 2022<sup>98</sup>. The CD20 CAR  $\gamma\delta$  T cells exhibited tumor killing, pro-inflammatory cytokine production *in vitro* and reduced tumor growth of B-cell lymphoma xenografts in NSG mice *in vivo*. Phenotypic analyses revealed that CD20 CAR<sup>+</sup> V $\delta$ 1  $\gamma\delta$  T cells co-express marker associated with both naïve (CD27, CD45RA, CD62L) and memory

(CD95, CD45RO) T cell phenotypes. Transcriptomic analyses showed upregulated genes involved in T-cell activation, cytotoxic function and innate immunity, which reveal that both innate and adaptive immune mechanisms are activated by CD20 CAR<sup>+</sup> V $\delta$ 1  $\gamma\delta$  T cells. Interleukin-15 (IL-15) and interleukin-2 (IL-2) potentiate the antitumor features of  $\gamma\delta$  T cells. It is noteworthy that mice lack species-specific homeostatic cytokines such as IL-2 and IL-15, which are required to maintain CAR-T cell persistence. Thus, human IL-2 is administered in combination with CD20 CAR<sup>+</sup> V $\delta$ 1  $\gamma\delta$  T cells to support their expansion and persistence in NSG mice<sup>98</sup>.

Despite the promising properties of  $\gamma\delta$  T cells, it is still a challenge to understand how to potentiate their antitumor cytotoxicity and their persistence. Another challenge is that cancer cells have evolved different mechanisms for immune escape and tolerance induction using various pathways. These strategies include upregulation of PD1 expression and secretion of inhibitory molecules, like TGF- $\beta$ , IL-10 and arginase-1, as well as reactive oxygen species (ROS), by regulatory T (Treg) cells and neutrophils, respectively<sup>99,100,101</sup>. More research and data are therefore necessary to harvest the therapeutic benefits of CAR  $\gamma\delta$  T cells.

## 1.7 Hypothesis and aims

Studies reveal increased tumor-specific toxicity and safety of CAR  $\gamma\delta$  T cells compared to natural  $\gamma\delta$  T cells against solid and liquid tumors<sup>102</sup>. In 2023, a study has generated a camelid nanobody-based CD19 CAR  $\alpha\beta$  T-cell product and compared it with its murine scFv-based counterpart<sup>103</sup>. The two designs showed comparable expansion rate as well as similar cytolytic reactions against CD19<sup>+</sup> cell lines. Moreover, both designs, the nanobody-CAR-T and the scFv-CAR-T, secreted significantly higher and similar levels of IFN- $\gamma$ , IL-2 and TNF- $\alpha$  upon stimulation with Ramos and Raji cell lines compared to those that were cultured alone or with K562 cell line.

Clinical studies to date have demonstrated that CAR-T cell therapies targeting CD22 have safety and toxicity profiles similar to those of CD19 CAR-Ts. In 2024, McComb et al. have initiated a Phase 1 clinical trial to test  $\alpha\beta$  T cells expressing a camelid CD22-targeted CAR nanobody against B-cell malignancies<sup>104</sup>. In their preclinical study, they found that constructs with a CD8 transmembrane (TM) domain had more sustained CAR expression and higher level of activation compared to those having a CD28 TM domain<sup>104</sup>. Among several nanobody-based CD22 CAR-T cell designs, they have identified that the 1ug36-CD22sdCAR construct, binding the 6<sup>th</sup> immunoglobulin-like subdomain of the CD22 antigen, represents the most promising candidate. Their CD22sdCAR construct surpassed the FMC63-scFv CD19 CAR construct, but not the benchmark m971 CD22 CAR construct. These constructs are composed of either an anti-CD19 (FMC63-scFv) or an anti-CD22 (m971-scFv) linked to a CD8 hinge and transmembrane domains, and a 4-1BB and CD3 $\zeta$  signaling domains. Nevertheless, CD22sdCAR showed higher on-target CD22 response activity with lower off-target response compared to the m971 CAR-T<sup>104</sup>.

Recent studies have highlighted the critical role of  $\gamma\delta$  T cell diversity and polyspecificity in mediating robust immune responses against a broad spectrum of antigens and immune

challenges<sup>105</sup>. Thus, our lab has developed a protocol for the *in vitro* expansion of polyclonal  $\gamma\delta$  T cells for preclinical cancer immunotherapy studies. This protocol achieves a high expansion rate, generating millions of cells from just a few thousands, and the resulting cells exhibit exceptionally long *in vivo* persistence in mice. Building on this platform, the primary objective of my research is to develop, as a proof of concept, two engineered human  $\gamma\delta$  T-cell products against B-lymphomas: one expressing a CD19 scFv-CAR and the other a CD22 sdAb-CAR, in collaboration with the McComb group (**Fig.4**). The CD19 CAR construct comprises a murine anti-CD19 scFv with a CD28-hinge domain, a 4-1BB costimulatory domain, and a CD3 $\zeta$  activation domain. The CD22 CAR construct incorporates a camelid anti-CD22 sdAb, also called nanobody, with a CD8 hinge-domain, a 4-1BB costimulatory domain, and a CD3 $\zeta$  activation domain. My hypothesis is that polyclonal human  $\gamma\delta$  T cells can be successfully engineered to express CAR constructs targeting B-cell antigens (CD19 or CD22), providing a platform for the development of novel  $\gamma\delta$  T cell-based immunotherapies for B-lymphomas. I tested this hypothesis through the two following aims:

***Aim 1:*** Production of CD19 scFv-CAR and CD22 sdAb-CAR lentiviruses in HEK 293SF-PacLV.

1A) Production of CD19 and CD22 CAR lentiviruses.

1B) Titration of CD19 CAR and CD22 CAR lentiviruses with HEK 293A cells.

***Aim 2:*** Transduction of  $\gamma\delta$  T cells with CD19 or CD22 CAR lentivirus.

2A) Generating CD19 CAR  $\gamma\delta$  T cells.

2B) Comparing different protocols of transduction to numerically transduce and expand CAR  $\gamma\delta$  T-cell products.

2C) Identification of the optimal MOI.

2D) Generating CD19 CAR and CD22 CAR  $\gamma\delta$  T cells.

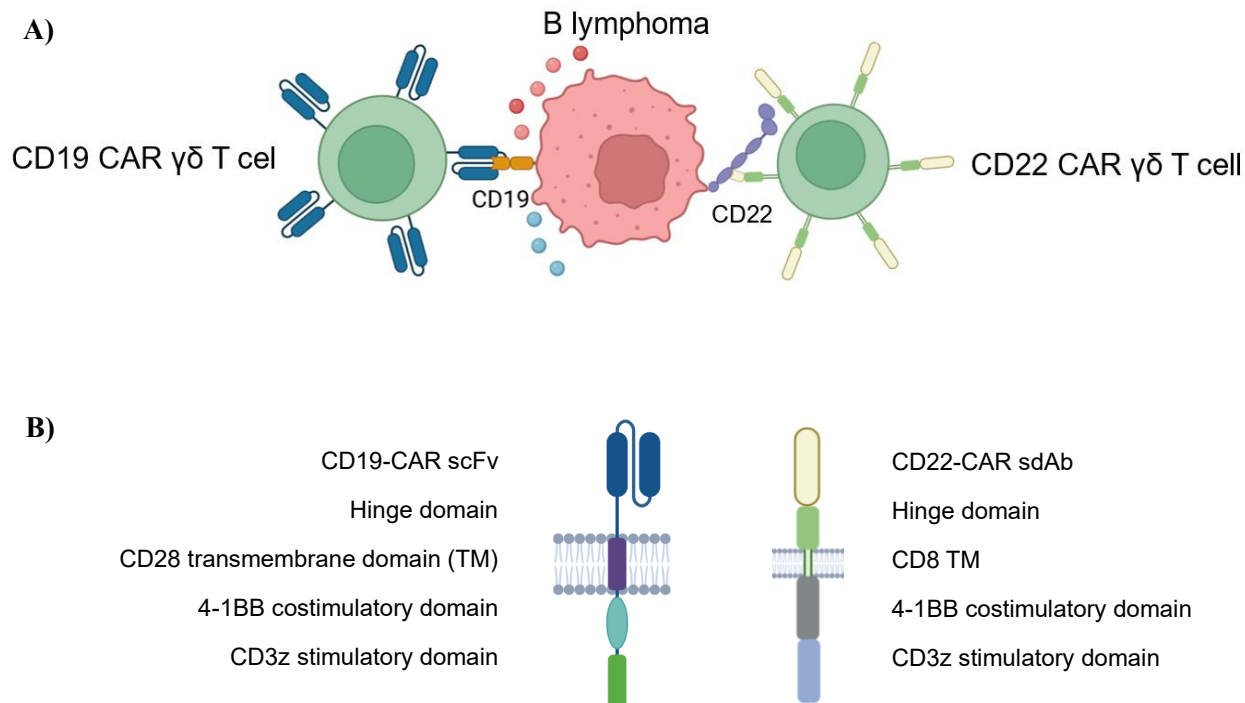


**Figure 4: The second-generation CAR constructs.** (A) The antigen binding domain of each CAR recognizes and binds to the TAA, which is either CD19 or CD22, on the tumor cell surface. This binding activates CAR T cell signaling through the CD3 $\zeta$  domain which elicits cytotoxic functions including the release of perforins and granzymes, as well as the production of pro-inflammatory cytokines. (B) The CD19-CAR was synthesized using the murine scFv, while the CD22-CAR was constructed using the camelid sdAb, also known as nanobody.

## 2. Materials and Methods

We have elaborated an optimized protocol allowing an *in vitro* expansion of polyclonal  $\gamma\delta$  T cells. This protocol was used to expand  $\gamma\delta$  T cells expressing CD19 or CD22 CAR. We have generated CD19 CAR  $\gamma\delta$  T cells and CD22 CAR  $\gamma\delta$  T cells, in collaboration with Dr. Scott McComb, a researcher at the National Research Council (NRC). His research mainly focuses on  $\alpha\beta$  T cells. Dr. Scott McComb provided us with these four standard operating procedures (SOPs):

1. SOP 00.P.65 - *Thawing, Subculturing, Counting and Banking of HEK Packaging and Producer Cell Lines.*
2. SOPs 00.P.068 - *Small-scale LV production in HEK293SF-PacLV.*
3. SOP 00.D.035 - *34 mL of Lentivirus or Virus Like Particle Concentration by Ultracentrifugation.*
4. SOP 00.T.28 - *Lentiviral vector-based gene transfer into human T lymphocytes.*

### 2.1 Cell Culture

LB broth medium (Gibco™) is used to culture *E. coli* DH5 $\alpha$ . 293SF-PacLV, the lentiviral packaging cell line, is cultivated in Hycell-Transfx-H medium (Hyclone). 293A cells used for the lentivirus' titration are cultured in DMEM high glucose medium (Gibco™) supplemented with 10% fetal bovine serum (FBS) (MilliporeSigma), 2 mM L-Glutamate, 100 U/mL penicillin and 100  $\mu$ g/mL streptomycin. Immortalized cancer cell line K562 is grown in standard culture conditions, using RPMI 1640 medium (Cytiva) supplemented with 10% FBS, 2 mM L-Glutamate, 100 U/mL penicillin and 100  $\mu$ g/mL streptomycin. Peripheral blood mononuclear cells (PBMCs) are thawed and incubated overnight in RPMI 1640 medium supplemented with 10% FBS, 2 mM

L-Glutamate, 100 U/mL penicillin and 100 µg/mL streptomycin. For the growth and expansion of isolated  $\gamma\delta$  T cells, cells are cultured in OpTmizer™ CTS™ medium (Gibco™) supplemented with 10% FBS, 2 mM L-Glu, 100 U/mL penicillin, 100 µg/mL streptomycin, 200 IU/ml human interleukin-2 (IL-2) (Novartis) and 70 ng/mL human interleukin-15 (IL-15) (PeproTech®).

## 2.2 Flow cytometry

For all flow cytometry experiments assessing CAR-GFP expression by  $\gamma\delta$  T cells,  $\gamma\delta$  T cells were stained with Zombie Aqua viability dye for 15 minutes in the dark at room temperature. The cells were washed with PBS and then fixed in 1% paraformaldehyde (PFA) solution for one hour in the dark at 4 °C. Flow cytometry was performed on the Northern Lights (©Cytek) at the CHEO RI II, affiliated with the Flow Cytometry & Virometry Core Facility of the University of Ottawa. Data were analyzed using the 10.10.0 version of FlowJo software (FlowJo™ 10). For the phenotypic analysis regarding the proportion of each  $\gamma\delta$  T cell subset within CAR-GFP<sup>+</sup> expressing cells,  $\gamma\delta$  T cells were stained using these following mouse anti-human mAbs: anti-TCR V $\delta$ 1-VioBlue (REA173; Miltenyi Biotec), anti-TCR V $\delta$ 2-PE (123R3; Miltenyi Biotec) and anti-TCR V $\gamma$ 9-FITC (B3; BioLegend). It was either V $\delta$ 1 and V $\delta$ 2 or V $\delta$ 1 and V $\gamma$ 9.

## 2.3 PMBC isolation

PBMCs were isolated from the blood of 62 healthy adult volunteers by gradient centrifugation on Ficoll-Paque (**Fig.5A**). All blood donors were recruited from Dr. Jonathan Angel Laboratory at the Ottawa Hospital Research Institute (OHRI) and informed consent was obtained from all individuals.

The heparinized blood was diluted to one-third in RPMI 1640 medium. In a separate tube, one volume unit of Ficoll solution (Sigma-Aldrich) was first transferred into 50 mL falcon tube and then two volume units of diluted blood were slowly added through the sides of the tube so that the blood overlaid the Ficoll solution. The tubes were then centrifuged at 1250 rcf with minimum acceleration and deceleration speed for 30 minutes at room temperature. Then, the ring of PBMCs, located between the Ficoll and the plasma/RPMI layer, was harvested and resuspended in one volume of RPMI into a new tube. The tube was spun down at 600 rcf for 10 minutes to remove any remaining platelets. Finally, the cells were washed twice with one volume of RPMI and counted using a trypan blue solution (Gibco™) on a hemocytometer. Isolated PBMCs were stored in cryogenic vials at -70°C in FBS supplemented with 10% dimethyl sulfoxide (DMSO) (Sigma-Aldrich). The PBMCs were transferred into the liquid nitrogen tank within 24-48 hours.

#### **2.4 Maxipreparation of CD19 CAR and CD22 CAR plasmids**

To increase the amount of the CD19 CAR construct (pQC4-CD19hCAR-BB-3z c1) and the CD22 CAR construct (pQC5-CD22-1ug36-CD8TM-BBz cG1), a maxipreparation of both plasmids was performed (**Fig.5B**). *E. coli* DH5 $\alpha$  strain was submitted to a heat shock transformation, which allowed the CD19 CAR or the CD22 CAR to enter the bacterial cells. Following overnight incubation on agar plate (pre-poured LB agar plates with 100  $\mu$ g/ml ampicillin), 5 colonies were selected for minipreparations. DNA isolation and purification were performed using the Quick-DNA™ Fungal/Bacterial Miniprep Kit (Zymo Research) and an electrophoresis gel was run, confirming the presence of CD19 CAR plasmid in DH5 $\alpha$  cells. Then, DNA plasmid was isolated and purified from maxipreparation using the PureLink™ HiPure Plasmid Maxiprep Kit (Life Technologies). To further confirm the plasmid identity, following the

maxipreparation, the isolated CD19 CAR plasmid was sent at the OHRI, more specifically at the StemCore Laboratories Genomics Core Facility, for Sanger sequencing.

## **2.5 Lentivirus production in HEK 293SF-PacLV**

I used a third-generation lentivirus packaging cell line, generated by Broussau et al.<sup>106</sup>, for producing lentiviral vectors (LVs) expressing either CD19 CAR or CD22 CAR (**Fig.5C**). The cell line, HEK 293SF-3F6, derives from human embryonic kidney cells (HEK cells), which were transfected with Gag-Pol and Rev genes from human immunodeficiency virus-1 (HIV-1) and VSV-G, the glycoprotein of vesicular stomatitis virus<sup>106</sup>. These HEK 293SF-PacLV are equipped with cumate- and coumermycin-inducible systems, enabling tight control of the expression of cytotoxic LV elements. In order to produce CD19 CAR and CD22 CAR lentiviruses, 19 million 293SF-PacLV were transfected with 8 µg of CAR plasmid and 16 µg of the polyethylenimine (PEI) transfection reagent (PEIpro® from Polyplus), in Hycell-Transfx-H medium. To induce lentivirus production, 10 nM of coumermycin (Enzo Life Sciences) and 80 µg of cumate (Sigma-Aldrich) were added 4h post-transfection and 7 mM of sodium butyrate (Sigma-Aldrich) was added 16h post-transfection to enhance transcription and thus, increase LV production. Then, to confirm whether the CD19 CAR or CD22 CAR plasmids were well integrated, GFP expression in HEK 293SF-PacLV cells was assessed using EVOS M5000 imaging system, since the plasmids encode GFP. The virus particles in the supernatants were ultracentrifuged at 4°C for 3 hours at 11,800 rpm using the Optima L-100 XP Ultracentrifuge (Beckam Coulter).

## 2.6 Titration of CD19 and CD22 CAR lentiviruses

The transduction units' titer (TU/mL) of the generated CD19 CAR and CD22 CAR lentiviruses was performed with HEK 293A cells (Invitrogen™) (**Fig.5D**). To do so, HEK 293A cells were transduced with serial dilutions of either CD19 CAR or CD22 CAR lentivirus in 8 µg/mL polybrene solution (made from hexadimethrine bromide) (Sigma Aldrich). At day 4 post-transduction, the cells were analysed for transduction efficiency by GFP expression using ©Cytek Northern Lights Flow Cytometry System. Finally, the infectious titer (TU/mL) was determined using data between 2% and 20% GFP-positive cells and the first formula shown below. Following the production of the CD19 CAR and CD22 CAR lentiviruses and knowing their infectious titer (TU/mL), it was possible to calculate the volume of LV, i.e volume from CAR lentivirus stock, required to test different multiplicities of infection (MOIs) by using the second formula shown below.

1. Formula to determine the infectious titer (TU/mL):

$$\text{TU/mL} = \frac{\frac{\% \text{ GFP Positive Cells}}{100} \times \# \text{Cells/well} \times \text{Dilution Factor}}{\text{Volume of Lentivirus used to transduce cells (mL)}}$$

2. Formula to test different multiplicities of infection (MOIs):

$$\text{Volume of viral vector} = \frac{\# \text{Cells}}{\text{Viral titer} \left( \frac{\text{TU}}{\text{mL}} \right)} \times \text{MOI}$$

## 2.7 Isolation of $\gamma\delta$ T cells

Given that  $\gamma\delta$  T cells represent only 5% of T cells,  $\gamma\delta$  T cells must be isolated from PBMCs prior to expansion (**Fig.6A-B**). To do so, a day before  $\gamma\delta$  T cells isolation (Day 0), 10 million PBMCs were thawed and incubated at 37°C overnight in RPMI 1640 medium supplemented with 10% FBS, 2 mM L-Glutamate, 100 U/mL penicillin and 100  $\mu\text{g}/\text{mL}$  streptomycin. In addition, 5  $\mu\text{g}/\text{mL}$  anti-human CD3 antibody (OKT3) (BioLegend®) was plated on a U-bottom 96-well-plate, protected from light and incubated at 4°C overnight. The next day (Day 1),  $\gamma\delta$  T cells were sorted from PBMCs using the EasySep™ Human Gamma/Delta T Cell Isolation Kit (STEMCELL™), as per the manufacturer's instructions. Then, isolated  $\gamma\delta$  T cells were resuspended in OpTmizer™ CTST™ medium containing 10% FBS with 200IU/mL IL-2 and 70 ng/mL human IL-15 on the OKT3 pre-plated U-bottom 96-well-plate.

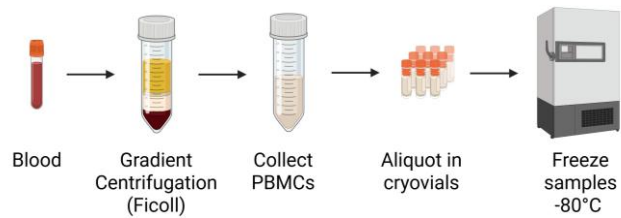
## 2.8 Production of CAR $\gamma\delta$ T cells

Two protocols were tested to identify the best protocol to transduce and expand the final product, expressing either CD19 CAR or CD22 CAR. In the first protocol (**Fig.6A-B**),  $\gamma\delta$  T cells were expanded after isolation and cocultured with 150,000 feeder cells and 5  $\mu\text{g}/\text{mL}$  OKT3 per well on a U-bottom 96-well-plate. Feeder cells are a mix of K562 and allogeneic PBMCs in a 1:1 ratio that were irradiated at 30 gray (Gy) using the X-ray irradiator (Precision X-Rad320) at the Pre-Clinical Imaging Core Facility (PCIC). At day 7 post-expansion,  $\gamma\delta$  T cells were transduced with different volumes corresponding to specific MOIs of CAR CD19 lentivirus or CD22 CAR lentivirus. To do so,  $\gamma\delta$  T cells were resuspended in TexMacs medium and transferred in a 15 mL tube, in which CD19 CAR or CD22 CAR lentivirus is added. A tube containing only expanded  $\gamma\delta$  T cells, without

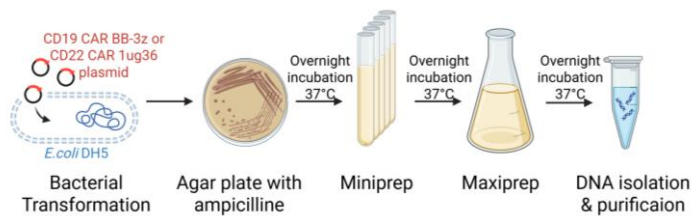
CAR lentivirus, served as a negative control. The 15 mL tubes were centrifugated for 2 hours at 800 rcf at 32°C. The transduced  $\gamma\delta$  T cells were resuspended in OpTmizer medium and transferred on a U-bottom 96-well-plate. The plate was monitored daily and fresh OpTmizer medium was added if needed. At day 7 post-transduction, the CAR transduction efficiency was evaluated by GFP expression using ©Cytek Northern Lights Flow Cytometry System.

A second protocol was tested in order to produce CAR  $\gamma\delta$  T cells (**Fig.7A-B**). PBMCs were thawed and incubated overnight at 37°C. A U-bottom 96-well-plate was coated with 5  $\mu\text{g/mL}$  of OKT3 and incubated overnight at 4°C. As in the previous protocol, the next day (Day 1),  $\gamma\delta$  T cells were sorted from PBMCs using the EasySep™ Human Gamma/Delta T Cell Isolation Kit. Isolated  $\gamma\delta$  T cells were then resuspended in OpTmizer medium containing 10% FBS with 200IU/mL IL-2, 70 ng/mL human IL-15 and transferred on the pre-coated OKT3 U-bottom 96-well-plate for an overnight incubation. Following the overnight incubation,  $\gamma\delta$  T cells were immediately resuspended in TexMacs and transduced with either CD19 CAR or CD22 CAR lentivirus, at different MOIs, on a flat-bottom 96 well-plate. The plate containing the  $\gamma\delta$  T cells and the CAR lentivirus was centrifugated for 2 hours at 800 rcf at 32°C. The plate was then incubated overnight at 37°C. The next day, the transduced  $\gamma\delta$  T cells were resuspended in OpTmizer medium and transferred on a U-bottom 96-well-plate, in which 150,000 irradiated feeder cells were added per well. At day 6 and day 10 post-transduction, the CAR transduction efficiency was evaluated by GFP expression on the ©Cytek Northern Lights Flow Cytometry System. The main difference between this protocol and the previous one lies in the time of transduction, as in this protocol,  $\gamma\delta$  T cells were transduced before expansion.

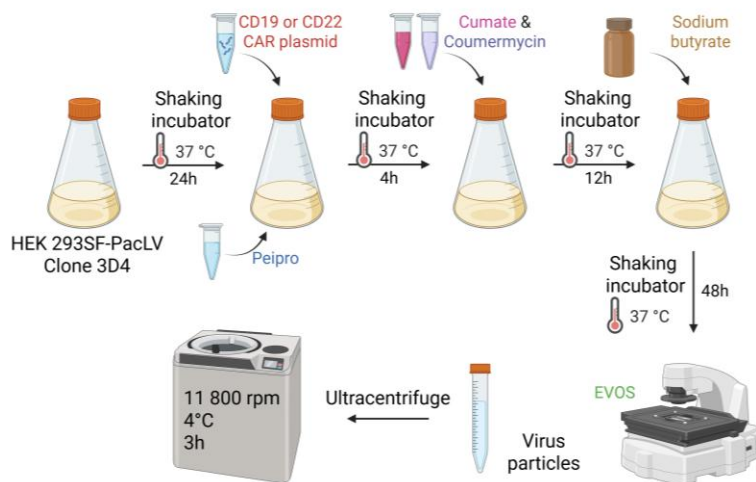
### A) Harvest peripheral blood mononuclear cells (PBMCs)



### B) Maxipreparation of both plasmids



### C) Transfection of HEK 293SF-PacLV with CD19 or CD22 CAR plasmid



### C) Titration of CD19 and CD22 CAR lentiviruses with HEK 293A cells

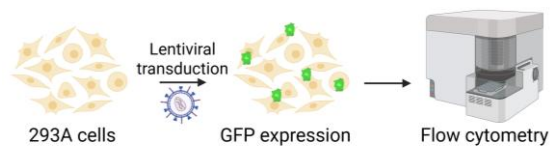
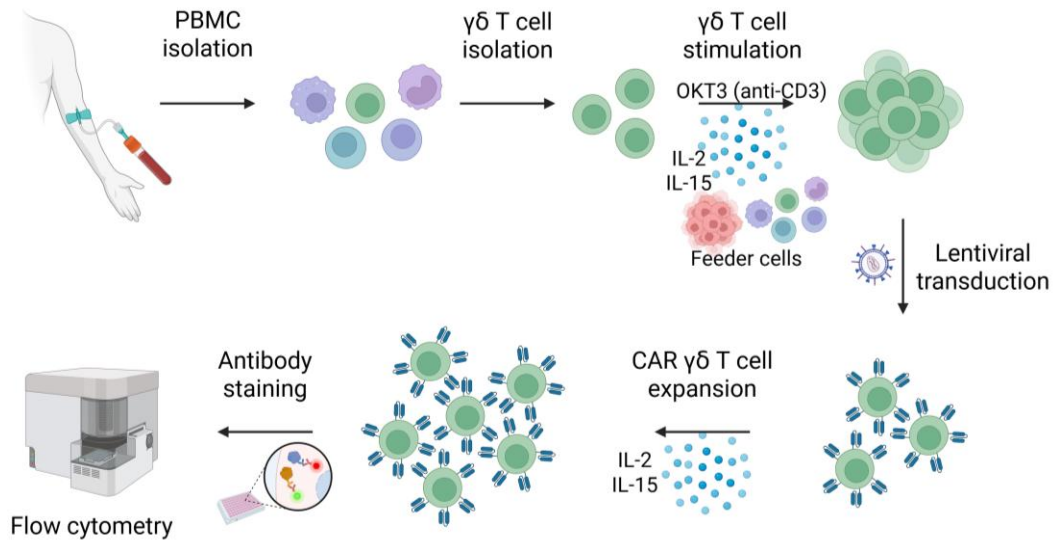


**Figure 5: Production of CD19 scFv-CAR or CD22 sdAb-CAR lentivirus in HEK 293SF-PacLV and titration with HEK 293A cells.** (A) Peripheral blood mononuclear cells (PBMCs) were collected from the blood of healthy adult volunteers. (B) *E.coli* DH5 $\alpha$  was transformed with the CD19 CAR BB-3z plasmid or the CD22 CAR 1ug36 plasmid that was then isolated and purified. (C) HEK 293SF-PacLV, a lentivirus packaging cell line, were transfected with the isolated CD19 CAR or CD22 CAR plasmid. (D) HEK 293A cells were transduced with CAR Lentivirus and were analysed for the expression of GFP to determine the viral titer.

**A) First protocol of transduction**



**B) First schedule of transduction**

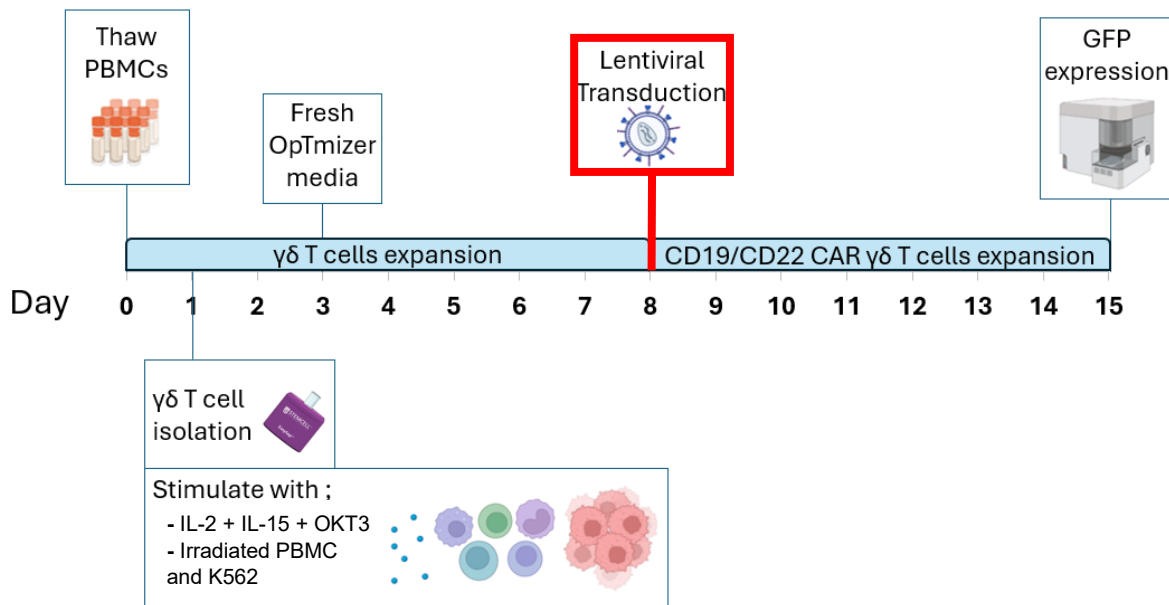
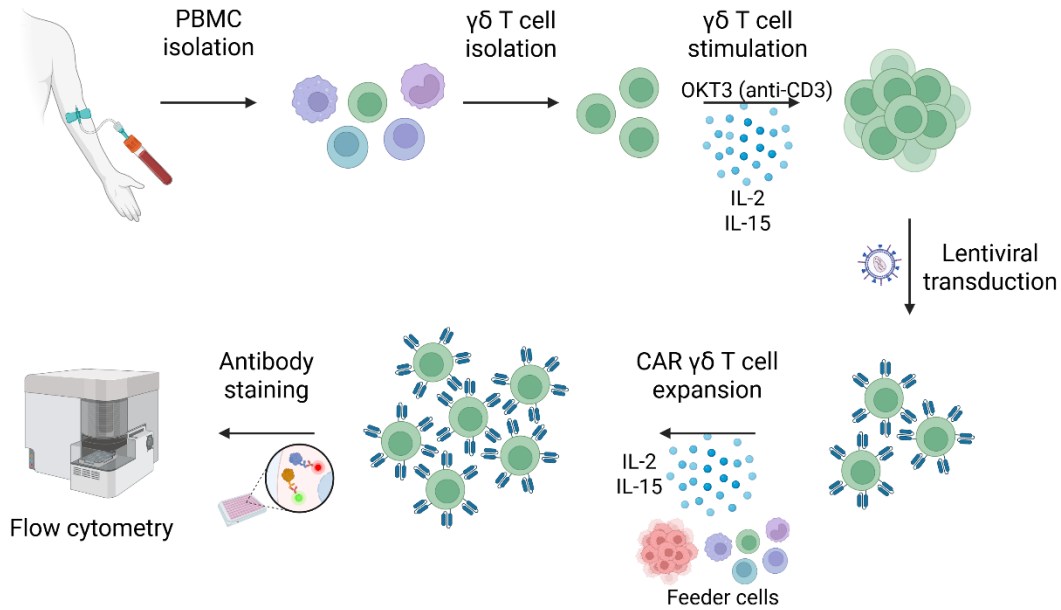


**Figure 6: First protocol for generating CD19 CAR and CD22 CAR  $\gamma\delta$  T cells.** (A) Schematic and (B) schedule of transduction followed for the first protocol.  $\gamma\delta$  T cells were isolated from PBMCs, expanded in the presence of IL-2, IL-15, anti-CD3 and feeder cells at Day 1, and transduced at Day 8 with either CD19 or CD22 CAR lentivirus. Feeder cells are PBMCs from another donor and K562 that have been irradiated at 30 Gy. Cells were assessed for the expression of CAR-GFP at Day 7 post-transduction. The control condition was expanded  $\gamma\delta$  T cells that were not transduced.

### A) Second protocol of transduction



### B) Second schedule of transduction

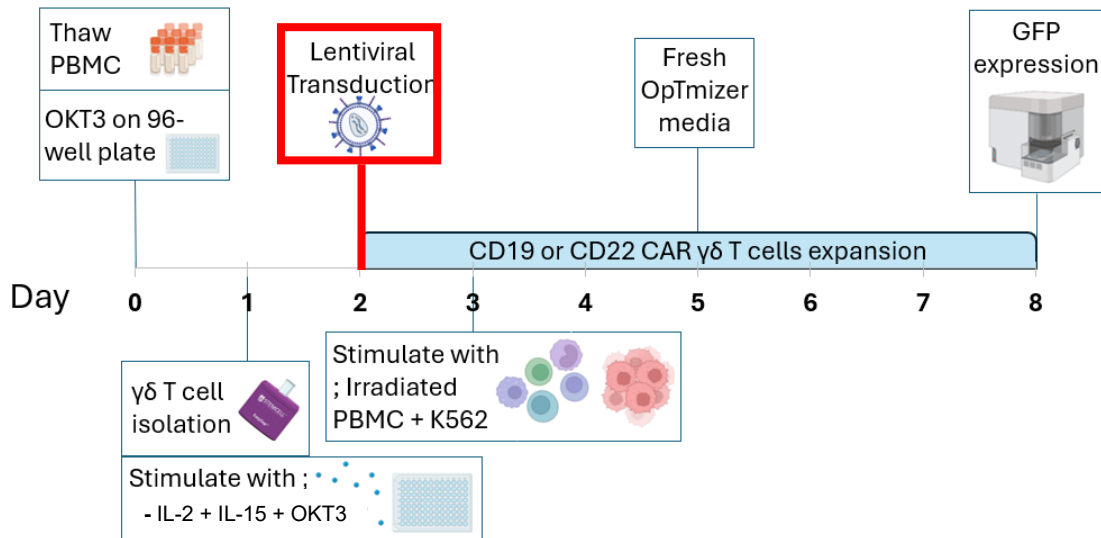


**Figure 7: Second protocol for generating CD19 CAR and CD22 CAR  $\gamma\delta$  T cells.** (A) Schematic and (B) schedule of transduction followed for the second protocol.  $\gamma\delta$  T cells were isolated from PBMCs, resuspended in the presence of IL-2, IL-15 and anti-CD3 at Day 1, and transduced at Day 2 with either CD19 or CD22 CAR lentivirus. Feeder cells were added at Day 3. These are PBMCs from another donor and K562 that have been irradiated at 30 Gy. Cells were assessed for the expression of CAR-GFP at Day 6 post-transduction. The control condition was expanded  $\gamma\delta$  T cells that were not transduced.

### **3. Results**

#### **3.1 Production of CD19 scFv-CAR and CD22 sdAb-CAR lentiviruses in HEK 293SF-PacLV**

##### **3.1.1 Both plasmids maintained their integrity upon maxipreparation**

Following the heat-shock step of *E. coli* DH5 $\alpha$  strain with one of the CAR plasmids and the overnight incubation of the petri dish, 5 colonies were selected and inoculated for minipreparations. To confirm the presence of the CAR plasmid in *E. coli* prior to the maxipreparation, DNA was isolated from these five individual minipreparations and electrophoresis gel analysis was performed (**Fig.8**). The agarose gel showed five similar bands corresponding to approximately 9,000 base pairs (bp), which corresponds to the 8,872 bp CD19 CAR plasmid. The fact that there is only one band in each column indicates that plasmids were well isolated and retained their integrity, confirming the presence of the CD19 CAR plasmid in the DH5 $\alpha$  cells. Furthermore, DNA concentrations, measured at a wavelength of 260 nm using a NanoDrop spectrophotometer, were all similar, further confirming the identity of the CAR CD19 plasmids.

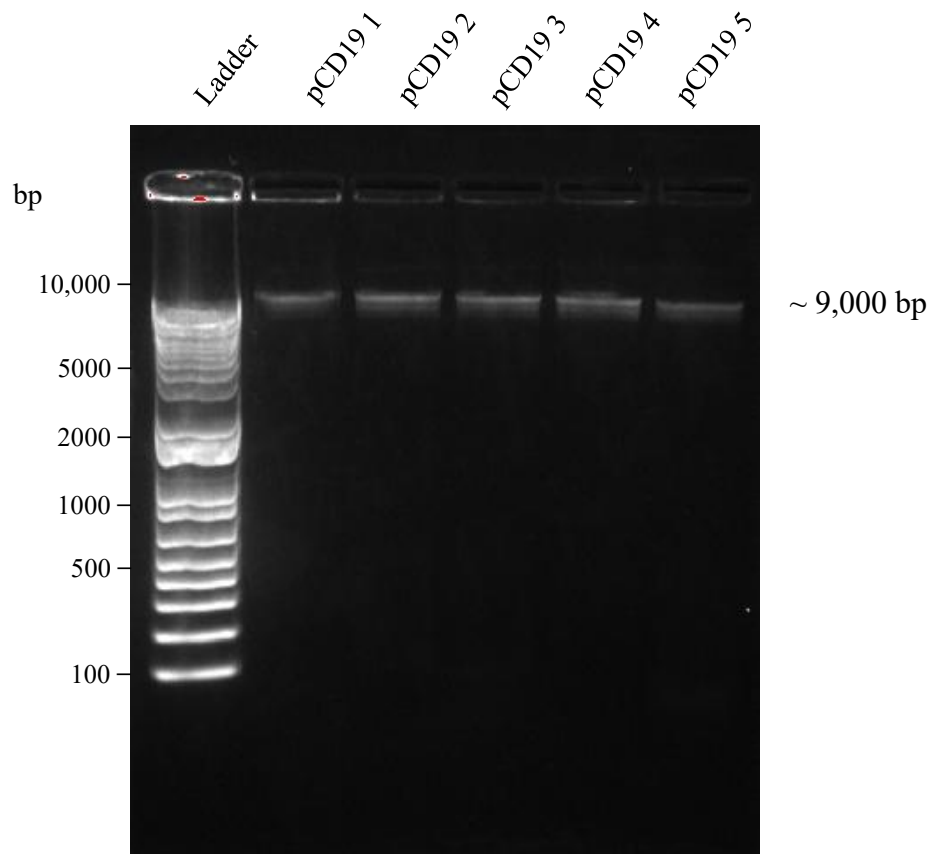


**Figure 8: CD19 CAR plasmids isolated from minipreparations.** The agarose gel shows 5 bands at approximately 9,000 bp corresponding to CD19 CAR plasmids that were isolated and purified from 5 minipreparations. The 1 kb plus ladder is in the first column whereas an aliquot of each pCD19 is in the second to the 6<sup>th</sup> column of the 1% agarose gel.

To ensure that the plasmid maintained its integrity upon maxipreparation, the CD19 CAR plasmid has been sent to the OHRI for Sanger sequencing. A forward and reverse primers were used to obtain the DNA sequence. Two primers, EFS-UTR-Test-F and EGFP-Seq-R, were used for sequencing: forward (5' CGC CAG AAC ACA GGT GTC GTG AC 3') and reverse (5' GGT GGC ATC GCC CTC GC 3'). Sanger sequencing results showed that primers cut two DNA sequences that aligned perfectly to the reference pSLCAR-CD19-BBz plasmid (pCD19) (Addgene: 135992), one sequence begins at the 2754<sup>th</sup> bp and ends at the 3590<sup>th</sup> bp, which is 838

bp in length, and the other one starts at the 3634<sup>th</sup> bp and finishes at the 4455<sup>th</sup> bp, which is 821 bp in length. These DNA sequences encode for CAR construct components: the FMC63-scFv domain, the CD28-hinge domain and the CD3 $\zeta$  activation domain (**Fig.9**), confirming that the CD19 CAR plasmid maintained its integrity and identity during the maxipreparation process. The concentration of the CD19 CAR and CD22 CAR plasmids, measured at 260 nm by a Nanodrop spectrophotometer, were 2.487  $\mu\text{g}/\mu\text{L}$  and 1.074  $\mu\text{g}/\mu\text{L}$ , respectively. To obtain an even more accurate concentration of CD19 CAR plasmid before sending it for Sanger sequencing, the DNA concentration was measured using the Qubit dsDNA kit. Plasmids were then preserved at -20 °C until further use.

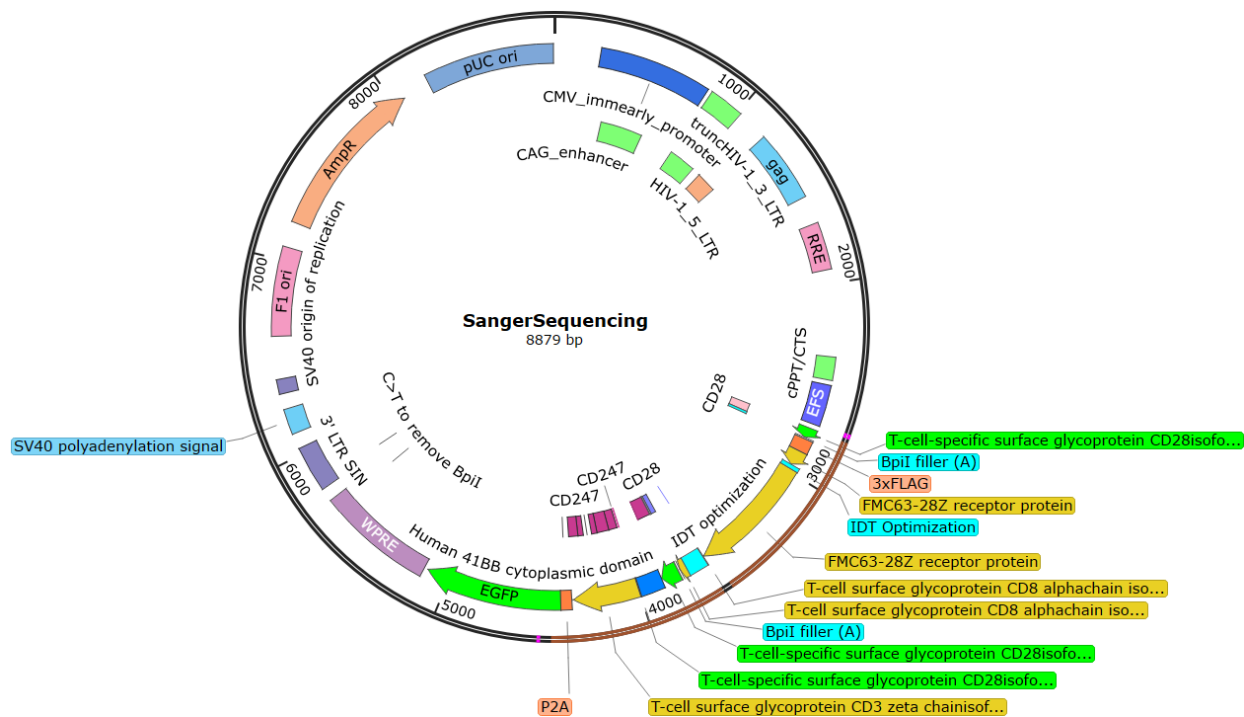


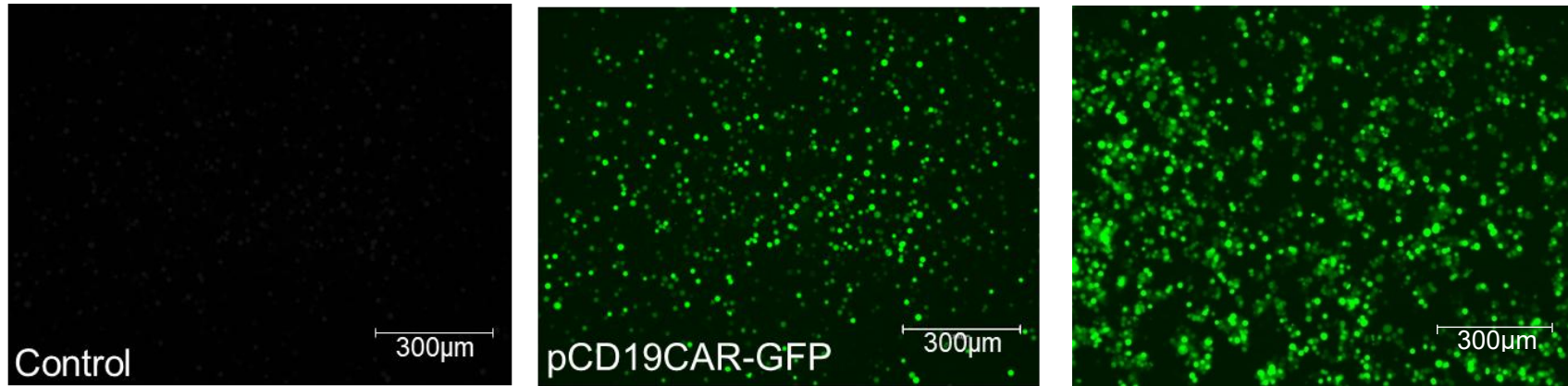
**Figure 9: DNA sequence of the CD19 CAR plasmid.** Plasmids were maxi-prepped to produce high yield transfection-grade plasmids. The identity of the isolated and purified CD19 CAR plasmids was confirmed by Sanger sequencing. (A) The plasmid map shows the two pCD19 DNA sequences, obtained from sequencing analysis, (in brown) aligned with the reference pSLCAR-CD19-BBz plasmid that can be found on Addgene (accession number 135992). A forward, 5' CGC CAG AAC ACA GGT GTC GTG AC 3', and reverse, 5' GGT GGC ATC GCC CTC GC 3', primers were used (in pink), allowing to cut two DNA sequences. The forward primer cut a DNA sequence of 838 whereas the reverse primer cut a DNA sequence of 821 bp.

### **3.1.2 Transfection of HEK 293SF-PacLV with the CD19 CAR plasmid showed higher levels of GFP-expressing cells than with the CD22 CAR plasmid**

A third-generation lentivirus packaging system, the safest generation due to its self-inactivating (SIN) sequence, was used for producing lentivirus encoding either CD19 CAR or CD22 CAR. To do so, HEK 293SF-PacLV, a lentivirus packaging cell line equipped with cumate and coumermycin inducible systems, were transfected with the isolated CD19 CAR or CD22 CAR plasmid<sup>92</sup>. More specifically, 19 million of HEK 293SF-PacLV were transfected with a PEI: DNA ratio of 2:1 since this ratio has been proven ideal for optimal transfection rate<sup>90</sup>. Cumate, a nontoxic inducible element, and coumermycin, an aminocoumarin that inhibits bacterial DNA gyrase, are added to induce the transfection. Cumate and coumermycin are acting together to tightly control the transcription of cytotoxic packaging elements, such as the protease encoded by the VSV-G gene.

A preliminary step prior to verifying the integration of CD19 CAR or CD22 CAR plasmid into the lentivirus packaging cell line is to evaluate the level of GFP expression in transfected HEK 293SF-PacLV cells using a fluorescence microscope. EVOS pictures were taken 72 hours post-transfection (**Fig.10**). Given that both CAR plasmids encode GFP, verifying the GFP expression level is necessary prior to confirm that CAR plasmids are well integrated to the lentiviral genome, under the third-generation lentivirus system. The same amount of CD19 or CD22 CAR plasmid was used to transfect HEK 293SF-PacLV. Indeed, for a flask containing 19 million of 293SF-PacLV, 8 µg of either CD19 or CD22 CAR plasmid were added with 16 µg of PEI so that the total DNA concentration in the production culture was 0.4 µg/mL. According to the EVOS pictures, the CD19 CAR plasmid was easier to transfect into HEK 293SF-PacLV than the CD22 CAR plasmid, as the transfection of CD19 CAR plasmid showed higher levels of GFP-expressing cells.

A)



B)

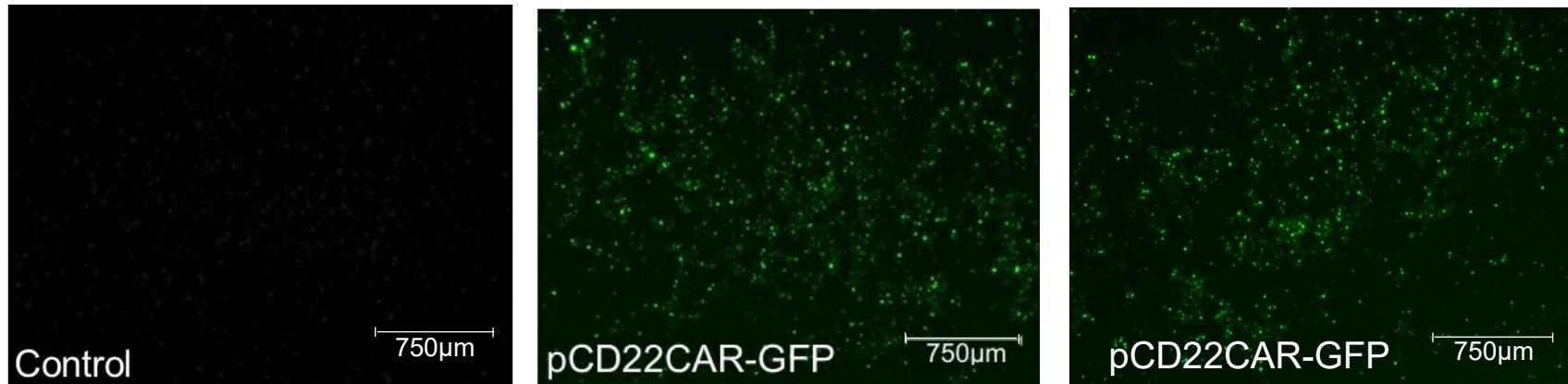
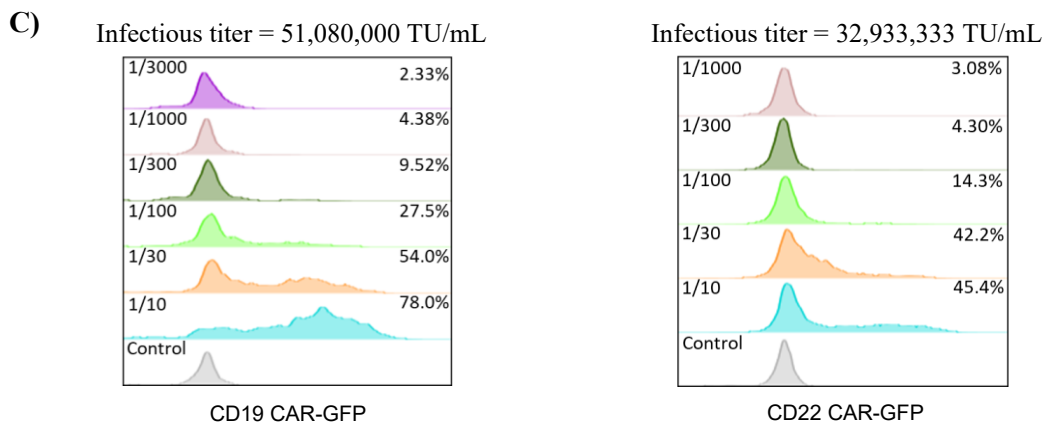
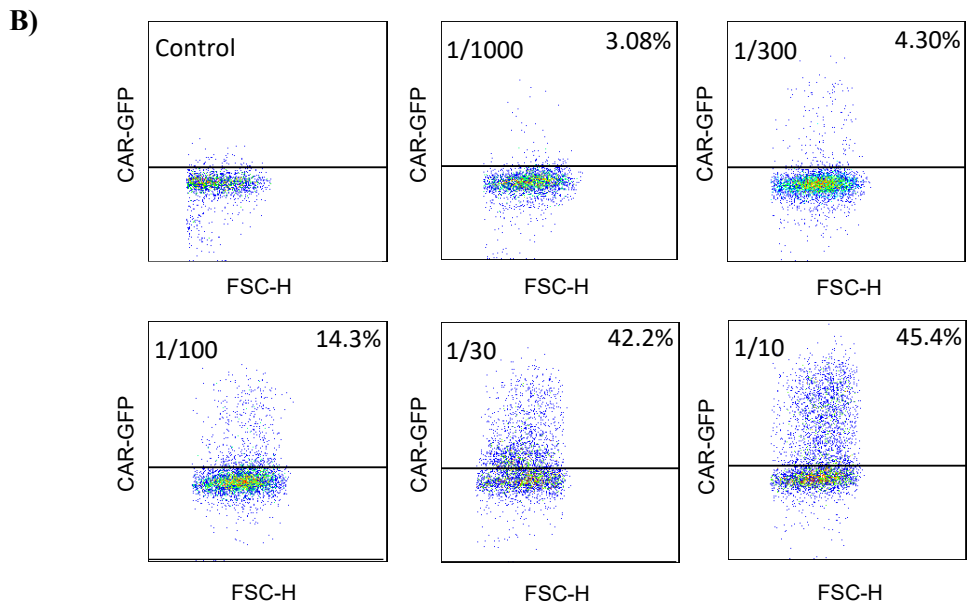
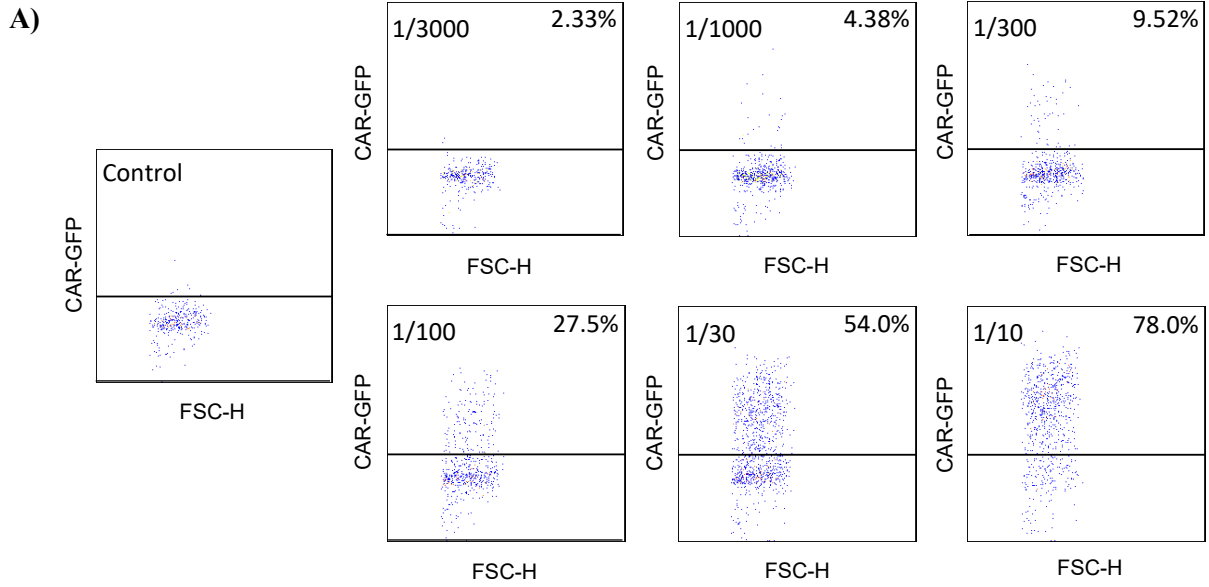


**Figure 10: GFP expression of HEK 293SF-PacLV.** (A) Evos pictures show the HEK 293SF-PacLV, a lentivirus packaging cell line, that has been transfected with the CD19 CAR plasmid (pCD19CAR-GFP). The two first pictures were taken from the same experiment. The first one shows the control, which no pCD19CAR-GFP was added to the flask, whereas the second one shows the HEK 293SF-PacLV transfected with pCD19CAR-GFP. The last picture at the right was taken from an independent transfection experiment. (B) Evos pictures show the HEK 293SF-PacLV transfected with the CD22 CAR plasmid (pCD22CAR-GFP). The first picture shows the control and the second shows the HEK 293SF-PacLV transfected with pCD22CAR-GFP. The last picture at the right was taken from an independent transfection experiment. All pictures were taken 72h post-transfection.

### 3.1.3 Titration of CD19 and CD22 CAR lentiviruses with HEK 293A cells

Following the production of CD19 and CD22 CAR lentiviruses, it is important to determine the infectious titer, which is measured as Transduction Unit per mL (TU/mL) and refers to the number of integration events in target cells. To do so, 20,000 HEK 293A cells were transduced with different volumes of viral stock corresponding to specific serial dilutions: 1/10, 1/100, 1/1000 and 1/30, 1/300, 1/3000. The volumes of viral stock were diluted in polybrene, a cationic polymer known to enhance the efficiency of lentiviral infection to mammalian cells. At day 4 post-transduction, GFP expression in transduced cells was assessed by flow cytometry. The infectious titer of the two CAR lentivirus stocks was calculated once the transduction efficiency was obtained from the percentages of HEK 293A cells expressing GFP. Only data between 2% and 20% GFP-positive cells (GFP<sup>+</sup>) were considered to calculate the infectious titer. The number of integrations is approximately equal to the number of transduced cells when the percentage of GFP<sup>+</sup> cells is lower than 20%, while the fraction of transduced cells with multiple integrations increases at transduction levels above 20%.

Regarding the CD19 CAR lentiviral titer, three results of transduction showed percentages of GFP<sup>+</sup> cells between 2 and 20%: 2.33%, 4.38% and 9.52%, which corresponded to dilutions 1/300, 1/1000 and 1/3000, respectively (**Fig.11A and C**). Concerning the CD22 CAR lentiviral titer, there were also three results of transduction that showed GFP<sup>+</sup> cells above 2% and under 20%: 3.08%, 4.30% and 14.30%, corresponding to 1/1000, 1/300 and 1/100, respectively (**Fig.11B and C**). Using the formula below and averaging the infectious titers obtained from the three percentages, we calculated infectious titers of 51,080,000 TU/mL for CD19 CAR lentivirus and 32,933,333 TU/mL for CD22 CAR lentivirus. Several batches of CD19 and CD22 CAR lentiviruses were produced during this project, all having different infectious titers (**Table 1-2**).



Formula to determine the infectious titer:

$$\frac{\% \text{ GFP Positive Cells}}{100} \times \# \text{ Cells/well} \times \text{Dilution Factor}$$

---

$$\text{Volume of Lentivirus used to transduce cells (mL)}$$

Infectious titer = 51,080,000 TU/mL

**Figure 11: CD19 and CD22 CAR lentiviruses titration on HEK 293A cells.** (A) Plots and (C) histogram (on the left) show the percentages of HEK 293A cells expressing GFP that have been transduced with CD19 CAR lentivirus according to its dilution. From the lentivirus stock, two series of dilution were tested and were as follows: 1/10, 1/100, 1/1000 and 1/30, 1/300, 1/3000. (B) Plots and (C) histogram (on the right) show the CD22 CAR lentivirus' titration using 293A cells. Serial dilutions of the lentivirus stock were tested to infect the HEK 293A cells. The infectious titer (TU/mL) of lentivirus was calculated from data in which GFP<sup>+</sup> cells ranged from 2 to 20%. The infectious titers were 51,080,000 TU/mL for CD19 CAR lentivirus and 32,933,333 TU/mL for CD22 CAR lentivirus.

**Table 1. Titrations of CD19 lentivirus stocks.**

Dilution	1		2		3		4		5	
	GFP%	TU/mL	GFP%	TU/mL	GFP%	TU/mL	GFP%	TU/mL	GFP%	TU/mL
1/10	74.6	14,920,000	78.0	15,600,000	98.6	19,600,000	90.1	18,020,000	84.3	16,860,000
1/30	45.0	27,000,000	54.0	32,400,000	89.8	53,880,000	89.5	53,700,000	78.1	46,860,000
1/100	32.5	65,000,000	27.5	55,000,000	81.2	162,400,000	73.4	146,800,000	71.1	142,200,000
1/300	13.7	27,400,000	9.52	19,040,000	36.3	72,600,000	*1.22	24,400,000	*22.4	44,800,000
1/1000	*17.4	348,000,000	4.38	87,600,000	*45.6	912,000,000	35.0	700,000,000	33.1	662,000,000
1/3000	7.43	148,600,000	2.33	46,600,000	13.0	260,000,000	0.12	2,400,000	3.80	76,000,000
Mean (TU/mL)	88,000,000		51,080,000		260,000,000		2,400,000		76,000,000	

\*Percentage of GFP expression that seemed wrong and is therefore not considered in calculating the average infectious titer. Numbers in magenta were taking into account to calculate the mean and thus obtain the infectious titer (TU/mL).

**Table 2. Titrations of CD22 lentivirus stocks.**

Dilution	1		2	
	GFP%	TU/mL	GFP%	TU/mL
1/10	48.4	96,800	45.4	9,080,000
1/30	22.5	13,500,000	42.2	25,320,000
1/100	7.35	14,700,000	14.3	28,600,000
1/300	*1.66	36,52	4.30	8,600,000
1/1000	*0.87	17.4	3.08	61,600,000
1/3000	*0.51	114,44	*21.6	432,000,000
Mean (TU/mL)	14,100,000		32,933,333	

**Calculation example:**

$$\text{Dilution } 1/300 \quad \frac{9.52}{100} \times \frac{20,000}{\text{well}} \times \frac{1}{300} = 19,040,000 \text{ TU/mL}$$

$$1/1000 \quad \frac{4.38}{100} \times \frac{20,000}{\text{well}} \times \frac{1}{1000} = 87,000,000 \text{ TU/mL}$$

$$1/3000 \quad \frac{2.33}{100} \times \frac{20,000}{\text{well}} \times \frac{1}{3000} = 46,600,000 \text{ TU/mL}$$

$$\frac{19,040,000 + 87,000,000 + 46,600,000}{3} = 51,080,000 \text{ TU/mL}$$

Infectious titer = 51,080,000 TU/mL

## 3.2 Aim 2: Transduction of $\gamma\delta$ T cells with CD19 or CD22 CAR lentivirus

### 3.2.1 Generating CD19 CAR $\gamma\delta$ T cells

Knowing the infectious titer of the CD19 CAR lentivirus determined using HEK 293A cells, different MOIs were tested to infect  $\gamma\delta$  T cells. Calculating the required volume of the CAR lentivirus stock for a given number of  $\gamma\delta$  T cells allows us to identify the MOI that yielded the highest transduction efficiency. First,  $\gamma\delta$  T cells were isolated from PBMCs, then expanded using IL-2, IL-15, and anti-CD3 (OKT3). Depending on the protocol of transduction followed (first or second), feeder cells were added to the OpTmizer medium at day 1 or day 3, respectively (**Fig.6B and 7B**).

Then, different MOIs were evaluated using the original CD19 lentiviral stock, provided by our collaborators, and based on the first protocol of transduction (**Fig.6**). Following  $\gamma\delta$  T cells isolation, expansion, transduction and a second expansion, CAR transduction rate was assessed by flow cytometry by analyzing the GFP expression at day 15. The original CD19 lentiviral stock had an infectious titer of 20,000,000 TU/mL. Therefore, to test MOI 4, 40  $\mu$ L of the CD19 lentivirus were used to infect 200,000  $\gamma\delta$  T cells, as shown below.

Calculation example:

$$\text{Volume required for MOI 4} = \frac{\#Cells}{\text{Viral titer} \left( \frac{TU}{mL} \right)} \times MOI$$
$$\frac{200,000}{\left( \frac{20,000,000}{mL} \right)} \times 4 = 0.04 \text{ mL}$$
$$\text{Volume of viral titer} = 40 \mu\text{L}$$

Flow cytometry analysis showed a CAR transduction rate of 35.7% at an MOI of 4, which exceeded our expectation (**Fig.12A**). Therefore, from the same experiment, a phenotypic analysis was performed to determine whether V $\delta$ 1, V $\delta$ 2 and V $\delta$ 1/2 neg  $\gamma\delta$  T cell subsets were efficiently transduced. As nearly all V $\delta$ 2 T cells express the V $\gamma$ 9 TCR chain, an anti-V $\gamma$ 9 TCR antibody was selected as a better fit for the panel design. The results show GFP expression across all subsets, confirming effective transduction (**Fig.12B**). V $\delta$ 1  $\gamma\delta$  T cell subsets (50.2%) were more abundant than V $\delta$ 2 (27.8%) and V $\delta$ 1/2 neg (17.5%)  $\gamma\delta$  T cell subsets. These results were surprising since V $\delta$ 2 T cell subsets are usually more present in the peripheral blood compared to V $\delta$ 1 T cell subsets. In our records, this donor was positive for the cytomegalovirus (CMV) ELISA test. Several studies showed that CMV might influence and shape the  $\gamma\delta$  T cells repertoire<sup>107,108</sup>. The CMV<sup>+</sup> status could therefore explain this observation.

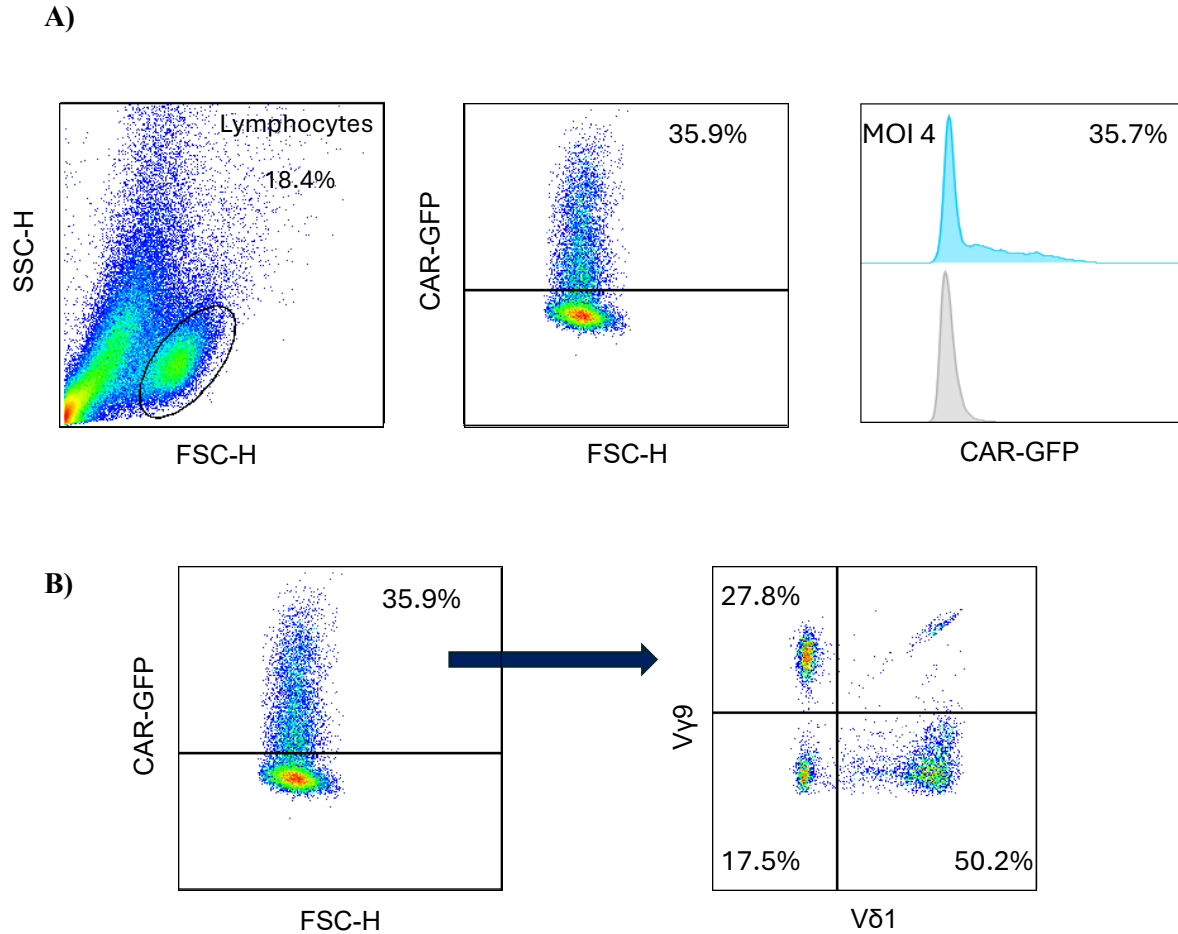


**Figure 12: Transduction of  $\gamma\delta$  T cells using the original CD19 CAR lentivirus stock and the first protocol of transduction.**  $\gamma\delta$  T cells were infected with CD19 CAR lentivirus at MOI 4. The infectious titer of the original CD19 CAR lentivirus stock was 20,000,000 TU/mL. Knowing the infectious titer, the number of  $\gamma\delta$  T cells and MOI, the volume of CD19 CAR lentiviral vector required was calculated. **(A)** Representative plots show the percentages of lymphocytes (left column) and the proportion of CAR<sup>+</sup>  $\gamma\delta$  T cells (middle column), while histograms compare the proportion of CAR-expressing  $\gamma\delta$  T cells to the control (left column) at day 7 post-transduction. **(B)** Flow cytometry plots show the proportion of CAR<sup>+</sup>  $\gamma\delta$  T cells from the experiment shown above and the percentage of the three main subsets, V $\delta$ 1, V $\delta$ 2 and V $\delta$ 1/2 neg, within CAR<sup>+</sup>  $\gamma\delta$  T cells (right panel).

### **3.2.2 Comparing different protocols of transduction to numerically transduce and expand CAR $\gamma\delta$ T-cell products**

Although the first transduction protocol yielded high transduction rates,  $\gamma\delta$  T cells viability was suboptimal, with the majority of cells dead by day 10 post-transduction, which corresponds to day 18 of the experiment. To circumvent this issue, a second protocol of transduction has been elaborated (**Fig.7**). This time,  $\gamma\delta$  T cells were infected with the original CD19 CAR lentivirus stock, at higher MOIs, and the second protocol of transduction was followed (**Fig.13**). CAR transduction efficiency was assessed at day 6 post-transduction. To test MOIs 25 and 90, 12,000 of  $\gamma\delta$  T cells were infected with 15  $\mu$ L and 50  $\mu$ L of the original CD19 CAR lentivirus stock, respectively. Flow cytometry plots showed that at an MOI of 25, 29.9% of  $\gamma\delta$  T cells were CAR-GFP<sup>+</sup>, whereas at an MOI of 90, 50.7% of  $\gamma\delta$  T cells were CAR-GFP<sup>+</sup>. Although these MOIs appear exceedingly high, they were calculated based on titration in HEK 293A cells and thus likely overestimate the effective MOIs for  $\gamma\delta$  T cells. The viability rates were better than the ones obtained with the first protocol based on the number of experiments performed. Therefore, the second procedure was selected as the optimized protocol for the transduction in this study.

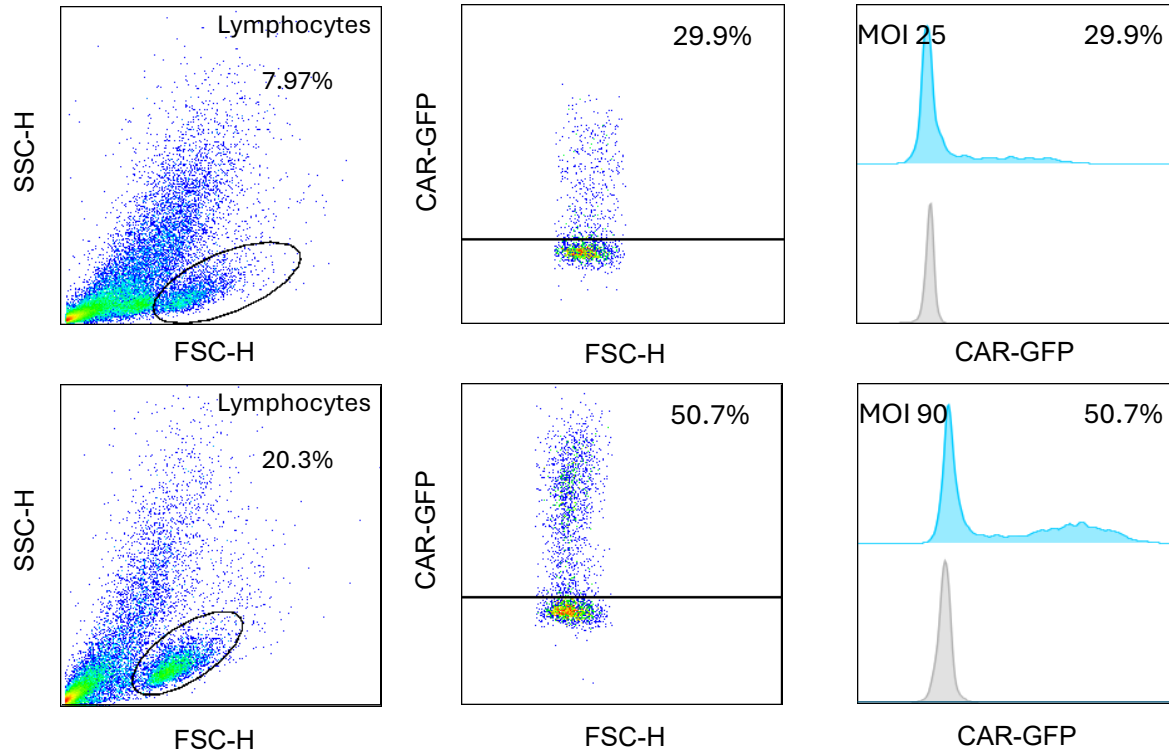


**Figure 13: Transduction of  $\gamma\delta$  T cells using the original CD19 CAR lentivirus stock and the second protocol of transduction.**  $\gamma\delta$  T cells were infected with CD19 CAR lentivirus at MOI 25 and 90. The infectious titer of the original CD19 CAR lentivirus stock was 20,000,000 TU/mL. The volume of CD19 CAR lentiviral vector required was calculated for each transduction, which were 15  $\mu$ L and 50  $\mu$ L, based on the infectious titer, the number of  $\gamma\delta$  T cells and MOI. (A) Representative plots show, from left to right, the percentages of lymphocytes, the proportion of CAR<sup>+</sup>  $\gamma\delta$  T cells, and histograms compare the proportion of CAR-expressing  $\gamma\delta$  T cells to the control,  $\gamma\delta$  T cells that were only expanded.

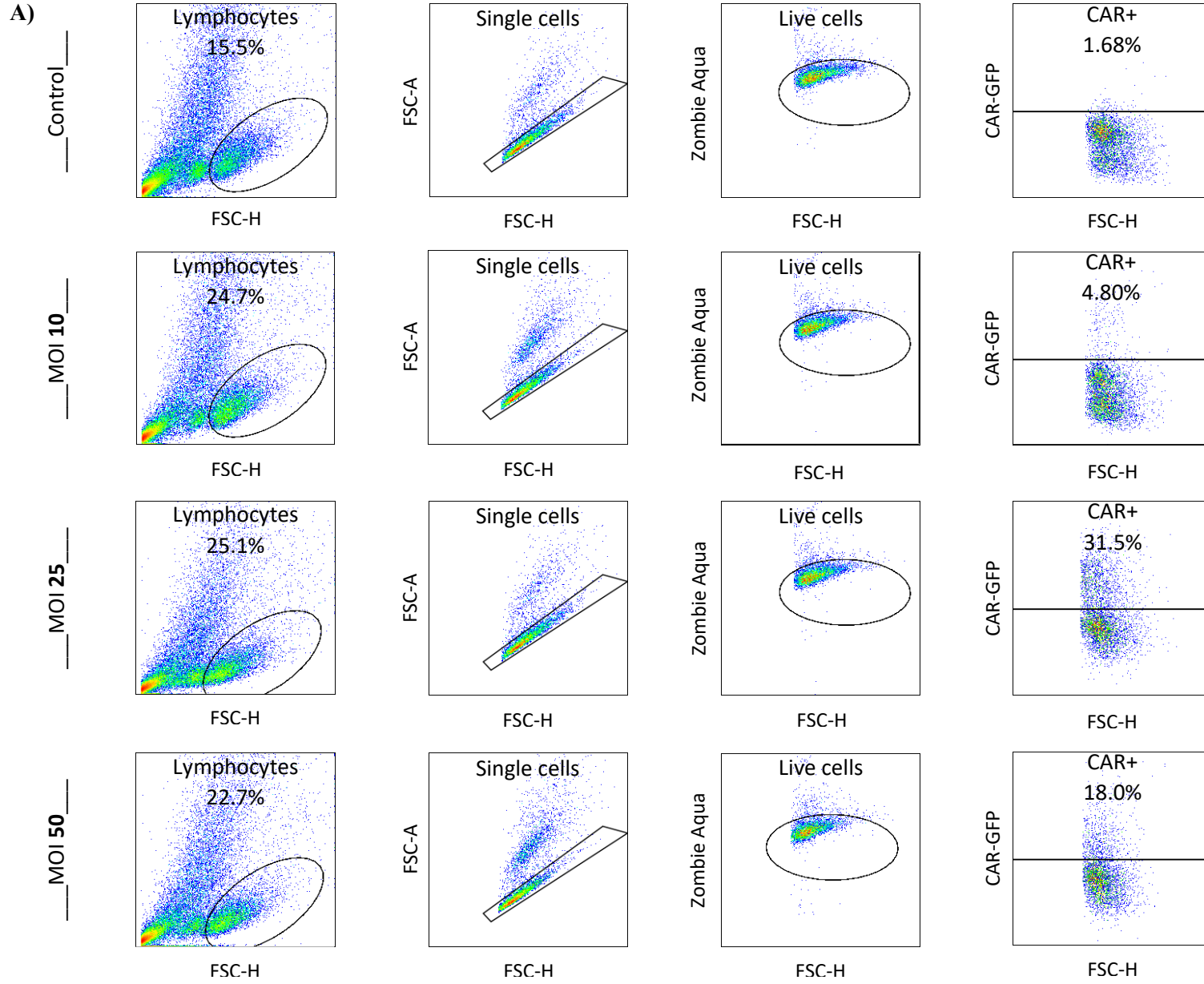
### 3.2.3 Identification of the optimal MOI

Next, from a CD19 CAR lentivirus stock that I generated, different MOIs were considered to evaluate their effect on the viability and transduction rate of  $\gamma\delta$  T cells. The infectious titer, obtained from titration with HEK293A cells, was 76,000,000 TU/mL for this specific CD19 CAR lentiviral stock. Thus, 1.3  $\mu$ L, 3.3  $\mu$ L and 6.6  $\mu$ L were used to transduce 10,000  $\gamma\delta$  T cells to test MOIs 10, 25 and 50, respectively. The transduction rates were assessed by GFP expression 6 days post-transduction. Flow cytometry analysis showed similar proportions of live cells for the three

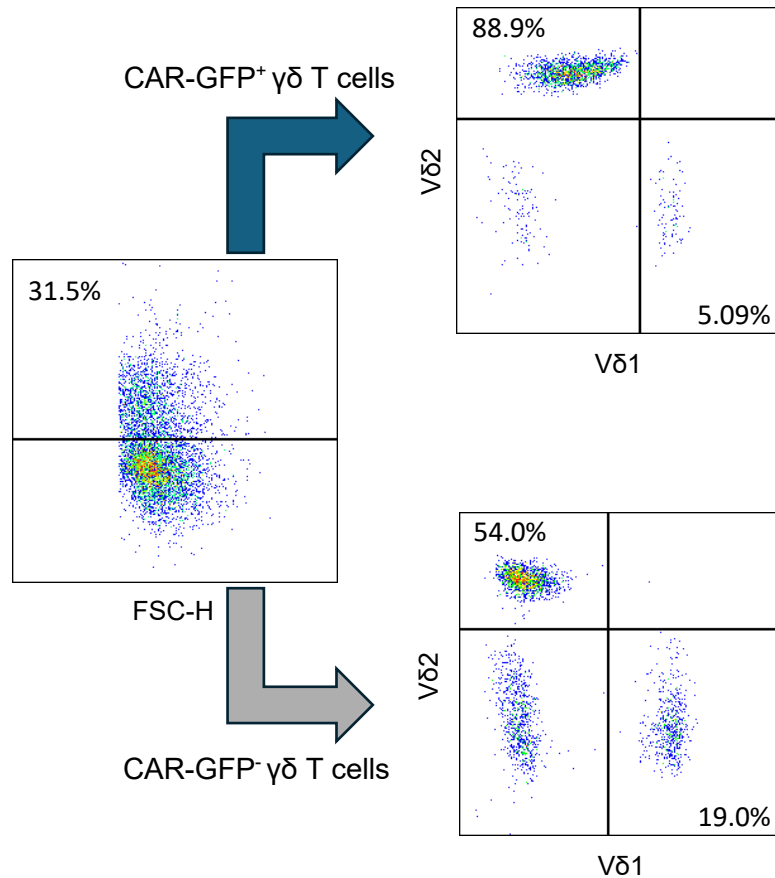
MOIs tested. Among these three MOIs, the MOI of 25 was optimal since it resulted in 31.5% of  $\gamma\delta$  T cells expressing CD19 CAR-GFP (**Fig.14A**), which represents a significant milestone in our research. CAR transduction efficacy of over 30% exceeds the clinical threshold for CAR therapy (about 20%)<sup>109</sup>,

From this same experiment, a phenotypic analysis was performed to compare the proportions of V $\delta$ 1, V $\delta$ 2 and V $\delta$ 1/2 neg T cells subsets within CAR-GFP<sup>-</sup>  $\gamma\delta$  T cells and CAR-GFP<sup>+</sup>  $\gamma\delta$  T cells. Flow cytometry analysis shows that the proportion of V $\delta$ 1  $\gamma\delta$  T cell subsets (19.0%) are lower in CAR-GFP<sup>-</sup>  $\gamma\delta$  T cells than that of V $\delta$ 2  $\gamma\delta$  T cell subsets (54.0%), in the bottom right panel (**Fig.14B**). Consequently, as shown in the upper right panel, the proportion of V $\delta$ 1  $\gamma\delta$  T cell subsets (5.09%) are also lower in CAR-GFP<sup>+</sup>  $\gamma\delta$  T cells, while V $\delta$ 2  $\gamma\delta$  T cell subsets are much higher (88.9%). These results align with the literature; V $\delta$ 2  $\gamma\delta$  T cell subsets are more abundant compared to V $\delta$ 1  $\gamma\delta$  T cell subsets in the peripheral blood. It should be noted that the transduction rate depends on the blood donor and the lentivirus stock.

Figure 14C shows the CAR transduction rates average for three experiments performed under the same conditions, where an MOI of 25 again yielded the highest transduction rate. Finally, to evaluate the transduction rate over time, for these three experiments, the GFP expression was assessed at day 8, 11 and 12 post-transductions (**Fig.15**). Unfortunately, all transduction rates decreased over time.



**B)**



**C)**

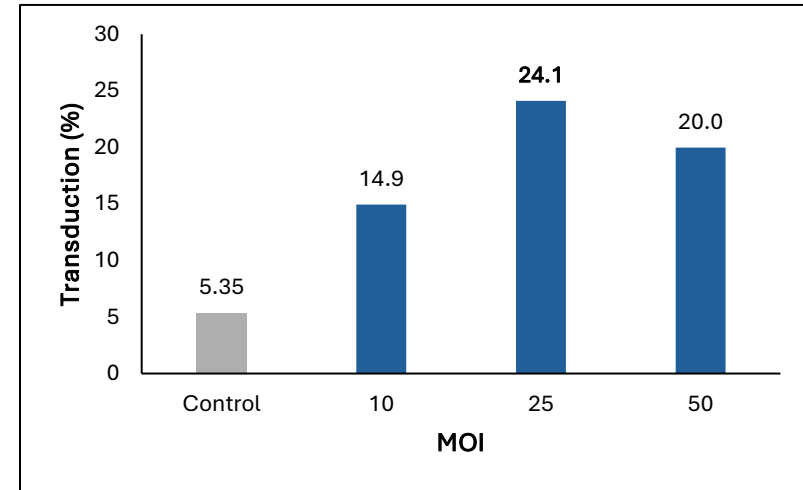


**Figure 14: Effects of different MOIs by using CD19 CAR lentivirus on the viability and transduction rate of  $\gamma\delta$  T cells.**  $\gamma\delta$  T cells were infected with CD19 CAR lentivirus at MOI 10, 25 and 50. The infectious titer of the CD19 CAR lentivirus was 76,000,000 TU/mL. (A) Representative plots show, from left to right, the percentage of lymphocytes, the single cells proportion, the percentage of live cells and the percentage of GFP<sup>+</sup>  $\gamma\delta$  T cells. The transduction rates were assessed by GFP expression and were compared to the control (top row),  $\gamma\delta$  T cells that were isolated from PBMCs and expanded. (B) Flow cytometry plots show the proportion of V $\delta$ 1, V $\delta$ 2 and V $\delta$ 1/2 neg  $\gamma\delta$  T cell subsets within CAR<sup>+</sup>  $\gamma\delta$  T cells. (C) Diagram showing the mean of transduction rate for three individual experiments conducted under the same conditions.

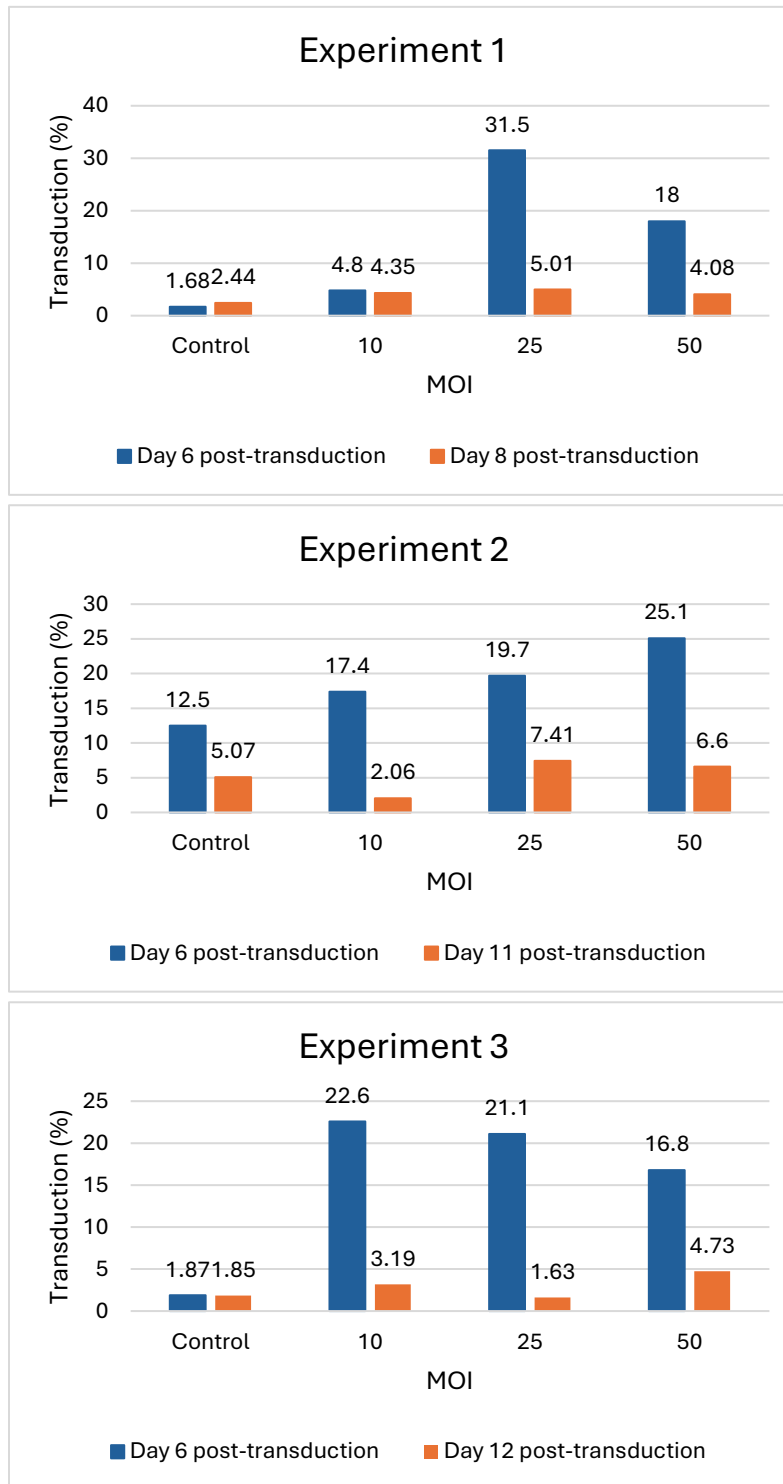


**Figure 15: Transduction rate assessed by GFP expression over time.** The bar graphs represent three experiments performed under the same conditions (i.e second protocol of transduction, blood donor and CD19 lentivirus stock). The infectious titer for the CD19 lentiviruses stock was 76,000,000 TU/mL. The volume of lentiviral vector used to transduce 10,000  $\gamma\delta$  T cells was 1.3  $\mu$ L, 3.3  $\mu$ L and 6.6  $\mu$ L to test MOIs 10, 25 and 50, respectively. GFP expression was assessed using flow cytometry at day 6 as well as day 8, 11 or 12 post-transduction, respectively.

### 3.2.4 Generating CD22 CAR $\gamma\delta$ T cells

The infectious titer of one of the two CD22 CAR lentivirus stocks that I generated was 14,100,000 TU/mL. Using this stock, I tested MOIs 10, 15 and 20. To infect 5,000  $\gamma\delta$  T cells at these MOIs, I used 3.6  $\mu$ L, 5.3  $\mu$ L and 7.1  $\mu$ L of CAR lentivirus, respectively. The transduction rates were evaluated at day 6 post-transduction. The proportions of live cells of all tested MOIs were similar to the control,  $\gamma\delta$  T cells that were not transduced (**Fig.16**). Flow cytometry plots on the right column show that the optimal MOI was 15, which corresponded to 5.18%  $\gamma\delta$  T cells CAR-GFP<sup>+</sup>. Similar transduction rates were obtained with the first protocol of transduction.

To exclude the possibility that some of the GFP<sup>+</sup> cells are feeder cells, wells of a 96-well plate containing only feeder cells were supplemented with OpTmizer as needed over 7 days. The feeder cells consisted of irradiated allogeneic PBMC and K562. At day 7 post-irradiation, the proportion of live cells was assessed to determine viability. Flow cytometry confirmed that the majority of feeder cells were dead by day 7, indicating they had been effectively cleared from the GFP<sup>+</sup> population (**Fig.S1**).

While transduction with the CD22 CAR lentivirus could be improved through further optimization, our results indicate that both protocols perform better with the CD19 construct, making CD19 CAR construct the more suitable candidate.

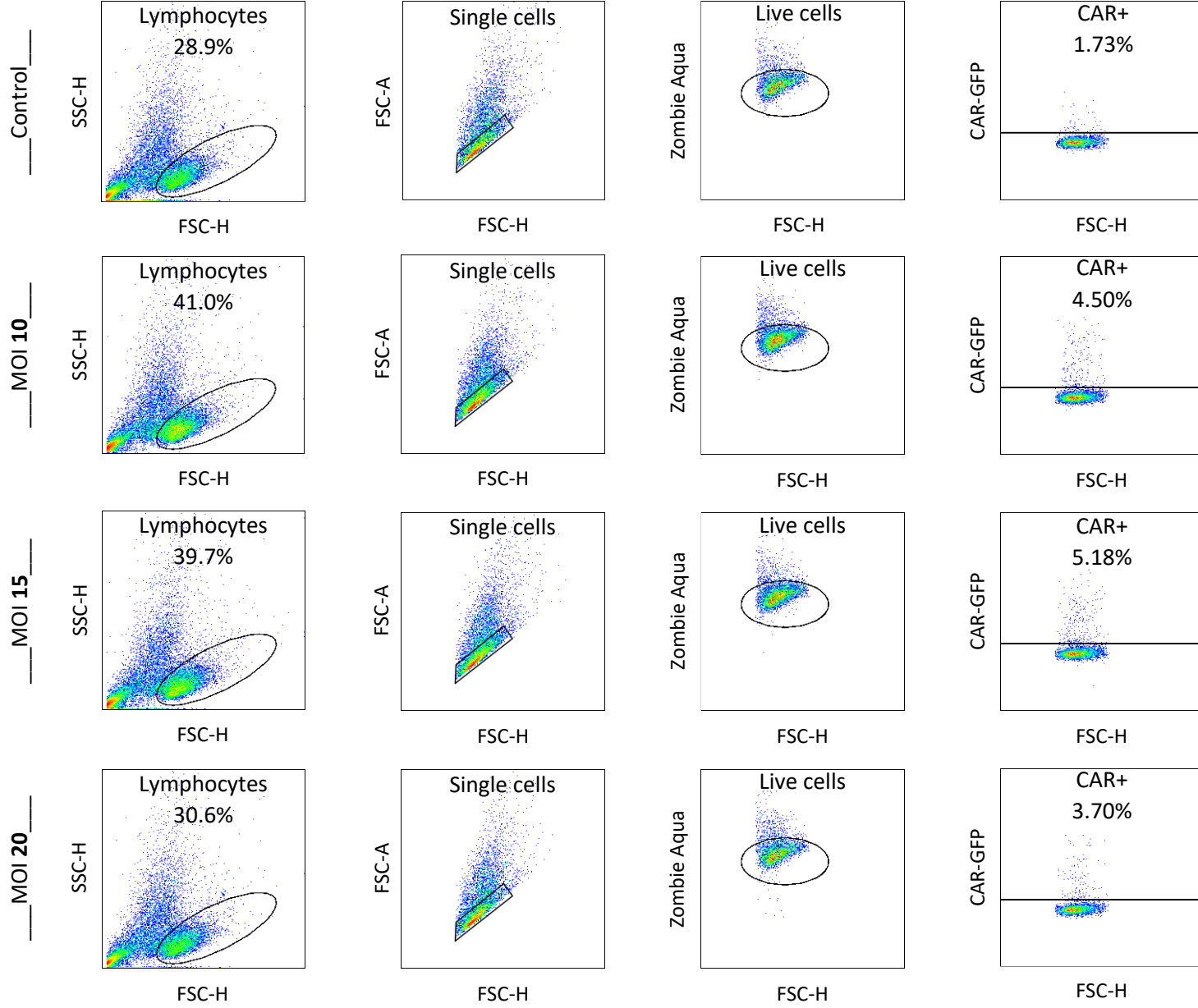


**Figure 16: Effects of different MOIs by using CD22 CAR lentivirus on the viability and transduction rate of  $\gamma\delta$  T cells.**  $\gamma\delta$  T cells were infected with CD22 CAR lentiviruses at MOI 10, 15 and 20. The infectious titer of the CD22 CAR lentivirus was 32,933,333 TU/mL. (A) Representative plots show, from left to right, the percentage of lymphocytes, the single cells proportion, the percentage of live cells and the percentage of GFP<sup>+</sup>  $\gamma\delta$  T cells. The transduction rates were assessed by GFP expression and were compared to the control (top row),  $\gamma\delta$  T cells that were isolated from PBMCs and expanded.

## 4. Discussion

CAR-T cell therapy, which is the combination of ACT with sophisticated engineering, is a new cancer treatment modality that has revolutionized the way to treat hematological malignancies including DLBCL, FL, MCL, B-cell acute lymphoblastic leukemia (B-ALL) and multiple myeloma (MM). In this study, we generated polyclonal CAR  $\gamma\delta$  T cells, as  $\gamma\delta$  T cells possess innate and adaptive immune properties and do not require HLA compatibility between patient and donor, making them ideal candidates for allogeneic CAR-T cell therapies. We decided to generate two CAR  $\gamma\delta$  T-cell products from two second-generation CAR constructs: 1) a CD19 murine scFv linked to a CD28-hinge domain, a 4-1BB costimulatory domain, and a CD3 $\zeta$  activation domain; and 2) a CD22 camelid sdAb linked to a CD8 hinge-domain, a 4-1BB costimulatory domain, and a CD3 $\zeta$  activation domain.

Our best infectious titers were 51,080,000 TU/mL and 32,933,333 TU/mL for CD19 and CD22 CAR LVs, respectively. Furthermore, EVOS microscope images of GFP expression, taken 72 hours after HEK293SF-PacLV cells were transfected with either CD19 or CD22 CAR plasmids, showed higher fluorescence in the cells transfected with the CD19 CAR. These results indicate that the HEK293SF-PacLV cells are easier to transfect with the CD19 CAR than with the CD22 CAR. Further experiments are needed to investigate the underlying cause. One possibility is that the CD19 CAR construct is more compatible with this third-generation lentiviral system than the CD22 CAR construct.

Flow cytometry analyses revealed that the optimal MOIs were 25 and 15 for CD19 CAR and CD22 CAR LVs, respectively. Despite the difficulty of comparing infectious titers obtained from different laboratories, a study of 2023 that generated a camelid nanobody-based CD19 CAR  $\alpha\beta$  T-

cell product and compared it with its murine scFv-based counterpart reported an optimal MOI of  $10^{103}$ . The discrepancy between their results and ours may be due to  $\gamma\delta$  T cells being inherently more resistant to lentiviral transduction than  $\alpha\beta$  T cells. Unfortunately, transduction rates for the CD22 CAR did not achieve expected results, with 5,18% being the highest transduction rate obtained. Nevertheless, flow cytometry analysis of CD19 CAR  $\gamma\delta$  T cell product showed a CAR transduction efficacy of over 30%, which surpasses the clinical threshold required for therapeutic applications. Notably, all  $\gamma\delta$  T cell subsets, V $\delta$ 1, V $\delta$ 2 and V $\delta$ 1/2 neg, were efficiently transduced. This high transduction rate represents a significant milestone in our research, as it confirms the feasibility of our approach.

Regarding the choice of target antigen for our CARs, we chose CD19 and CD22 as they are both antigens highly expressed in B-NHLs and have shown efficacy in several preclinical studies and clinical trials<sup>40,46,49,110-111</sup>. There are currently six CAR  $\alpha\beta$  T-cell therapies that were granted approval by the FDA, four of which targeting CD19 for the treatment of B-cell leukemia and lymphoma and two targeting BCMA for the treatment of MM. *Axicabtagene ciloleucel* (2017)<sup>40,110</sup>, *Tisagenlecleucel* (2017)<sup>48</sup>, *Brexucabtagene autoleucel* (2020)<sup>46,49</sup> and *Lisocabtagene maraleucel* (2021)<sup>111</sup> are all CD19 CAR  $\alpha\beta$  T-cell therapies that have been approved for DLBCL, FL and MCL. They have led to high rates of durable complete remission (CR) for patients with r/r DLBCL that had few other treatment options<sup>40,46,48,49,110-117</sup>. From three pivotal trials evaluating the safety and efficacy of CD19 CAR  $\alpha\beta$  T-cell therapies using *axi-cel*, *tisagenlecleucel* or *liso-cel* for the treatment of r/r DLBCL, the overall response rate (ORR) was 83%, 53% and 73% while the CR was 58%, 39% and 53%, respectively<sup>40,48,110,117</sup>. Despite the promising results, approximately 60% of patients do not respond or relapse within 2 years of treatment with CD19  $\alpha\beta$  CAR-T cell

therapies, mostly due to CD19 antigen expression loss on the surface of cancer cells, which accounts for up to 30% of reported relapse<sup>119,120,121</sup>.

Studies trying to elucidate relapse mechanisms in patients with *axi-cel*-treated DLBCL, evaluated protein and transcription levels of the CD19 antigen from biopsy samples collected before treatment and after relapse. These studies identified two differential relapse mechanisms: 1) target-related through evasion with CD19 antigen expression loss; and 2) suboptimal *in vivo* CAR-T expansion that can be attributed to premature exhaustion, impaired trafficking or immunosuppressive mechanisms occurring in the TME<sup>119,121</sup>. Moreover, CD19 CAR  $\alpha\beta$  T-cell therapies have been associated with cytokine release syndrome (CRS), immune effector cell-associated neurotoxicity syndrome (ICANS), as well as GvHD caused by the primary population of  $\alpha\beta$  T cells in the end product<sup>122-125</sup>. One way to overcome these challenges and avoid serious adverse events such as GvHD is to use another primary cell population to generate CAR-T cells, such as  $\gamma\delta$  T cells. Polyclonal CAR  $\gamma\delta$  T cells are HLA-independent and their natural diverse TCR repertoire could help compensate for CD19 loss by mediating intrinsic cytotoxicity.  $\gamma\delta$  T cells are implicated in both tumor surveillance and antitumor immunity, and among all immune cells,  $\gamma\delta$  T cells are the immune cell population whose tumor infiltration is the most significantly correlated with survival<sup>94</sup>.

Second generation CAR constructs are used because the addition of a co-stimulatory molecule enhances proliferation, activation and persistence of CAR-T cells compared to the first-generation of CARs<sup>126,127</sup>. All CAR-T cell products approved by the FDA are second generation. Even though a third generation, equipped with two co-stimulatory molecules, a fourth generation, having a cytokine inducer, and a fifth generation, supplied with a truncated cytokine receptor with STAT3 inducer, have been developed, they do not show better results than the second generation. Though

innovative and exciting, not all new constructs lead to better outcomes, as these generations showed CAR-T cell exhaustion or severe toxicity.

Furthermore, we selected CAR constructs composed of a 4-1BB costimulatory domain instead of CD28-based CAR constructs because studies support that 4-1BB-based CAR-T cells had a memory-like phenotype, which could help for *in vivo* persistence. Indeed, it has been shown that CAR-T cells with a CD28 costimulatory domain usually undergo high proliferation within 7 days of cell transfer but only persist for about 60 days after infusion<sup>39,40</sup>. In contrast, 4-1BB-based CAR-T cells take about 7 to 14 days to reach their peak number after ACT and can persist for several months<sup>41,42</sup>. For instance, in 2020, a preclinical study regarding an allogeneic CD123 CAR-Delta One T (DOT) cells for the treatment of acute myeloid leukemia (AML) showed higher persistence and cytotoxicity of second generation 4-1BB-based CAR-T cells compared to second generation CD28-based CAR-T cells in preclinical AML models<sup>125</sup>. It is worth mentioning that the recently approved allogeneic CD20 V $\delta$ 1 CAR  $\gamma\delta$  T-cell product for treating B-cell malignancies is a second generation 4-1BB-based CAR-T therapy (NCT04735471)<sup>98</sup>. In their preclinical study, the CD20 V $\delta$ 1 CAR  $\gamma\delta$  T-cell product showed significant tumor growth inhibition in B-cell lymphoma xenograft models. The mean volume tumor, observed at day 14 post-treatment in Raji-bearing mice ( $\sim 250 \text{ mm}^3$ ) and at day 30 post-treatment in JVM-2 mantle cell lymphoma-bearing mice ( $\sim 150 \text{ mm}^3$ ) was significantly smaller compared to control mice ( $\sim 2\,000 \text{ mm}^3$ )<sup>98</sup>. Thus, we opted for second generation CARs composed of a costimulatory domain that could persist longer throughout the body.

It is well known that LVs derived from lentivirus can efficiently deliver their genetic material into dividing cells and non-dividing cells, resulting in stable integration of the genes they carry into the host's genome. The HEK 293SF-PacLV that was used in this project contains all elements

necessary for LV assembly<sup>106</sup>. These elements include two packaging plasmids, one containing the *gag/pol* gene, which encodes for the capsid and three enzymes (the reverse transcriptase, integrase and transcriptase) and another plasmid containing the *rev* gene that encodes for the Rev protein. It also includes a plasmid carrying the *Env* gene, which in this case encodes VSV-G protein, enabling the infection of a broad range of cell types. These three plasmids were transfected simultaneously in HEK 293SF-3F6 cells that were previously engineered with the cumate and coumermycin inducible systems, in order to produce the HEK 293SF-PacLV and producer clones for self-inactivating (SIN) LV pseudotyped with VSV-G<sup>128,129,130</sup>. We specifically used the 3D4 clone derived from the HEK 293SF-PackLVIIIb stock<sup>106</sup>.

A great advantage of using a packaging cell line is that it allowed us to do one transfection with only one plasmid, the transgene of interest (TOI) (i.e CD19 or CD22 CARs), instead of with four plasmids, which represents the most straightforward method to produce LVs. Moreover, we chose this cell line because it has been shown that the third-generation system is safer to produce LVs compared to the second-generation system, largely due to the separation of *gag/pol* and *rev* genes split into two plasmids<sup>131,132</sup>. Additional safety features are in the transfer plasmid, which includes the chimeric 5'LTR fused to a CMV promoter, eliminating the need for HIV Tat to drive transcription. Most importantly, a deletion in 3'LTR enables its transfer to the 5'LTR after one round of reverse transcription, inhibiting transcription of the LV genome after integration into the host genome. We therefore used the safest generation system to produce our SIN LVs, equipped with the cumate and coumermycin inducible system, which ensures a tight control of the expression of genes required for LV assembly.

Clinical studies employing CAR  $\gamma\delta$  T cells are currently in early clinical stages, with only a few studies providing preliminary data. There are only eight active clinical trials on CAR  $\gamma\delta$  T cells,

according to ClinicalTrials.gov, which shows how new this field of study is. In 2021, the first-in-class allogeneic CAR V $\delta$ 1<sup>+</sup>  $\gamma\delta$  T-cell therapy aiming to target the B-cell antigen CD20 in patients with r/r advanced B-cell lymphoma has initiated a Phase 1 clinical trial, which was completed in June 2025 (NCT04735471)<sup>97</sup>. This CAR-T therapy is also currently tested for autoimmune diseases (NCT06375993) and has just started, in August, another Phase 1 clinical trial for treating rheumatoid arthritis (RA) (NCT07100873). The recent approval of this allogeneic CD20 CAR  $\gamma\delta$  T-cell product has led to the elaboration of others CAR-T cell based on  $\gamma\delta$  T cells. Five CAR  $\gamma\delta$  T-cell therapies were registered and entered Phase 1 clinical trials in 2024. One targets CD19 and is intended for treating patients with systemic lupus erythematosus (SLE) (NCT06106893), while another focuses on advanced solid tumors or hematological malignancies (NCT05302037)<sup>122,123,133-136</sup> and targets NKG2DL ligands. A third therapy is intended for treating autoimmune diseases such as lupus nephritis (NCT06375993) and targets CD20, whereas the fourth focuses on clear cell renal cell carcinoma (ccRCC) (NCT06480565)<sup>137</sup> and targets CD70. Finally, the last one is an HLA-G-CAR.BiTE allogeneic  $\gamma\delta$  T-cell product tested in r/r solid cancers such as non-small cell lung cancer (NSCLC), triple negative breast cancer (TNBC), colorectal cancer (CRC) and glioblastoma multiforme (GBM) (NCT06150885)<sup>138</sup>. All these therapies are based on V $\delta$ 1 or V $\delta$ 2 T cells. The novelty of our product is that it encompasses all V $\delta$ 1, V $\delta$ 2 and V $\delta$ 1/2 neg  $\gamma\delta$  T cell subsets, aiming to target a broad range of antigens through the cells' inherent antigen-recognition capabilities and to compensate for potential antigen loss.

#### 4.1 Conclusion and future directions

In conclusion, I have generated a first polyclonal CD19 CAR  $\gamma\delta$  T-cell product, achieving a CAR transduction efficiency of 30% and encompassing all  $\gamma\delta$  T cell subsets. The protocol used supports the expansion of the transduced cells, demonstrating feasibility of our approach and enabling future preclinical studies in our lab. The protocol for CD22 CAR  $\gamma\delta$  T cells is still being optimized. Of note, the transduction rates were variable across individuals and in the phenotypic analyses, one blood donor was CMV<sup>+</sup>, while all other blood donors were CMV<sup>-</sup>, which may have had an impact on the proportions of  $\gamma\delta$  T cell subset in their peripheral blood.

The future directions of this research include further phenotyping of the generated CAR  $\gamma\delta$  T cells using spectral flow cytometry with a large antibody panel that targets surface proteins, intracellular cytokines and transcriptional factors. Additionally, *in vitro* killing assays against both wild-type and CD19-negative Ramos and Raji B cell lines should be performed to assess specificity to B lymphoma. Finally, following *in vitro* studies, the CD19 CAR  $\gamma\delta$  T cells should be evaluated for *in vivo* efficacy using mouse models.

## 4.1 References

1. Canadian Cancer Society's Advisory Committee on Cancer Statistics. Canadian Cancer Statistics 2017. Toronto, ON: Canadian Cancer Society; 2017. Available at: [www.cancer.ca/en/cancer-information/cancer-101/canadian-cancer-statistics-publication](http://www.cancer.ca/en/cancer-information/cancer-101/canadian-cancer-statistics-publication)
2. Brenner DR, Gillis J, Demers AA, Ellison LF, Billette JM, Zhang SX, Liu JL, Woods RR, Finley C, Fitzgerald N, Saint-Jacques N, Shack L, Turner D. Projected estimates of cancer in Canada. *Canadian Medical Association J.* 2024 May 196 (18) E615-E623. doi: <https://doi.org/10.1503/cmaj.240095>
3. Myllykangas S, Himberg J, Böhling T, Nagy B, Hollmén J, Knuutila S. DNA copy number amplification profiling of human neoplasms. *Oncogene.* 2006 Nov 23;25(55):7324-32. doi: 10.1038/sj.onc.1209717. Epub 2006 Jun 5. PMID: 16751803.
4. Hanahan D, Weinberg RA. The hallmarks of cancer. *Cell.* 2000 Jan 7;100(1):57-70. doi: 10.1016/s0092-8674(00)81683-9. PMID: 10647931.
5. Hanahan D, Weinberg RA. Hallmarks of cancer: the next generation. *Cell.* 2011 Mar 4;144(5):646-74. doi: 10.1016/j.cell.2011.02.013. PMID: 21376230.
6. Kroemer G, Pouyssegur J. Tumor cell metabolism: cancer's Achilles' heel. *Cancer Cell.* 2008 Jun;13(6):472-82. doi: 10.1016/j.ccr.2008.05.005. PMID: 18538731.
7. Jones S, Zhang X, Parsons DW, Lin JC, Leary RJ, Angenendt P, Mankoo P, Carter H, Kamiyama H, Jimeno A, Hong SM, Fu B, Lin MT, Calhoun ES, Kamiyama M, Walter K, Nikolskaya T, Nikolsky Y, Hartigan J, Smith DR, Hidalgo M, Leach SD, Klein AP, Jaffee EM, Goggins M, Maitra A, Iacobuzio-Donahue C, Eshleman JR, Kern SE, Hruban RH, Karchin R, Papadopoulos N, Parmigiani G, Vogelstein B, Velculescu VE, Kinzler KW. Core signaling pathways in human pancreatic cancers revealed by global genomic analyses. *Science.* 2008 Sep 26;321(5897):1801-6. doi: 10.1126/science.1164368. Epub 2008 Sep 4. PMID: 18772397; PMCID: PMC2848990.
8. Cox AD, Fesik SW, Kimmelman AC, Luo J, Der CJ. Drugging the undruggable RAS: Mission possible? *Nat Rev Drug Discov.* 2014 Nov;13(11):828-51. doi: 10.1038/nrd4389. Epub 2014 Oct 17. PMID: 25323927; PMCID: PMC4355017.
9. Conroy M, Cowzer D, Kolch W, Duffy AG. Emerging RAS-directed therapies for cancer. *Cancer Drug Resist.* 2021 Apr 8;4(3):543-558. doi: 10.20517/cdr.2021.07. PMID: 35582302; PMCID: PMC9094076.
10. Degirmenci U, Wang M, Hu J. Targeting Aberrant RAS/RAF/MEK/ERK Signaling for Cancer Therapy. *Cells.* 2020 Jan 13;9(1):198. doi: 10.3390/cells9010198. PMID: 31941155; PMCID: PMC7017232.
11. Castellano E, Downward J. RAS Interaction with PI3K: More Than Just Another Effector Pathway. *Genes Cancer.* 2011 Mar;2(3):261-74. doi: 10.1177/1947601911408079. PMID: 21779497; PMCID: PMC3128635.
12. Coelho MA, de Carné Trécesson S, Rana S, Zecchin D, Moore C, Molina-Arcas M, East P, Spencer-Dene B, Nye E, Barnouin K, Snijders AP, Lai WS, Blackshear PJ, Downward J. Oncogenic RAS Signaling Promotes Tumor Immuno-resistance by Stabilizing PD-L1 mRNA. *Immunity.* 2017 Dec 19;47(6):1083-1099.e6. doi: 10.1016/j.immuni.2017.11.016. Epub 2017 Dec 12. PMID: 29246442; PMCID: PMC5746170.
13. Connell PP, Hellman S. Advances in radiotherapy and implications for the next century: a historical perspective. *Cancer Res.* 2009 Jan 15;69(2):383-92. doi: 10.1158/0008-5472.CAN-07-6871. PMID: 19147546.

14. DeVita VT Jr, Chu E. A history of cancer chemotherapy. *Cancer Res.* 2008 Nov 1;68(21):8643-53. doi: 10.1158/0008-5472.CAN-07-6611. PMID: 18974103.
15. Baskar R, Lee KA, Yeo R, Yeoh KW. Cancer and radiation therapy: current advances and future directions. *Int J Med Sci.* 2012;9(3):193-9. doi: 10.7150/ijms.3635. Epub 2012 Feb 27. PMID: 22408567; PMCID: PMC3298009
16. Welty NE, Gill SI. Cancer Immunotherapy Beyond Checkpoint Blockade: JACC: CardioOncology State-of-the-Art Review. *JACC CardioOncol.* 2022 Dec 20;4(5):563-578. doi: 10.1016/j.jacc.2022.11.006. PMID: 36636439; PMCID: PMC9830230.
17. Silkenstedt E, Salles G, Campo E, Dreyling M. B-cell non-Hodgkin lymphomas. *Lancet.* 2024 May 4;403(10438):1791-1807. doi: 10.1016/S0140-6736(23)02705-8. Epub 2024 Apr 10. PMID: 38614113; PMCID: PMC12261310.
18. Freeman AM, Matto P. Lymphadenopathy. 2023 Feb 20. In: StatPearls [Internet]. Treasure Island (FL): StatPearls Publishing; 2025 Jan-. PMID: 30020622.
19. Alfaifi A, Refai MY, Alsaadi M, Bahashwan S, Malhan H, Al-Kahiry W, Dammag E, Ageel A, Mahzary A, Albiheyri R, Almehdar H, Qadri I. Metabolomics: A New Era in the Diagnosis or Prognosis of B-Cell Non-Hodgkin's Lymphoma. *Diagnostics (Basel).* 2023 Feb 23;13(5):861. doi: 10.3390/diagnostics13050861. PMID: 36900005; PMCID: PMC10000528.
20. Xu W, Berning P, Lenz G. Targeting B-cell receptor and PI3K signaling in diffuse large B-cell lymphoma. *Blood.* 2021 Sep 30;138(13):1110-1119. doi: 10.1182/blood.2020006784. PMID: 34320160.
21. Canadian Cancer Society. 2030 Oct Available at: [Diffuse large B-cell lymphoma | Canadian Cancer Society](#)
22. Moleti ML, Testi AM, Foà R. Treatment of relapsed/refractory paediatric aggressive B-cell non-Hodgkin lymphoma. *Br J Haematol.* 2020 Jun;189(5):826-843. doi: 10.1111/bjh.16461. Epub 2020 Mar 6. PMID: 32141616.
23. Dreyling M, Ghielmini M, Rule S, Salles G, Vitolo U, Ladetto M; ESMO Guidelines Committee. Newly diagnosed and relapsed follicular lymphoma: ESMO Clinical Practice Guidelines for diagnosis, treatment and follow-up. *Ann Oncol.* 2016 Sep;27(suppl 5):v83-v90. doi: 10.1093/annonc/mdw400. Erratum in: *Ann Oncol.* 2017 Dec 1;28(12):3109. doi: 10.1093/annonc/mdx020. PMID: 27664263.
24. Tilly H, Gomes da Silva M, Vitolo U, Jack A, Meignan M, Lopez-Guillermo A, Walewski J, André M, Johnson PW, Pfreundschuh M, Ladetto M; ESMO Guidelines Committee. Diffuse large B-cell lymphoma (DLBCL): ESMO Clinical Practice Guidelines for diagnosis, treatment and follow-up. *Ann Oncol.* 2015 Sep;26 Suppl 5:v116-25. doi: 10.1093/annonc/mdv304. PMID: 26314773.
25. Eichhorst B, Robak T, Montserrat E, Ghia P, Hillmen P, Hallek M, Buske C; ESMO Guidelines Committee. Chronic lymphocytic leukaemia: ESMO Clinical Practice Guidelines for diagnosis, treatment and follow-up. *Ann Oncol.* 2015 Sep;26 Suppl 5:v78-84. doi: 10.1093/annonc/mdv303. PMID: 26314781.
26. Wilson WH, Young RM, Schmitz R, Yang Y, Pittaluga S, Wright G, Lih CJ, Williams PM, Shaffer AL, Gerecitano J, de Vos S, Goy A, Kenkre VP, Barr PM, Blum KA, Shustov A, Advani R, Fowler NH, Vose JM, Elstrom RL, Habermann TM, Barrientos JC, McGreivy J, Fardis M, Chang BY, Clow F, Munneke B, Moussa D, Beaupre DM, Staudt LM. Targeting B cell receptor signaling with ibrutinib in diffuse large B cell lymphoma. *Nat Med.* 2015 Aug;21(8):922-6. doi: 10.1038/nm.3884. Epub 2015 Jul 20. PMID: 26193343; PMCID: PMC8372245.

27. Sauter CS, Matasar MJ, Schoder H, Devlin SM, Drullinsky P, Gerecitano J, Kumar A, Noy A, Palomba ML, Portlock CS, Straus DJ, Zelenetz AD, McCall SJ, Miller ST, Courtien AI, Younes A, Moskowitz CH. A phase 1 study of ibrutinib in combination with R-ICE in patients with relapsed or primary refractory DLBCL. *Blood*. 2018 Apr 19;131(16):1805-1808. doi: 10.1182/blood-2017-08-802561. Epub 2018 Jan 31. PMID: 29386196; PMCID: PMC5909762.
28. Zinzani PL, Ribrag V, Moskowitz CH, Michot JM, Kuruvilla J, Balakumaran A, Zhang Y, Chlosta S, Shipp MA, Armand P. Safety and tolerability of pembrolizumab in patients with relapsed/refractory primary mediastinal large B-cell lymphoma. *Blood*. 2017 Jul 20;130(3):267-270. doi: 10.1182/blood-2016-12-758383. Epub 2017 May 10. PMID: 28490569; PMCID: PMC5766837.
29. Armand P, Rodig S, Melnichenko V, Thieblemont C, Bouabdallah K, Tumyan G, Özcan M, Portino S, Fogliatto L, Caballero MD, Walewski J, Gulbas Z, Ribrag V, Christian B, Perini GF, Salles G, Svoboda J, Zain J, Patel S, Chen PH, Ligon AH, Ouyang J, Neuberg D, Redd R, Chatterjee A, Balakumaran A, Orlowski R, Shipp M, Zinzani PL. Pembrolizumab in Relapsed or Refractory Primary Mediastinal Large B-Cell Lymphoma. *J Clin Oncol*. 2019 Dec 1;37(34):3291-3299. doi: 10.1200/JCO.19.01389. Epub 2019 Oct 14. PMID: 31609651; PMCID: PMC6881098.
30. Tomassetti S, Chen R, Dandapani S. The role of pembrolizumab in relapsed/refractory primary mediastinal large B-cell lymphoma. *Ther Adv Hematol*. 2019 Apr 22;10:2040620719841591. doi: 10.1177/2040620719841591. PMID: 31040936; PMCID: PMC6477766.
31. Awasthi A, Ayello J, Van de Ven C, Elmacken M, Sabulski A, Barth MJ, Czuczman MS, Islam H, Klein C, Cairo MS. Obinutuzumab (GA101) compared to rituximab significantly enhances cell death and antibody-dependent cytotoxicity and improves overall survival against CD20(+) rituximab-sensitive/-resistant Burkitt lymphoma (BL) and precursor B-acute lymphoblastic leukaemia (pre-B-ALL): potential targeted therapy in patients with poor risk CD20(+) BL and pre-B-ALL. *Br J Haematol*. 2015 Dec;171(5):763-75. doi: 10.1111/bjh.13764. Epub 2015 Oct 16. PMID: 26471982.
32. Advani A, Coiffier B, Czuczman MS, Dreyling M, Foran J, Gine E, Gisselbrecht C, Ketterer N, Nasta S, Rohatiner A, Schmidt-Wolf IG, Schuler M, Sierra J, Smith MR, Verhoef G, Winter JN, Boni J, Vandendries E, Shapiro M, Fayad L. Safety, pharmacokinetics, and preliminary clinical activity of inotuzumab ozogamicin, a novel immunoconjugate for the treatment of B-cell non-Hodgkin's lymphoma: results of a phase I study. *J Clin Oncol*. 2010 Apr 20;28(12):2085-93. doi: 10.1200/JCO.2009.25.1900. Epub 2010 Mar 22. PMID: 20308665.
33. Goebeler ME, Knop S, Viardot A, Kufer P, Topp MS, Einsele H, Noppeney R, Hess G, Kallert S, Mackensen A, Rupertus K, Kanz L, Libicher M, Nagorsen D, Zugmaier G, Klinger M, Wolf A, Dorsch B, Quednau BD, Schmidt M, Scheele J, Baeuerle PA, Leo E, Bargou RC. Bispecific T-Cell Engager (BiTE) Antibody Construct Blinatumomab for the Treatment of Patients With Relapsed/Refractory Non-Hodgkin Lymphoma: Final Results From a Phase I Study. *J Clin Oncol*. 2016 Apr 1;34(10):1104-11. doi: 10.1200/JCO.2014.59.1586. Epub 2016 Feb 16. PMID: 26884582.
34. Viardot A, Goebeler ME, Hess G, Neumann S, Pfreundschuh M, Adrian N, Zettl F, Libicher M, Sayehli C, Stieglmaier J, Zhang A, Nagorsen D, Bargou RC. Phase 2 study of the bispecific T-cell engager (BiTE) antibody blinatumomab in relapsed/refractory diffuse large B-cell lymphoma. *Blood*. 2016 Mar 17;127(11):1410-6. doi: 10.1182/blood-2015-06-651380. Epub 2016 Jan 11. PMID: 26755709; PMCID: PMC4797019.
35. Brudno JN, Maus MV, Hinrichs CS. CAR T Cells and T-Cell Therapies for Cancer: A Translational Science Review. *JAMA*. 2024 Dec 10;332(22):1924-1935. doi: 10.1001/jama.2024.19462. PMID: 39495525; PMCID: PMC11808657.

36. Maalej KM, Merhi M, Inchakalody VP, Mestiri S, Alam M, Maccalli C, Cherif H, Uddin S, Steinhoff M, Marincola FM, Dermime S. CAR-cell therapy in the era of solid tumor treatment: current challenges and emerging therapeutic advances. *Mol Cancer*. 2023 Jan 30;22(1):20. doi: 10.1186/s12943-023-01723-z. PMID: 36717905; PMCID: PMC9885707.
37. Kandra P, Nandigama R, Eul B, Huber M, Kobold S, Seeger W, Grimminger F, Savai R. Utility and Drawbacks of Chimeric Antigen Receptor T Cell (CAR-T) Therapy in Lung Cancer. *Front Immunol*. 2022 Jun 2;13:903562. doi: 10.3389/fimmu.2022.903562. PMID: 35720364; PMCID: PMC9201083.
38. Eshhar Z, Waks T, Gross G, Schindler DG. Specific activation and targeting of cytotoxic lymphocytes through chimeric single chains consisting of antibody-binding domains and the gamma or zeta subunits of the immunoglobulin and T-cell receptors. *Proc Natl Acad Sci U S A*. 1993 Jan 15;90(2):720-4. doi: 10.1073/pnas.90.2.720. PMID: 8421711; PMCID: PMC45737.
39. Kochenderfer JN, Dudley ME, Kassim SH, Somerville RP, Carpenter RO, Stetler-Stevenson M, Yang JC, Phan GQ, Hughes MS, Sherry RM, Raffeld M, Feldman S, Lu L, Li YF, Ngo LT, Goy A, Feldman T, Spaner DE, Wang ML, Chen CC, Kranick SM, Nath A, Nathan DA, Morton KE, Toomey MA, Rosenberg SA. Chemotherapy-refractory diffuse large B-cell lymphoma and indolent B-cell malignancies can be effectively treated with autologous T cells expressing an anti-CD19 chimeric antigen receptor. *J Clin Oncol*. 2015 Feb 20;33(6):540-9. doi: 10.1200/JCO.2014.56.2025. Epub 2014 Aug 25. PMID: 25154820; PMCID: PMC4322257.
40. Neelapu SS, Locke FL, Bartlett NL, Lekakis LJ, Miklos DB, Jacobson CA, Braunschweig I, Oluwole OO, Siddiqi T, Lin Y, Timmerman JM, Stiff PJ, Friedberg JW, Flinn IW, Goy A, Hill BT, Smith MR, Deol A, Farooq U, McSweeney P, Munoz J, Avivi I, Castro JE, Westin JR, Chavez JC, Ghobadi A, Komanduri KV, Levy R, Jacobsen ED, Witzig TE, Reagan P, Bot A, Rossi J, Navale L, Jiang Y, Aycock J, Elias M, Chang D, Wiezorek J, Go WY. Axicabtagene Ciloleucel CAR T-Cell Therapy in Refractory Large B-Cell Lymphoma. *N Engl J Med*. 2017 Dec 28;377(26):2531-2544. doi: 10.1056/NEJMoa1707447. Epub 2017 Dec 10. PMID: 29226797; PMCID: PMC5882485.
41. Turtle CJ, Hanafi LA, Berger C, Gooley TA, Cherian S, Hudecek M, Sommermeyer D, Melville K, Pender B, Budiarto TM, Robinson E, Steevens NN, Chaney C, Soma L, Chen X, Yeung C, Wood B, Li D, Cao J, Heimfeld S, Jensen MC, Riddell SR, Maloney DG. CD19 CAR-T cells of defined CD4+:CD8+ composition in adult B cell ALL patients. *J Clin Invest*. 2016 Jun 1;126(6):2123-38. doi: 10.1172/JCI85309. Epub 2016 Apr 25. PMID: 27111235; PMCID: PMC4887159.
42. Maude SL, Laetsch TW, Buechner J, Rives S, Boyer M, Bittencourt H, Bader P, Verneris MR, Stefanski HE, Myers GD, Qayed M, De Moerloose B, Hiramatsu H, Schlis K, Davis KL, Martin PL, Nemecek ER, Yanik GA, Peters C, Baruchel A, Boissel N, Mechinaud F, Balduzzi A, Krueger J, June CH, Levine BL, Wood P, Taran T, Leung M, Mueller KT, Zhang Y, Sen K, Lebwohl D, Pulsipher MA, Grupp SA. Tisagenlecleucel in Children and Young Adults with B-Cell Lymphoblastic Leukemia. *N Engl J Med*. 2018 Feb 1;378(5):439-448. doi: 10.1056/NEJMoa1709866. PMID: 29385370; PMCID: PMC5996391.
43. Salter AI, Ivey RG, Kennedy JJ, Voillet V, Rajan A, Alderman EJ, Voytovich UJ, Lin C, Sommermeyer D, Liu L, Whiteaker JR, Gottardo R, Paulovich AG, Riddell SR. Phosphoproteomic analysis of chimeric antigen receptor signaling reveals kinetic and quantitative differences that affect cell function. *Sci Signal*. 2018 Aug 21;11(544):eaat6753. doi: 10.1126/scisignal.aat6753. PMID: 30131370; PMCID: PMC6186424.

44. Cappell KM, Kochenderfer JN. Long-term outcomes following CAR T cell therapy: what we know so far. *Nat Rev Clin Oncol*. 2023 Jun;20(6):359-371. doi: 10.1038/s41571-023-00754-1. Epub 2023 Apr 13. PMID: 37055515; PMCID: PMC10100620.
45. Chen L, Xie T, Wei B, Di DL. Current progress in CAR-T cell therapy for tumor treatment. *Oncol Lett*. 2022 Aug 25;24(4):358. doi: 10.3892/ol.2022.13478. PMID: 36168313; PMCID: PMC9478623.
46. Wang M, Munoz J, Goy A, Locke FL, Jacobson CA, Hill BT, Timmerman JM, Holmes H, Jaglowski S, Flinn IW, McSweeney PA, Miklos DB, Pagel JM, Kersten MJ, Bouabdallah K, Khanal R, Topp MS, Houot R, Beitinjaneh A, Peng W, Fang X, Shen RR, Siddiqi R, Kloos I, Reagan PM. Three-Year Follow-Up of KTE-X19 in Patients With Relapsed/Refractory Mantle Cell Lymphoma, Including High-Risk Subgroups, in the ZUMA-2 Study. *J Clin Oncol*. 2023 Jan 20;41(3):555-567. doi: 10.1200/JCO.21.02370. Epub 2022 Jun 4. PMID: 35658525; PMCID: PMC9870225.
47. Papadouli I, Mueller-Berghaus J, Beuneu C, Ali S, Hofner B, Petavy F, Tzogani K, Miermont A, Norga K, Kholmanskikh O, Leest T, Schuessler-Lenz M, Salmonson T, Gisselbrecht C, Garcia JL, Pignatti F. EMA Review of Axicabtagene Ciloleucel (Yescarta) for the Treatment of Diffuse Large B-Cell Lymphoma. *Oncologist*. 2020 Oct;25(10):894-902. doi: 10.1634/theoncologist.2019-0646. Epub 2020 Apr 27. PMID: 32339368; PMCID: PMC7543293.
48. Schuster SJ, Bishop MR, Tam CS, Waller EK, Borchmann P, McGuirk JP, Jäger U, Jaglowski S, Andreadis C, Westin JR, Fleury I, Bachanova V, Foley SR, Ho PJ, Mielke S, Magenau JM, Holte H, Pantano S, Pacaud LB, Awasthi R, Chu J, Anak Ö, Salles G, Maziarz RT; JULIET Investigators. Tisagenlecleucel in Adult Relapsed or Refractory Diffuse Large B-Cell Lymphoma. *N Engl J Med*. 2019 Jan 3;380(1):45-56. doi: 10.1056/NEJMoa1804980. Epub 2018 Dec 1. PMID: 30501490.
49. Wang M, Munoz J, Goy A, Locke FL, Jacobson CA, Hill BT, Timmerman JM, Holmes H, Jaglowski S, Flinn IW, McSweeney PA, Miklos DB, Pagel JM, Kersten MJ, Milpied N, Fung H, Topp MS, Houot R, Beitinjaneh A, Peng W, Zheng L, Rossi JM, Jain RK, Rao AV, Reagan PM. KTE-X19 CAR T-Cell Therapy in Relapsed or Refractory Mantle-Cell Lymphoma. *N Engl J Med*. 2020 Apr 2;382(14):1331-1342. doi: 10.1056/NEJMoa1914347. PMID: 32242358; PMCID: PMC7731441.
50. Sterner RC, Sterner RM. CAR-T cell therapy: current limitations and potential strategies. *Blood Cancer J*. 2021 Apr 6;11(4):69. doi: 10.1038/s41408-021-00459-7. PMID: 33824268; PMCID: PMC8024391.
51. Stepanov AV, Xie J, Zhu Q, Shen Z, Su W, Kuai L, Soll R, Rader C, Shaver G, Douthit L, Zhang D, Kalinin R, Fu X, Zhao Y, Qin T, Baran PS, Gabibov AG, Bushnell D, Neri D, Kornberg RD, Lerner RA. Control of the antitumour activity and specificity of CAR T cells via organic adapters covalently tethering the CAR to tumour cells. *Nat Biomed Eng*. 2023 Oct 5. doi: 10.1038/s41551-023-01102-5. Epub ahead of print. PMID: 37798444.
52. Cornel AM, Mimpfen IL, Nierkens S. MHC Class I Downregulation in Cancer: Underlying Mechanisms and Potential Targets for Cancer Immunotherapy. *Cancers (Basel)*. 2020 Jul 2;12(7):1760. doi: 10.3390/cancers12071760. PMID: 32630675; PMCID: PMC7409324.
53. Liu Y, Zhang C. The Role of Human  $\gamma\delta$  T Cells in Anti-Tumor Immunity and Their Potential for Cancer Immunotherapy. *Cells*. 2020 May 13;9(5):1206. doi: 10.3390/cells9051206. PMID: 32413966; PMCID: PMC7290839.
54. Saito H, Kranz DM, Takagaki Y, Hayday AC, Eisen HN, Tonegawa S. Complete primary structure of a heterodimeric T-cell receptor deduced from cDNA sequences. *Nature*. 1984 Jun 28-Jul 4;309(5971):757-62. doi: 10.1038/309757a0. PMID: 6330561.

55. Brenner MB, McLean J, Dialynas DP, Strominger JL, Smith JA, Owen FL, Seidman JG, Ip S, Rosen F, Krangel MS. Pillars Article: Identification of a Putative Second T-cell Receptor. *Nature*. 1986. 322: 145-149. *J Immunol*. 2016 May 1;196(9):3509-13. Epub 2016 Apr 18. PMID: 27183647.
56. Bank I, DePinho RA, Brenner MB, Cassimeris J, Alt FW, Chess L. Pillars Article: A Functional T3 Molecule Associated with a Novel Heterodimer on the Surface of Immature Human Thymocytes. *Nature*. 1986. 322: 179-181. *J Immunol*. 2016 May 1;196(9):3514-6. Epub 2016 Apr 18. PMID: 27183648.
57. Loh EY, Lanier LL, Turck CW, Littman DR, Davis MM, Chien YH, Weiss A. Identification and sequence of a fourth human T cell antigen receptor chain. *Nature*. 1987 Dec 10-16;330(6148):569-72. doi: 10.1038/330569a0. PMID: 2825032.
58. Giri S, Girdhari L. Differentiation and functional plasticity of gamma-delta ( $\gamma\delta$ ) T cells under homeostatic and disease conditions. *Mol Immunol*. (2021) 136:138–49. doi: 10.1016/j.molimm.2021.06.006
59. Porritt HE, Rumfelt LL, Tabrizifard S, Schmitt TM, Zúñiga-Pflücker JC, Petrie HT. Heterogeneity among DN1 prothymocytes reveals multiple progenitors with different capacities to generate T cell and non-T cell lineages. *Immunity*. (2004) 20:735–45. doi: 10.1016/j.immuni.2004.05.004
60. Hernandez JB, Newton RH, Walsh CM. Life and death in the thymus—cell death signaling during T cell development. *Curr Opin Cell Biol*. (2010) 22:865–71. doi: 10.1016/j.ceb.2010.08.003
61. Biały S, Bogunia-Kubik K. Uncovering the mysteries of human gamma delta T cells: from origins to novel therapeutics. *Front Immunol*. 2025 Apr 10;16:1543454. doi: 10.3389/fimmu.2025.1543454. PMID: 40276509; PMCID: PMC12018481.
62. Hayes SM, Li L, Love PE. TCR signal strength influences alphabeta/gammadelta lineage fate. *Immunity*. (2005) 22:583–93. doi: 10.1016/j.immuni.2005.03.014
63. Fahl SP, Coffey F, Wiest DL. Origins of  $\gamma\delta$  T cell effector subsets: a riddle wrapped in an enigma. *J Immunol* (Baltimore Md: 1950). (2014) 193:4289–94. doi: 10.4049/jimmunol.1401813
64. Elliott JF, Rock EP, Patten PA, Davis MM, Chien YH. The adult T-cell receptor delta-chain is diverse and distinct from that of fetal thymocytes. *Nature*. 1988 Feb 18;331(6157):627-31. doi: 10.1038/331627a0. PMID: 2963227.
65. Kabelitz D, Serrano R, Kouakanou L, Peters C, Kalyan S. Cancer immunotherapy with  $\gamma\delta$  T cells: many paths ahead of us. *Cell Mol Immunol*. 2020 Sep;17(9):925-939. Doi: 10.1038/s41423-020-0504-x. Epub 2020 Jul 22. Erratum in: *Cell Mol Immunol*. 2020 Sep 1;: PMID : 32699351; PMCID : PMC7609273.
66. Silva-Santos B, Strid J. Working in "NK Mode": Natural Killer Group 2 Member D and Natural Cytotoxicity Receptors in Stress-Surveillance by  $\gamma\delta$  T Cells. *Front Immunol*. 2018 Apr 24;9:851. doi: 10.3389/fimmu.2018.00851. PMID: 29740448; PMCID: PMC5928212.
67. Willcox BE, Willcox CR.  $\gamma\delta$  TCR ligands: the quest to solve a 500-million-year-old mystery. *Nat Immunol*. 2019 Feb;20(2):121-128. doi: 10.1038/s41590-018-0304-y. Epub 2019 Jan 21. Erratum in: *Nat Immunol*. 2019 Apr;20(4):516. doi: 10.1038/s41590-019-0358-5. PMID: 30664765.
68. Born WK, Kemal Aydintug M, O'Brien RL. Diversity of  $\gamma\delta$  T-cell antigens. *Cell Mol Immunol*. 2013 Jan;10(1):13-20. doi: 10.1038/cmi.2012.45. Epub 2012 Oct 22. PMID: 23085946; PMCID: PMC4003174.
69. Rigau M, Ostrouska S, Fulford TS, Johnson DN, Woods K, Ruan Z, McWilliam HEG, Hudson C, Tutuka C, Wheatley AK, Kent SJ, Villadangos JA, Pal B, Kurts C, Simmonds J, Pelzing M, Nash AD, Hammet A, Verhagen AM, Vairo G, Maraskovsky E, Panousis C, Gherardin NA, Cebon J, Godfrey DI,

- Behren A, Uldrich AP. Butyrophilin 2A1 is essential for phosphoantigen reactivity by  $\gamma\delta$  T cells. *Science*. 2020 Feb 7;367(6478):eaay5516. doi: 10.1126/science.aay5516. Epub 2020 Jan 9. PMID: 31919129.
70. Viey E, Fromont G, Escudier B, Morel Y, Da Rocha S, Chouaib S, Caignard A. Phosphostim-activated gamma delta T cells kill autologous metastatic renal cell carcinoma. *J Immunol*. 2005 Feb 1;174(3):1338-47. doi: 10.4049/jimmunol.174.3.1338. PMID: 15661891.
  71. Alexander AA, Maniar A, Cummings JS, Hebbeler AM, Schulze DH, Gastman BR, Pauza CD, Strome SE, Chapoval AI. Isopentenyl pyrophosphate-activated CD56+  $\{\gamma\}\{\delta\}$  T lymphocytes display potent antitumor activity toward human squamous cell carcinoma. *Clin Cancer Res*. 2008 Jul 1;14(13):4232-40. doi: 10.1158/1078-0432.CCR-07-4912. PMID: 18594005; PMCID: PMC2614380.
  72. Todaro M, D'Asaro M, Caccamo N, Iovino F, Francipane MG, Meraviglia S, Orlando V, La Mendola C, Gulotta G, Salerno A, Dieli F, Stassi G. Efficient killing of human colon cancer stem cells by gammadelta T lymphocytes. *J Immunol*. 2009 Jun 1;182(11):7287-96. doi: 10.4049/jimmunol.0804288. PMID: 19454726.
  73. D'Asaro M, La Mendola C, Di Liberto D, Orlando V, Todaro M, Spina M, Guggino G, Meraviglia S, Caccamo N, Messina A, Salerno A, Di Raimondo F, Vigneri P, Stassi G, Fournié JJ, Dieli F. V gamma 9V delta 2 T lymphocytes efficiently recognize and kill zoledronate-sensitized, imatinib-sensitive, and imatinib-resistant chronic myelogenous leukemia cells. *J Immunol*. 2010 Mar 15;184(6):3260-8. doi: 10.4049/jimmunol.0903454. Epub 2010 Feb 12. PMID: 20154204.
  74. Dokouhaki P, Schuh NW, Joe B, Allen CA, Der SD, Tsao MS, Zhang L. NKG2D regulates production of soluble TRAIL by ex vivo expanded human  $\gamma\delta$  T cells. *Eur J Immunol*. 2013 Dec;43(12):3175-82. doi: 10.1002/eji.201243150. Epub 2013 Sep 10. PMID: 24019170.
  75. Li Z, Xu Q, Peng H, Cheng R, Sun Z, Ye Z. IFN- $\gamma$  enhances HOS and U2OS cell lines susceptibility to  $\gamma\delta$  T cell-mediated killing through the Fas/Fas ligand pathway. *Int Immunopharmacol*. 2011 Apr;11(4):496-503. doi: 10.1016/j.intimp.2011.01.001. Epub 2011 Jan 14. PMID: 21238618.
  76. Couzi L, Pitard V, Sicard X, Garrigue I, Hawchar O, Merville P, Moreau JF, Déchanet-Merville J. Antibody-dependent anti-cytomegalovirus activity of human  $\gamma\delta$  T cells expressing CD16 (Fc $\gamma$ RIIIa). *Blood*. 2012 Feb 9;119(6):1418-27. doi: 10.1182/blood-2011-06-363655. Epub 2011 Dec 16. PMID: 22180442.
  77. Tokuyama H, Hagi T, Mattarollo SR, Morley J, Wang Q, So HF, Moriyasu F, Nieda M, Nicol AJ. V gamma 9 V delta 2 T cell cytotoxicity against tumor cells is enhanced by monoclonal antibody drugs--rituximab and trastuzumab. *Int J Cancer*. 2008 Jun 1;122(11):2526-34. doi: 10.1002/ijc.23365. Erratum in: *Int J Cancer*. 2011 Dec 1;129(11):2761. Fai-So, Hang [corrected to So, Hang-Fai]. PMID: 18307255.
  78. Gertner-Dardenne J, Bonnafous C, Bezombes C, Capietto AH, Scaglione V, Ingoure S, Cendron D, Gross E, Lepage JF, Quillet-Mary A, Ysebaert L, Laurent G, Sicard H, Fournié JJ. Bromohydrin pyrophosphate enhances antibody-dependent cell-mediated cytotoxicity induced by therapeutic antibodies. *Blood*. 2009 May 14;113(20):4875-84. doi: 10.1182/blood-2008-08-172296. Epub 2009 Mar 10. PMID: 19278954.
  79. Schiller CB, Braciak TA, Fenn NC, Seidel UJ, Roskopf CC, Wildenhain S, Honegger A, Schubert IA, Schele A, Lämmermann K, Fey GH, Jacob U, Lang P, Hopfner KP, Oduncu FS. CD19-specific triplebody SPM-1 engages NK and  $\gamma\delta$  T cells for rapid and efficient lysis of malignant B-lymphoid cells. *Oncotarget*. 2016 Dec 13;7(50):83392-83408. doi: 10.18632/oncotarget.13110. PMID: 27825135; PMCID: PMC5347777.

80. Bauer S, Groh V, Wu J, Steinle A, Phillips JH, Lanier LL, Spies T. Pillars Article: Activation of NK Cells and T Cells by NKG2D, a Receptor for Stress-Inducible MICA. *Science*. 1999. 285: 727-729. *J Immunol*. 2018 Apr 1;200(7):2231-2233. PMID: 29555676.
81. Kong Y, Cao W, Xi X, Ma C, Cui L, He W. The NKG2D ligand ULBP4 binds to TCRgamma9/delta2 and induces cytotoxicity to tumor cells through both TCRgammadelta and NKG2D. *Blood*. 2009 Jul 9;114(2):310-7. doi: 10.1182/blood-2008-12-196287. Epub 2009 May 12. PMID: 19436053.
82. Groh V, Rhinehart R, Secrist H, Bauer S, Grabstein KH, Spies T. Broad tumor-associated expression and recognition by tumor-derived gamma delta T cells of MICA and MICB. *Proc Natl Acad Sci U S A*. 1999 Jun 8;96(12):6879-84. doi: 10.1073/pnas.96.12.6879. PMID: 10359807; PMCID: PMC22010.
83. Lança T, Correia DV, Moita CF, Raquel H, Neves-Costa A, Ferreira C, Ramalho JS, Barata JT, Moita LF, Gomes AQ, Silva-Santos B. The MHC class Ib protein ULBP1 is a nonredundant determinant of leukemia/lymphoma susceptibility to gammadelta T-cell cytotoxicity. *Blood*. 2010 Mar 25;115(12):2407-11. doi: 10.1182/blood-2009-08-237123. Epub 2010 Jan 25. PMID: 20101024.
84. Silva-Santos B, Mensurado S, Coffelt SB.  $\gamma\delta$  T cells: pleiotropic immune effectors with therapeutic potential in cancer. *Nat Rev Cancer*. 2019 Jul;19(7):392-404. doi: 10.1038/s41568-019-0153-5. PMID: 31209264; PMCID: PMC7614706.
85. Rezende RM, Lanser AJ, Rubino S, Kuhn C, Skillin N, Moreira TG, Liu S, Gabriely G, David BA, Menezes GB, Weiner HL.  $\gamma\delta$  T cells control humoral immune response by inducing T follicular helper cell differentiation. *Nat Commun*. 2018 Aug 8;9(1):3151. doi: 10.1038/s41467-018-05487-9. PMID: 30089795; PMCID: PMC6082880.
86. Nicol AJ, Tokuyama H, Mattarollo SR, Hagi T, Suzuki K, Yokokawa K, Nieda M. Clinical evaluation of autologous gamma delta T cell-based immunotherapy for metastatic solid tumours. *Br J Cancer*. 2011 Sep 6;105(6):778-86. doi: 10.1038/bjc.2011.293. Epub 2011 Aug 16. PMID: 21847128; PMCID: PMC3171009.
87. Kunzmann V, Smetak M, Kimmel B, Weigang-Koehler K, Goebeler M, Birkmann J, Becker J, Schmidt-Wolf IG, Einsele H, Wilhelm M. Tumor-promoting versus tumor-antagonizing roles of  $\gamma\delta$  T cells in cancer immunotherapy: results from a prospective phase I/II trial. *J Immunother*. 2012 Feb-Mar;35(2):205-13. doi: 10.1097/CJI.0b013e318245bb1e. PMID: 22306909.
88. Wilhelm M, Kunzmann V, Eckstein S, Reimer P, Weissinger F, Ruediger T, Tony HP. Gammadelta T cells for immune therapy of patients with lymphoid malignancies. *Blood*. 2003 Jul 1;102(1):200-6. doi: 10.1182/blood-2002-12-3665. Epub 2003 Mar 6. PMID: 12623838.
89. Kobayashi H, et al. Safety profile and anti-tumor effects of adoptive immunotherapy using  $\gamma\delta$  T cells against advanced renal cell carcinoma: a pilot study. *Cancer Immunol Immunother*. 2007;56:469-476. doi: 10.1007/s00262-006-0199-6.
90. Fournie JJ, et al. What lessons can be learned from  $\gamma\delta$  T cell-based cancer immunotherapy trials? *Cell Mol Immunol*. 2013;10:35-41. doi: 10.1038/cmi.2012.39. A review providing an insightful discussion of the limited success of cancer clinical trials based on V $\gamma$ 9V $\delta$ 2 T cells.
91. Jonus HC, Burnham RE, Ho A, Pilgrim AA, Shim J, Doering CB, Spencer HT, Goldsmith KC. Dissecting the cellular components of ex vivo  $\gamma\delta$  T cell expansions to optimize selection of potent cell therapy donors for neuroblastoma immunotherapy trials. *Oncoimmunology*. 2022 Mar 26;11(1):2057012. doi: 10.1080/2162402X.2022.2057012. PMID: 35371623; PMCID: PMC8966991.
92. Marcu-Malina V, et al. Redirecting  $\alpha\beta$  T cells against cancer cells by transfer of a broadly tumor-reactive  $\gamma\delta$ T-cell receptor. *Blood*. 2011;118:50-59. doi: 10.1182/blood-2010-12-325993. A work that

- establishes a proof of principle for transferring V $\gamma$ 9V $\delta$ 2 TCRs into  $\alpha\beta$  T cells to improve their antitumour efficacy and safety.
93. Straetemans T, et al. GMP-grade manufacturing of T cells engineered to express a defined  $\gamma\delta$ TCR. *Front Immunol.* 2018;9:1062. doi: 10.3389/fimmu.2018.01062.
  94. Gentles, A. J. et al. The prognostic landscape of genes and infiltrating immune cells across human cancers. *Nat Med* 21, 938–945 (2015)
  95. Rischer M, Pscherer S, Duwe S, Vormoor J, Jürgens H, Rossig C. Human gammadelta T cells as mediators of chimaeric-receptor redirected anti-tumour immunity. *Br J Haematol.* 2004 Aug;126(4):583-92. doi: 10.1111/j.1365-2141.2004.05077.x. PMID: 15287953.
  96. Deniger DC, Maiti SN, Mi T, Switzer KC, Ramachandran V, Hurton LV, Ang S, Olivares S, Rabinovich BA, Huls MH, Lee DA, Bast RC Jr, Champlin RE, Cooper LJ. Activating and propagating polyclonal gamma delta T cells with broad specificity for malignancies. *Clin Cancer Res.* 2014 Nov 15;20(22):5708-19. doi: 10.1158/1078-0432.CCR-13-3451. Epub 2014 May 15. PMID: 24833662; PMCID: PMC4233015.
  97. Rozenbaum M, Meir A, Aharony Y, Itzhaki O, Schachter J, Bank I, Jacoby E, Besser MJ. Gamma-Delta CAR-T Cells Show CAR-Directed and Independent Activity Against Leukemia. *Front Immunol.* 2020 Jul 2;11:1347. doi: 10.3389/fimmu.2020.01347. PMID: 32714329; PMCID: PMC7343910.
  98. Nishimoto KP, Barca T, Azameera A, Makkouk A, Romero JM, Bai L, Brodey MM, Kennedy-Wilde J, Shao H, Papaioannou S, Doan A, Masri C, Hoang NT, Tessman H, Ramanathan VD, Giner-Rubio A, Delfino F, Sharma K, Bray K, Hoopes M, Satpayev D, Sengupta R, Herrman M, Abbot SE, Aftab BT, An Z, Panuganti S, Hayes SM. Allogeneic CD20-targeted  $\gamma\delta$  T cells exhibit innate and adaptive antitumor activities in preclinical B-cell lymphoma models. *Clin Transl Immunology.* 2022 Feb 2;11(2):e1373. doi: 10.1002/cti2.1373. PMID: 35136603; PMCID: PMC8809437.
  99. Yi Y, et al. The functional impairment of HCC-infiltrating  $\gamma\delta$  T cells, partially mediated by regulatory T cells in a TGF $\beta$ -and IL-10-dependent manner. *J Hepatol.* 2013;58:977–983. doi: 10.1016/j.jhep.2012.12.015.
  100. Sacchi A, et al. Myeloid-derived suppressor cells specifically suppress IFN- $\gamma$  production and antitumor cytotoxic activity of V $\delta$ 2 T cells. *Front Immunol.* 2018;9:1271. doi: 10.3389/fimmu.2018.01271.
  101. Sabbione F, et al. Neutrophils suppress  $\gamma\delta$  T cell function. *Eur J Immunol.* 2014;44:819–830. doi: 10.1002/eji.201343664.
  102. Ganapathy T, Radhakrishnan R, Sakshi S, Martin S. CAR  $\gamma\delta$  T cells for cancer immunotherapy. Is the field more yellow than green? *Cancer Immunol Immunother.* 2023 Feb;72(2):277-286. doi: 10.1007/s00262-022-03260-y. Epub 2022 Aug 12. PMID: 35960333.
  103. Nasiri F, Safarzadeh Kozani P, Rahbarizadeh F. T-cells engineered with a novel VHH-based chimeric antigen receptor against CD19 exhibit comparable tumoricidal efficacy to their FMC63-based counterparts. *Front Immunol.* 2023 Feb 16;14:1063838. doi: 10.3389/fimmu.2023.1063838. PMID: 36875091; PMCID: PMC9978144.
  104. McComb S, Arbabi-Ghahroudi M, Hay KA, Keller BA, Faulkes S, Rutherford M, Nguyen T, Shepherd A, Wu C, Marcil A, Aubry A, Hussack G, Pinto DM, Ryan S, Raphael S, van Faassen H, Zafer A, Zhu Q, Maclean S, Chattopadhyay A, Gurnani K, Gilbert R, Gadoury C, Iqbal U, Fatehi D, Jezierski A, Huang J, Pon RA, Sigrist M, Holt RA, Nelson BH, Atkins H, Kekre N, Yung E, Webb J, Nielsen JS, Weeratna RD. Discovery and preclinical development of a therapeutically active nanobody-

- based chimeric antigen receptor targeting human CD22. *Mol Ther Oncol*. 2024 Feb 13;32(1):200775. doi: 10.1016/j.omton.2024.200775. PMID: 38596311; PMCID: PMC10914482.
105. Guo J, Chowdhury RR, Mallajosyula V, Xie J, Dubey M, Liu Y, Li J, Wei YL, Palanski BA, Wang C, Qiu L, Ohanyan M, Kask O, Sola E, Kamalyan L, Lewis DB, Scriba TJ, Davis MM, Dodd D, Zeng X, Chien YH.  $\gamma\delta$  T cell antigen receptor polyspecificity enables T cell responses to a broad range of immune challenges. *Proc Natl Acad Sci U S A*. 2024 Jan 23;121(4):e2315592121. doi: 10.1073/pnas.2315592121. Epub 2024 Jan 16. PMID: 38227652; PMCID: PMC10823224.
  106. Broussau S, Lytvyn V, Simoneau M, Guilbault C, Leclerc M, Nazemi-Moghaddam N, Coulombe N, Elahi SM, McComb S, Gilbert R. Packaging cells for lentiviral vectors generated using the cumate and coumermycin gene induction systems and nanowell single-cell cloning. *Mol Ther Methods Clin Dev*. 2023 Feb 26;29:40-57. doi: 10.1016/j.omtm.2023.02.013. PMID: 36936448; PMCID: PMC10018046.
  107. Ravens S, Schultze-Florey C, Raha S, Sandrock I, Drenker M, Oberdörfer L, Reinhardt A, Ravens I, Beck M, Geffers R, von Kaisenberg C, Heuser M, Thol F, Ganser A, Förster R, Koenecke C, Prinz I. Human  $\gamma\delta$  T cells are quickly reconstituted after stem-cell transplantation and show adaptive clonal expansion in response to viral infection. *Nat Immunol*. 2017 Apr;18(4):393-401. doi: 10.1038/ni.3686. Epub 2017 Feb 20. Erratum in: *Nat Immunol*. 2018 Sep;19(9):1037. doi: 10.1038/s41590-018-0054-x. PMID: 28218745.
  108. Davey MS, Willcox CR, Hunter S, Kasatskaya SA, Remmerswaal EBM, Salim M, Mohammed F, Bemelman FJ, Chudakov DM, Oo YH, Willcox BE. The human  $V\delta 2^+$  T-cell compartment comprises distinct innate-like  $V\gamma 9^+$  and adaptive  $V\gamma 9^-$  subsets. *Nat Commun*. 2018 May 2;9(1):1760. doi: 10.1038/s41467-018-04076-0. PMID: 29720665; PMCID: PMC5932074.
  109. Wang L, Gong W, Wang S, Neuber B, Sellner L, Schubert ML, Hückelhoven-Krauss A, Kunz A, Gern U, Michels B, Hinkelbein M, Mechler S, Richter P, Müller-Tidow C, Schmitt M, Schmitt A. Improvement of in vitro potency assays by a resting step for clinical-grade chimeric antigen receptor engineered T cells. *Cytotherapy*. 2019 May;21(5):566-578. doi: 10.1016/j.jcyt.2019.02.013. Epub 2019 Mar 23. PMID: 30910382.
  110. Nastoupil LJ, Jain MD, Feng L, Spiegel JY, Ghobadi A, Lin Y, Dahiya S, Lunning M, Lekakis L, Reagan P, Oluwole O, McGuirk J, Deol A, Sehgal AR, Goy A, Hill BT, Vu K, Andreadis C, Munoz J, Westin J, Chavez JC, Cashen A, Bennani NN, Rapoport AP, Vose JM, Miklos DB, Neelapu SS, Locke FL. Standard-of-Care Axicabtagene Ciloleucel for Relapsed or Refractory Large B-Cell Lymphoma: Results From the US Lymphoma CAR T Consortium. *J Clin Oncol*. 2020 Sep 20;38(27):3119-3128. doi: 10.1200/JCO.19.02104. Epub 2020 May 13. PMID: 32401634; PMCID: PMC7499611.
  111. Abramson JS, Palomba ML, Gordon LI, Lunning MA, Wang M, Arnason J, Mehta A, Purev E, Maloney DG, Andreadis C, Sehgal A, Solomon SR, Ghosh N, Albertson TM, Garcia J, Kostic A, Mallaney M, Ogasawara K, Newhall K, Kim Y, Li D, Siddiqi T. Lisocabtagene maraleucel for patients with relapsed or refractory large B-cell lymphomas (TRANSCEND NHL 001): a multicentre seamless design study. *Lancet*. 2020 Sep 19;396(10254):839-852. doi: 10.1016/S0140-6736(20)31366-0. Epub 2020 Sep 1. PMID: 32888407.
  112. Jacobson C, Locke FL, Ghobadi A, Miklos DB, Lekakis LJ, Oluwole OO, Lin Y, Hill BT, Timmerman JM, Deol A, Reagan PM, Stiff P, Flinn IW, Farooq U, Goy AH, Munoz J, Siddiqi T, Shen RR, Bot A, Dong J, Singh K, Spooner C, Karalliyadda R, Kin JJ, Zheng Yan, Neelapu SS. Long-Term ( $\geq 4$  Year and  $\geq 5$  Year) Overall Survival (OS) By 12- and 24-Month Event-Free Survival (EFS): An

- Updated Analysis of ZUMA-1, the Pivotal Study of Axicabtagene Ciloleucel (Axi-Cel) in Patients (Pts) with Refractory Large B-Cell Lymphoma (LBCL). *Blood*. 2021; 138:1764
113. Hirayama AV, Gauthier J, Hay KA, Voutsinas JM, Wu Q, Pender BS, Hawkins RM, Vakil A, Steinmetz RN, Riddell SR, Maloney DG, Turtle CJ. High rate of durable complete remission in follicular lymphoma after CD19 CAR-T cell immunotherapy. *Blood*. 2019 Aug 15;134(7):636-640. doi: 10.1182/blood.2019000905. PMID: 31648294; PMCID: PMC6695558.
  114. Cappell KM, Sherry RM, Yang JC, Goff SL, Vanasse DA, McIntyre L, Rosenberg SA, Kochenderfer JN. Long-Term Follow-Up of Anti-CD19 Chimeric Antigen Receptor T-Cell Therapy. *J Clin Oncol*. 2020 Nov 10;38(32):3805-3815. doi: 10.1200/JCO.20.01467. Epub 2020 Oct 6. PMID: 33021872; PMCID: PMC7655016.
  115. Chong EA, Ruella M, Schuster SJ; Lymphoma Program Investigators at the University of Pennsylvania. Five-Year Outcomes for Refractory B-Cell Lymphomas with CAR T-Cell Therapy. *N Engl J Med*. 2021 Feb 18;384(7):673-674. doi: 10.1056/NEJMc2030164. PMID: 33596362.
  116. Locke FL, Miklos DB, Jacobson CA, Perales MA, Kersten MJ, Oluwole OO, Ghobadi A, Rapoport AP, McGuirk J, Pagel JM, Muñoz J, Farooq U, van Meerten T, Reagan PM, Sureda A, Flinn IW, Vandenberghe P, Song KW, Dickinson M, Minnema MC, Riedell PA, Leslie LA, Chaganti S, Yang Y, Filosto S, Shah J, Schupp M, To C, Cheng P, Gordon LI, Westin JR; All ZUMA-7 Investigators and Contributing Kite Members. Axicabtagene Ciloleucel as Second-Line Therapy for Large B-Cell Lymphoma. *N Engl J Med*. 2022 Feb 17;386(7):640-654. doi: 10.1056/NEJMoa2116133. Epub 2021 Dec 11. PMID: 34891224.
  117. Bock TJ, Colonne CK, Fiorenza S, Turtle CJ. Outcome correlates of approved CD19-targeted CAR T cells for large B cell lymphoma. *Nat Rev Clin Oncol*. 2025 Apr;22(4):241-261. doi: 10.1038/s41571-025-00992-5. Epub 2025 Feb 18. PMID: 39966627.
  118. Locke FL, Rossi JM, Neelapu SS, Jacobson CA, Miklos DB, Ghobadi A, Oluwole OO, Reagan PM, Lekakis LJ, Lin Y, Sherman M, Better M, Go WY, Wiezorek JS, Xue A, Bot A. Tumor burden, inflammation, and product attributes determine outcomes of axicabtagene ciloleucel in large B-cell lymphoma. *Blood Adv*. 2020 Oct 13;4(19):4898-4911. doi: 10.1182/bloodadvances.2020002394. PMID: 33035333; PMCID: PMC7556133.
  119. Avanzi MP, Yeku O, Li X, Wijewarnasuriya DP, van Leeuwen DG, Cheung K, Park H, Purdon TJ, Daniyan AF, Spitzer MH, Brentjens RJ. Engineered Tumor-Targeted T Cells Mediate Enhanced Anti-Tumor Efficacy Both Directly and through Activation of the Endogenous Immune System. *Cell Rep*. 2018 May 15;23(7):2130-2141. doi: 10.1016/j.celrep.2018.04.051. PMID: 29768210; PMCID: PMC5986286.
  120. Plaks V, Rossi JM, Chou J, Wang L, Poddar S, Han G, Wang Z, Kuang SQ, Chu F, Davis RE, Vega F, Bashir Z, Jacobson CA, Locke FL, Reagan PM, Rodig SJ, Lekakis LJ, Flinn IW, Miklos DB, Bot A, Neelapu SS. CD19 target evasion as a mechanism of relapse in large B-cell lymphoma treated with axicabtagene ciloleucel. *Blood*. 2021 Sep 23;138(12):1081-1085. doi: 10.1182/blood.2021010930. PMID: 34041526; PMCID: PMC8462361.
  121. Lee DW, Gardner R, Porter DL, Louis CU, Ahmed N, Jensen M, Grupp SA, Mackall CL. Current concepts in the diagnosis and management of cytokine release syndrome. *Blood*. 2014 Jul 10;124(2):188-95. doi: 10.1182/blood-2014-05-552729. Epub 2014 May 29. Erratum in: *Blood*. 2015 Aug 20;126(8):1048. Dosage error in article text. Erratum in: *Blood*. 2016 Sep 15;128(11):1533. doi: 10.1182/blood-2016-07-730689. PMID: 24876563; PMCID: PMC4093680.

122. Neelapu SS, Tummala S, Kebriaei P, Wierda W, Gutierrez C, Locke FL, Komanduri KV, Lin Y, Jain N, Daver N, Westin J, Gulbis AM, Loghin ME, de Groot JF, Adkins S, Davis SE, Rezvani K, Hwu P, Shpall EJ. Chimeric antigen receptor T-cell therapy - assessment and management of toxicities. *Nat Rev Clin Oncol*. 2018 Jan;15(1):47-62. doi: 10.1038/nrclinonc.2017.148. Epub 2017 Sep 19. PMID: 28925994; PMCID: PMC6733403.
123. Neelapu SS. Managing the toxicities of CAR T-cell therapy. *Hematol Oncol*. 2019 Jun;37 Suppl 1:48-52. doi: 10.1002/hon.2595. PMID: 31187535.
124. Chou CK, Turtle CJ. Insight into mechanisms associated with cytokine release syndrome and neurotoxicity after CD19 CAR-T cell immunotherapy. *Bone Marrow Transplant*. 2019 Aug;54(Suppl 2):780-784. doi: 10.1038/s41409-019-0602-5. PMID: 31431714.
125. Baroni ML, Sanchez Martinez D, Gutierrez Aguera F, Roca Ho H, Castella M, Zanetti SR, Velasco Hernandez T, Diaz de la Guardia R, Castaño J, Anguita E, Vives S, Nomdedeu J, Lapillone H, Bras AE, van der Velden VHJ, Junca J, Marin P, Bataller A, Esteve J, Vick B, Jeremias I, Lopez A, Sorigue M, Bueno C, Menendez P. 41BB-based and CD28-based CD123-redirection T-cells ablate human normal hematopoiesis in vivo. *J Immunother Cancer*. 2020 Jun;8(1):e000845. doi: 10.1136/jitc-2020-000845. PMID: 32527933; PMCID: PMC7292050.
126. Kowolik CM, Topp MS, Gonzalez S, Pfeiffer T, Olivares S, Gonzalez N, Smith DD, Forman SJ, Jensen MC, Cooper LJ. CD28 costimulation provided through a CD19-specific chimeric antigen receptor enhances in vivo persistence and antitumor efficacy of adoptively transferred T cells. *Cancer Res*. 2006 Nov 15;66(22):10995-1004. doi: 10.1158/0008-5472.CAN-06-0160. PMID: 17108138.
127. Philipson BI, O'Connor RS, May MJ, June CH, Albelda SM, Milone MC. 4-1BB costimulation promotes CAR T cell survival through noncanonical NF- $\kappa$ B signaling. *Sci Signal*. 2020 Mar 31;13(625):eaay8248. doi: 10.1126/scisignal.aay8248. PMID: 32234960; PMCID: PMC7883633.
128. Côté J, Garnier A, Massie B, Kamen A. Serum-free production of recombinant proteins and adenoviral vectors by 293SF-3F6 cells. *Biotechnol Bioeng*. 1998 Sep 5;59(5):567-75. PMID: 10099373.
129. Mullick A, Xu Y, Warren R, Koutroumanis M, Guilbault C, Broussau S, Malenfant F, Bourget L, Lamoureux L, Lo R, Caron AW, Pilote A, Massie B. The cumate gene-switch: a system for regulated expression in mammalian cells. *BMC Biotechnol*. 2006 Nov 3;6:43. doi: 10.1186/1472-6750-6-43. PMID: 17083727; PMCID: PMC1654148.
130. Zhao HF, Boyd J, Jolicoeur N, Shen SH. A coumermycin/novobiocin-regulated gene expression system. *Hum Gene Ther*. 2003 Nov 20;14(17):1619-29. doi: 10.1089/104303403322542266. PMID: 14633404.
131. Dull T, Zufferey R, Kelly M, Mandel RJ, Nguyen M, Trono D, Naldini L. A third-generation lentivirus vector with a conditional packaging system. *J Virol*. 1998 Nov;72(11):8463-71. doi: 10.1128/JVI.72.11.8463-8471.1998. PMID: 9765382; PMCID: PMC110254.
132. Zufferey R, Dull T, Mandel RJ, Bukovsky A, Quiroz D, Naldini L, Trono D. Self-inactivating lentivirus vector for safe and efficient in vivo gene delivery. *J Virol*. 1998 Dec;72(12):9873-80. doi: 10.1128/JVI.72.12.9873-9880.1998. PMID: 9811723; PMCID: PMC110499.
133. Wilhelm M, Smetak M, Schaefer-Eckart K, Kimmel B, Birkmann J, Einsele H, Kunzmann V. Successful adoptive transfer and in vivo expansion of haploidentical  $\gamma\delta$  T cells. *J Transl Med*. 2014 Feb 15;12:45. doi: 10.1186/1479-5876-12-45. PMID: 24528541; PMCID: PMC3926263.
134. Wada I, Matsushita H, Noji S, Mori K, Yamashita H, Nomura S, Shimizu N, Seto Y, Kakimi K. Intraperitoneal injection of in vitro expanded V $\gamma$ 9V $\delta$ 2 T cells together with zoledronate for the

- treatment of malignant ascites due to gastric cancer. *Cancer Med.* 2014 Apr;3(2):362-75. doi: 10.1002/cam4.196. Epub 2014 Feb 7. PMID: 24515916; PMCID: PMC3987085.
135. Nakajima J, Murakawa T, Fukami T, Goto S, Kaneko T, Yoshida Y, Takamoto S, Kakimi K. A phase I study of adoptive immunotherapy for recurrent non-small-cell lung cancer patients with autologous gammadelta T cells. *Eur J Cardiothorac Surg.* 2010 May;37(5):1191-7. doi: 10.1016/j.ejcts.2009.11.051. PMID: 20137969.
136. Demoulin B, Cook WJ, Murad J, Graber DJ, Sentman ML, Loney C, Gilham DE, Sentman CL, Agaugue S. Exploiting natural killer group 2D receptors for CAR T-cell therapy. *Future Oncol.* 2017 Aug;13(18):1593-1605. doi: 10.2217/fon-2017-0102. Epub 2017 Jun 14. PMID: 28613086.
137. Nishimoto KP, Lamture G, Chanthery Y, Teague AG, Verma Y, Au M, Smith-Boeck M, Salum M, Murthy P, Gundurao SRY, Kaur R, Zhang J, Azameera A, Wong JTS, Speltz EB, Wang KM, Doan A, Sethuraman J, Bhatwala D, Giner-Rubio A, Puligujja P, Budworth H, Rold CJ, Panuganti S, Jakobovits A, Herrman M, Bhat A, Green S, Aftab BT. ADI-270: an armored allogeneic gamma delta T cell therapy designed to target CD70-expressing solid and hematologic malignancies. *J Immunother Cancer.* 2025 Jul 1;13(7):e011704. doi: 10.1136/jitc-2025-011704. PMID: 40592738; PMCID: PMC12215124.
138. Huang SW, Pan CM, Lin YC, Chen MC, Chen Y, Jan CI, Wu CC, Lin FY, Wang ST, Lin CY, Lin PY, Huang WH, Chiang YT, Tsai WC, Chiu YH, Lin TH, Chiu SC, Cho DY. BiTE-Secreting CAR- $\gamma\delta$ T as a Dual Targeting Strategy for the Treatment of Solid Tumors. *Adv Sci (Weinh).* 2023 Jun;10(17):e2206856. doi: 10.1002/advs.202206856. Epub 2023 Apr 20. PMID: 37078788; PMCID: PMC10265101.

## 4.2 Contribution of collaborators

Dr. Scott McComb, Adjunct Professor (Department of Biochemistry, Microbiology and Immunology, University of Ottawa, Ottawa, ON, Canada.) and Research Officer (Human Health Therapeutics Research Centre, National Research Council, Ottawa, ON, Canada), highly contributed to this project by providing four standard operating procedures (SOP); 1) Thawing, Subculturing, Counting and Banking of HEK Packaging and Producer Cell Lines, 2) Small-scale LV production in HEK293SF-PacLV, 3) 34 mL of Lentivirus or Virus Like Particle Concentration by Ultracentrifugation and 4) Lentiviral vector-based gene transfer into human T lymphocytes.

Dr. Jonathan Angel, Professor (Department of Biochemistry, Microbiology and Immunology, University of Ottawa, Ottawa, ON, Canada), Tier 1 Clinical Research Chair and Senior Scientist (Ottawa Hospital Research Institute, Ottawa, ON, Canada), recruited healthy blood donors and provided all blood donor samples.

Shahriar, laboratory technician (StemCore Laboratories Genomics Core Facility (OHRI, uOttawa), RRID:SCR\_012601), prepared DNA samples for Sanger sequencing that contributed to Figure 9.

### 4.3 Supplementary materials

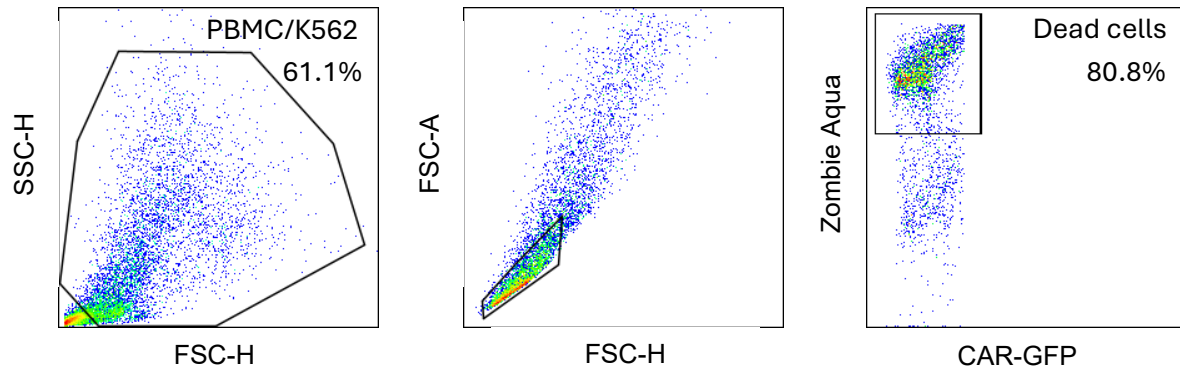


**Figure S1. Feeder cells viability at day 7 post-irradiation.** Feeder cells were resuspended in OpTmizer supplemented with IL-2, IL-15 and 10% FBS, and plated in wells of a 96-well plate. Cellular viability was assessed at day 7 post-irradiation by using the viability dye zombie aqua. Flow cytometry plots, from left to right, show the feeder cells' population (i.e PBMC/K562), the proportions of single cells and the dead cells.